Systemic Risk in Modern Financial Systems

Inaugural-Dissertation
zur Erlangung des akademischen Grades eines Doktors
der Wirtschafts- und Sozialwissenschaften
der Wirtschafts- und Sozialwissenschaftlichen Fakultät
der Christian-Albrechts-Universität zu Kiel

vorgelegt von
M.Sc., Mattia Montagna
aus Pavia/Italy

Frankfrut am Main, 2015

Gedruckt mit Genehmigung der
Wirtschafts- und Sozialwissenschaftlichen Fakultät
der Christian-Albrechts-Universität zu Kiel

Dekan/in:	Prof. Dr. Achim Walter
Erstbegutachtung:	Prof. Dr., Thomas Lux
Zweitbegutachtung:	Prof. Dr., Hans-Werner Wohltmann
Tag der Abgabe der Arbeit:	22.12.2015
Tag der mündlichen Prüfung:	11.05.2016

To Giuseppina Maria Ciceri, my beloved mother whose loyalty, love for life, energy and beauty inspires my whole existence.

Do not pretend that things will change if we always do the same.
The crisis is the best blessing that can happen to people and countries,
because the crisis brings progress. Creativity is born from the distress,
as the day is born from the dark night.
It is in crisis that invention, discovery and large strategies are born.
Who ever overcomes crisis, outdoes himself without being overcome.

ALBERT EINSTEIN

Acknowledgements

First and foremost I would like to thank my advisor Professor Dr. Thomas Lux, who has been the best supervisor I could ever wish for. I would like to thank him for encouraging my research and allowing me to grow as a young scientist. His advises on both, my research and my career have been invaluable. For my future life, I wish to be surrounded by people with the same passion for science.

I would like to thank Lorenzo Cappiello, who has been and still is a great adviser, a great teacher and a great friend to me. His view on life is always enlightening, and his authenticity has been a reference for me in several situations. I am grateful for his presence in my life.

My beloved aunt Laura was probably the closest person to me in the past 10 years. Knowing that she is in my life, gives me a terrific feeling of safeness. She has been my lifeline in uncountable situations. Her ability to turn my mood up every time it is down, is unique.

During my Ph.D I had the great opportunity to travel a lot, and I would like to thank all the amazing people I met throughout my adventure in the last 4 years of my life. In particular Christian Freund, my dear fellow adventurer and friend. I would also like to thank Massimo Schiavo, Veronika Penner, Evelin Melissa Villegas Alonzo, Stephan Fahr, Gabriele La Spada, Assunta Di Chiara, Philipp Kolberg, Stefano Pegoraro, Maribel Lagar, Andrea Corvatta, Giulia Provenzano, the great team of researchers at the Economic Department of Castellón de la Plana and among them in particular Simone and Eva. All of them enriched me in a unique way.

My life time friends deserve special thanks. They are always patient with me, they push me when I need to be pushed, and they stop me in case I take the wrong path. Also if they are all over the world, I still feel their warmth every time we talk to each other. In particular, I wish to thank Francesco Rigamonti, Alessio Elia, Andrea Capozzi and Silvia Entradi.

Last but not least a distinctive gratitude goes to my family, for all their love and encouragement. For my parents, who raised me with the love for science and supported me in all my pursuits. Without them this work would not have been possible. Thank you.

Contents

List of Figures

Glossary

BCBS	Basel Committee for Banking Supervision
BIS	Bank for International Settlements
CRWA	Constant Risk Weighted Assets
EBA	European Banking Authority
ECB	European Central Bank
IbM	Interbank Market
ML	Multi Layered
OTC	Over the Counter
ROA	Return on Assets
ROE	Return on Equity
RWA	Risk Weighted Assets
RWCR	Risk Weighted Capital Ratio
VaR	Value at Risk

1

Introduction

Although widely used, the concept of systemic risk remains elusive and hard to measure and quantify. As noted by Hansen (40), systemic risk refers to a variety of phenomena, which include asset bubbles (Rosengren (63)), contagion (Acemoglu et al. (1)), correlated exposures (Acharya et al. (2)), etc. – see Bisias et al. (16) for a comprehensive survey. However, despite the large number of economic and financial crises (see Reinhart and Rogoff (62)), systemic risk still lacks an accepted definition, and its roots are not totally understood.

The goal of this thesis is to investigate how the structure of a financial system is affecting its resilience against different kinds of economic, financial and structural shocks. The main idea behind the study presented here is the following. Consider a financial system, composed by a certain number of financial institutions (hereafter, banks, for simplicity), whose investments are risky. Those investments can be thought of as loans to the real economy, for simplicity (although during the thesis other kinds of assets will be taken into account, for example financial securities). Moreover, suppose banks can lend money to each other through simple interbank, non-collateralized loans. The uncertainty in such a financial system should in principle only come from the uncertainty of the loans provided by the banks to the real economy. This level of uncertainty is responsible for what can be defined as *real risk*, and in principle this level of risk should bind the amount of *financial risk*, i.e. the final risk the financial system is bearing (see Rajan (61) for a discussion on this point). This assumption is true in a context where there are no feedbacks *within* the financial system, and between the financial system and the real economy. The interbank loans in the simple example above provide such a feedback: distressed institutions, which suffered (idiosyncratic) losses because of the materialization of the real risk, can transmit distress to their counterparties in the interbank market (i.e., their lender banks), which in turn can be unable to absorb such losses and transmit further to their own counterparties. In this way, single idiosyncratic shocks can be transformed into systemic crisis.

During the last decades, the financial world was marked by a large rate of growth of financial innovations. Several new financial instruments have become available to banks, and their principal scope was to enable more risk-sharing within the financial system. Liquidity risk can be hedged through interbank money markets, interest rate risk and credit risk through the derivative markets, and so on. These instruments, while obviously improving the efficiency of the financial system, have uncertain effects on the financial stability. The complexity of modern financial contracts among institutions, and their opacity, makes it hard to track how the risk is generated by and shared within the financial system. Moreover, in case shocks occur, the same financial contracts can transmit distress from bank to bank, through the whole financial system: contagion is the dark side of financial interconnectedness.

Interbank contracts, whatever their kind is, always involve the transfer of risk from one (or more) banks, to others. In principle, this risk sharing mechanism improves the efficiency of the financial system. Banks who can not bear their risks can simply sell them to other entities which in that moment have enough capacity (in terms of capital, liquidity or skills) to do it. However, if the number of contracts, together with their disposition within the system, becomes too large, it can become hard - if not impossible - to take track of those risks. The pioneering work of Allen and Gale (4) clearly shows this simple but powerful concept: ex-ante, interbank relationships are extremely useful for sharing risk in an efficient way within the banking system. Ex-post, after a shock occurs, the exact same contracts can become channels through which losses propagate, making the system fragile against single idiosyncratic shocks. There is therefore a certain probability to see financial breakdowns not because a *systematic* shock hits several banks at the same time, but because the structure of the financial system allows idiosyncratic shocks to become systemic.

The way financial systems are able to absorb and allocate losses depends therefore on how several kinds of interbank contracts among banks are transferring risk among them: in other words, systemic risk depends on the topology of the interbank network.

With interbank network we mean the mathematical object composed by a set of nodes (representing the banks) connected to each other by a set of links (representing the interbank contracts among them). Going back to the previous example, one can imagine to fix the structure (i.e. the amount and the risk) of loans that each bank provides to the real economy. This is equivalent to saying that the amount of real risk in the system is fixed. A natural question then is the following: is there an *optimal* structure for interbank network such that the system is better able to absorb particular kinds of shocks? While a universal answer to this question does not exist, *network theory*, i.e. the branch of mathematics devoted to study graphs and their properties, can shed some light on how the topology of financial systems affect systemic risk. Network theory has been historically employed by natural scientists, in particular physicists and biologists, to study systems of interconnected elements, ranging from neural networks, to molecular networks, to social networks (see Newman (59) and Caldarelli (24)). After the financial crisis emerged in 2007, economists started to draw from this fascinating branch of mathematics as well, since it became clear that the internal structure of financial systems was key to understand systemic risk, and network theory seemed to be the natural candidate to study the properties of such systems.

A crucial difference between networks in financial (and, more in general, economic) systems and other natural systems regards the complexity of the elements composing them. The nodes in financial and economic systems, indeed, represent in general economic agents, being them banks, households or corporations. Their mathematical modeling generally involves a very complex internal structure. Moreover, economic agents are in general connected by *different* kinds of links, i.e. links of different nature, with an implied contagion mechanism that changes from link to link. It is enough to think of interbank contracts: they can range from derivative contracts (and already inside this category a wide spectrum is in place), to interbank unsecured loans, to short term repurchase agreements (repo) contracts, etc. Different contracts in general involve different kinds of risk, which implies different ways of distress propagation in case a shock occurs. Those kinds of interbank links can be defined as *direct* links, since a contract involving two or more parties is in place, which defines clearly how losses are allocated in case one of the parties can not fulfill its obligations.

In parallel to direct links, financial systems are also characterized by *indirect* links: an indirect link exists between two (or more) financial institutions if the actions of one of them negatively affect the other(s) through market mechanisms, and generally through prices. An example of indirect links is an overlap in the mark-to-market portfolio of two financial institutions. Indeed, suppose that one of the two institutions suffers losses and, for example for regulatory reasons, needs to deleverage, by selling part of its portfolio of securities. In case the liquidity in the market is not enough to absorb the sale, prices will drop, and the second institution will have to book losses because of its mark-to-market portfolio (see Acharya et al. (3) for a complete discussion on this mechanism). Again, the idiosyncratic risk which materializes in the first bank is transmitted to the second, and this process can continue until a systemic crisis materializes.

Both direct and indirect links among banks, therefore, have the final effect to increase the correlation among banks default probabilities. This has a major impact on macroprudential policy and regulation. Before the last financial crisis, indeed, it was assumed that the stability of each financial institution, considered as an isolated entity, was a condition necessary and sufficient to guarantee the stability of the system as a whole. I present here a simple example based on the contribution of Vasicek (69), and reported in detail in Cappiello et al. (25), that clarifies the problem with micro-prudential regulation. Consider a set of N financial institutions, $i = 1, 2, \ldots, N$, each characterized by a certain default probability p_i. Such default probabilities are fixed by the regulation for banks acting under the Basel international regulatory framework (see BCBS (9)), and are specified as probability of default over a certain time period, generally one year. Calling e_i the equity of bank i, the regulator requires:

$$Pr\left\{e_i < 0\right\} < \alpha$$

This very simplified framework is actually not far away from the one specified in the Basel international regulatory framework. To define risk weights for each asset, and to require banks to hold a certain percentage of the risk-weighted assets the bank holds, is equivalent to require the bank to keep a certain amount of capital reflecting the amount of losses that materialize with a predefined confidence level. In other words, the regulator is fixing an acceptable default probability that each bank in the system needs to meet.

Consider then the set of variables n_i, defined as:

$$n_i = \begin{cases} 1 & \text{if } eq_i < 0 \\ 0 & \text{otherwise} \end{cases}$$

and given the regulatory requirement, this is equivalent to say:

$$n_i = \begin{cases} 1 & \text{with probability } \alpha \\ 0 & \text{with probability} 1-\alpha \end{cases}$$

In this simplified framework, one can compute the probability to have a systemic crisis starting from the distribution of the number of defaults. In mathematical words, we need to compute the distribution of the variable $N_d = \sum_{i=1}^{N} n_i$. If banks default probabilities are not correlated among each other, the distribution of the yearly number of defaults approaches a Gaussian distribution as the number of banks tends to infinity. This is a direct consequences of the central limit theorem:

$$\frac{N_d}{N} \xrightarrow{d} Z$$

where Z is a Gaussian variable with mean α and variance $\alpha(1-\alpha)$. To give a numerical example, suppose the regulator fixes α at the value 0.001. For a banking system composed by 1000 units, the probability to see more than 20 defaults is 10^{-20}: a systemic event is virtually impossible.

The situation totally change when banks' default probabilities are pairwise correlated among each other, ρ being the correlation. As shown in Cappiello et al. (25), the distribution of the number of defaults N_d converges now to[1]:

$$\sqrt{\frac{1-\rho}{\rho}} exp\left\{-\frac{1}{2\rho}\left(\sqrt{1-\rho}\cdot G^{-1}(N_d) - G^{-1}(\alpha)\right)^2 + \frac{1}{2}\left(G^{-1}\left(N_d\right)\right)^2\right\}$$

Again, consider a banking system composed of 1000 units, a value α equal to 0.001, and a correlation among banks default probabilities $\rho = 0.3$. The probability to have more than 20 defaults is now equal to $7 \cdot 10^{-3}$: systemic events become possible. Moreover, the two banking systems (with and without correlation among banks default probabilities) are equivalent for a micro-prudential regulator, since the margin default probability of the banks in both systems is constant and equal to α.

[1] $G(\cdot)$ is the Gaussian cumulative distribution.

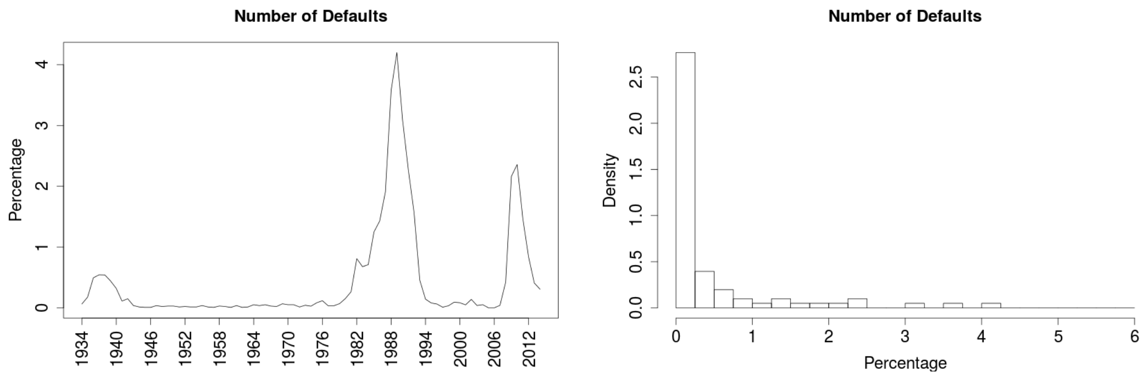

Figure 1.1: LHS chart: yearly number of defaults in the U.S. for the period 1934-2014. Numbers reported as a fraction of the total number of banks. RHS chart: distribution of the number of defaults.

It is interesting to see the real distribution of the number of defaults. This is available only for the U.S. banking system, where the series of defaulting banks is reported by the Federal Deposit Insurance Corporation[1]. The left-hand side of Fig. 1.1 reports the yearly number of defaults in the U.S for the period 1934-2014, expressed as a fraction of the number of active banks at the beginning of each year. On the right-hand side, instead, the distribution of the same quantity is shown. The average and standard deviation of the distribution are, respectively, 0.4 and 0.8. If no correlation among banks default probabilities where in place, events like the savings and loans crisis in the 80-90s', where more than 3% of the total number of banks failed in one single year, should happen once every 700 years. It is obvious from the LHS of Fig. 1.1 that such crises are much more frequent, implying a correlation among banks' default probabilities.

The correlations among banks' default probabilities can be generated by several factors. Common systematic shocks, hitting banks balance sheets at the same moment, generate systemic events, where a large number of banks fail at the same time. One of the goals of this thesis is to understand to what extent *idiosyncratic* shocks can generate such systemic events. In other words, the question is whether the structure of the banking system can be responsible for producing a large number of defaults, triggered by idiosyncratic and not systematic shocks. And the general answer to this

[1] See `https://www.fdic.gov`.

question is yes.

In the last years, two streams of literature studying systemic risk have developed. The first one builds on the pioneering contributions of Bernanke and Gertler (14), Bernanke et al. (15) and Kiyotaki and Moore (51) and explores the dynamics of economies characterized by financial frictions. More recent contributions (for example, among others, Brunnermeier and Sannikov (22), Gerali et al. (36), Gertler and Karadi (37)) extensively study the role of the financial sector in business cycle fluctuations, where agents act in imperfect markets and under asymmetric information. This approach has the advantage of modeling endogenous interactions among agents, and therefore it describes the endogenous dynamic evolution of the system. On the other hand, it lacks of a realistic representation of the financial markets, usually missing important components like heterogeneity and interconnectedness.

The second stream of literature builds on the pioneering contribution of Allen and Gale (4), and, borrowing methodologies usually employed by natural scientists, like network theory and statistical mechanics, studies the influence of the interbank networks on the resilience of the financial system (for example, among others, see Acemoglu et al. (1), Battiston et al. (6), Iori et al. (48)). This approach comes with a realistic representation of the architecture of modern financial systems, though this advantage often comes together with a missing micro-foundation. Merging the two approaches seems to be one of the great academic challenge for the near future.

This thesis contributes to the second of the two streams of literature described above. The rest of this Chapter is devoted to describe the structure of the thesis itself and its contributions in the current debate about systemic risk.

1.1 Content Overview and Contributions

Chapter 2 uses a toy financial system to study systemic risk in scale-free interbank networks. Networks are produced according to a *fitness* algorithm, combined with a representation of the balance sheets of the banks. The fitness algorithm is used to specify the way banks are connected to each other, and it is designed in a way to reproduce the frequently documented features of disassortative behavior, power laws in the degree distributions and power laws in the distribution of bank sizes. Those topological characteristics of a network play an important role when a shock is propagating.

The results show the presence of a particular shell structure affecting the spread of an endogenous shock, which take the form of one bank failing on its obligations to its own creditor banks. This contribution has been developed by myself together with prof. Dr. Thomas Lux. The two authors contributed equally to this work.

Banks have become increasingly interconnected via interbank credit and other forms of liabilities (see, for example, Sole and Espinosa-Vega (64)). As a consequence of the increased interconnectedness, the failure of one node in the interbank network might constitute a threat to the survival of large parts of the entire system. How important this effect of "too-big-too-fail" and "too-interconnected-too-fail" is, depends on the exact topology of the network on which the supervisory authorities have typically very incomplete knowledge. In Chapter 3, which is intimately related to Chapter 2, we propose a probabilistic model to combine some important known quantities (like the size of the banks) with a realistic stochastic representation of the remaining structural elements. Our approach allows us to evaluate relevant measures for the contagion after default of one unit (i.e. number of expected subsequent defaults, or their probabilities). For some quantities we are able to derive closed form solutions, others can be obtained via computational mean-field approximations. The approach can also be used to quantify *network* risk, i.e. the risk of single institutions coming from the structure of the network banks are immerse, including eventual uncertainty regarding the structure itself. This contribution has been developed by myself together with prof. Dr. Thomas Lux. The two authors contributed equally to this work.

In Chapter 4, we develop an agent-based multi-layered interbank network model based on a sample of large EU banks. The model allows for taking a more holistic approach to interbank contagion than is standard in the literature. A key finding of the paper is that there are non-negligible non-linearities in the propagation of shocks to individual banks when taking into account that banks are related to each other in various market segments. In a nutshell, the contagion effects when considering the shock propagation simultaneously across multiple layers of interbank networks can be substantially larger than the sum of the contagion-induced losses when considering the network layers individually. This effect emerges from the ability of banks to transform different kinds of risks into each other. For example, a bank that suffers losses from its mark-to-market portfolio can, as a consequence, withdraw liquidity from the interbank money market. The borrower of the first bank will therefore suffer a liquidity shock:

the materialization of market risk for the first bank has been transformed into liquidity risk for another bank. In addition, a bank's "systemic importance" measure based on the multi-layered network model is developed and is shown to outperform standard network centrality indicators. This contribution has been developed by myself, together with Christoffer Kok, during my internship at the European Central Bank. The two authors contributed equally to this work.

The topic of Chapter 5 is slightly different, detached from networks and focusing more on another structural change of financial markets which took place starting from the 70s: the massive use of derivative products. Current regulation foreseen by the Basel international regulatory framework relies on risk weights to compute the regulatory capital that banks have to hold against their portfolio of assets. The regulation also imposes a cap on leverage as a backstop to enhance the resilience of individual banks and of the whole financial system. Against this background, this paper assesses whether commonly used measures of leverage (e.g. assets over equity) adequately capture the "effective" leverage that a financial institution takes on, in particular when it uses derivatives. By using a standard equivalent portfolio technique to unbundle derivatives into their underlying securities, this paper shows that banks' net positions in derivatives contribute to increasing their leverage beyond the level which is captured by the ratio currently proposed by regulators. Furthermore, the study investigates whether because of the effective leverage embedded in a derivative contract banks can engage in capital arbitrage. Depending on the composition of a bank's balance sheet and on whether the average risk weights of a bank are above or below a given threshold, capital arbitrage opportunities can materialise. By employing aggregate statistics provided by the Bank for International Settlements (BIS) the study provides a rough approximation of the effective leverage embedded in outstanding OTC net derivative positions for banks in 13 jurisdictions. From 2005 until 2007, in the run-up to the financial crisis, effective leverage more than doubled. At the end of 2007 it started to decline and it reached its minimum value after the demise of Lehman Brothers in September 2008. Recently, effective leverage has peaked up again. A breakdown by type of instruments shows that before the eruption of the financial crisis, CDS and forward contracts played the most prominent role in terms of effective leverage.

By correcting the standard measure of leverage using the exposures implied by derivative contracts, the paper also estimates the discrepancy between such a measure and the banking system's effective leverage. There is tentative evidence that effective leverage is above regulatory limits in certain jurisdictions. A bank-level analysis would be necessary in order to give more precise indications about which institutions are more highly leveraged than they appear and which ones elude the leverage requirement. This analysis provides a simple approximation of how to calculate effective leverage, which leads to two policy messages. When assessing risk at the individual institution and system level effective leverage should be preferred to the standard measure proposed in current regulation. Furthermore, by adopting the effective leverage, regulation would rule out capital arbitrage opportunities. This contribution has been developed by myself.

2

Financial Contagion in a Simulated Banking System

2.1 Introduction

In the last decades more and more efforts have been directed to the study of interbank financial data using tools initially developed in the natural sciences, with the aim to shed light on the contagions effects of shocks through interbank linkages. In particular, a better understanding of the link between the topology of a financial system, where an intricate network of financial entities (like banks and hedge funds) are connected together through a complex web of financial instruments, and the stability of the system itself, namely the ability of networks to absorb shocks and adapt the structure in order to maintain efficiency, became a major issue (Battiston et al. (7)). The relevance of the network structure for regulatory reform of the banking sector has been emphasized by Johnson and Lux (50), among others[1].

The risk of a global systemic failure of the whole system is strongly connected to the topological features of the financial network, and it gives rise to the crucial concept of systemic risk. Since the pioneering work of Allen and Gale (4) in which the relevance of the structure of a financial system for its stability has been highlighted, the study of systemic risk using network approaches has attracted the attention of economists and scientists in general. Nier et al. (60) have studied a simple but versatile random network structure, where the nodes of the networks represent banks and the edges

[1] See also `http://www.imf.org/external/pubs/ft/survey/so/2014/RES052314A.htm`.

represent interbank liabilities, combined with a representation of the balance sheets of banks. They show how the resilience of the whole system to idiosyncratic shocks is affected by the topological features of the system, such as the connectivity of the nodes. May and Arinaminpathy (56) provide an analytical explanation of these results using a mean-field approach, providing more insights into the connections between complexity and stability.

The main aim of this paper is to expand this line of research into the determinants of systemic risk in simulated banking systems. By systemic risk we mean the risk of a whole financial system, in this case a set of banks, to collapse as an aftereffect to the initial default of a single unit or a small cluster. After the default of the first bank, the shock is transmitted through the whole system due to a web of debt relationships. This domino effect may cause the whole system to fail. As in the case considered by Nier et al. (60) and May and Arinaminpathy (56), our networks are static since the single nodes, namely the banks, are not allowed to change their behavior during the spread of the shock, they just passively absorb the propagation of the losses. We are, therefore, considering a situation in which the spread of the shock through the system is faster than the potential changes of the topological features of the interbank network that would be manifested after the reaction of the banks themselves.

In network theory, if high-degree vertices attach to low-degree ones, the resulting graph is said to display a *disassortative mixing* or *disassortative behavior*. A simple way to identify such a structure consists in studying the distribution of the average degree of the neighbours of the vertices belonging to the network. In the case of disassortative mixing, this distribution should be a decreasing function in the degree of the nodes, as a consequence of the attitude of high-degree vertices to link with low-degree ones, and *vice versa*. Disassortative mixing is a frequent feature of real networks, examples are the internet, the World Wide Web, protein interactions and neural networks (Caldarelli (24)). Interestingly, also most of the interbank money markets seem to be characterized by disassortative behavior, as documented by Boss et al. (19) for the Austrian interbank market, Soramäki et al. (65) for the US Fedwire Network, Iori (47) for the Italian interbank market, and Imakubo and Soejima (43) for the Japanese interbank money market. Therefore, it seems important to include the well-established stylized fact of disassortative mixing also in the study of artificial financial networks, since this particular structure could affect the ability of a system to absorb shocks. Another feature that is often present in real networks is a characteristic power law degree distribution, that produces the so-called *scale-free networks*. Scale-free networks are characterized by the presence of hubs, namely nodes with a degree that is much higher than the mean degree of the other nodes. Therefore, in a scale-free network, there is a high probability that many transactions would take place through one of the high-degree nodes of the network. The presence of such hubs make systems in general more prone to a break-down in case of targeted attacks, as the downside of their high connectivity in terms of the shortest paths between any two nodes belonging to the system. Again, in real interbank money markets scale-free degree distributions have been frequently reported. Examples are Inaoka et al. (45) and Imakubo and Soejima (43) for the Japanese interbank market, and Boss et al. (19) for the Austrian interbank market, while there exist divergent results for the Italian interbank market (De Masi et al. (28) and Finger et al. (33)).

Empirical evidence on the size distribution of bank's balance sheets can be found in, for example, Ennis (32) and Janicki and Prescott (49). For the U.S., the banking system is characterized by a large number of small banks and a few large banks, and the size distribution seems to be lognormal with a Pareto-distributed tail. A study on the evolution of the banking system in a European Country can be found in Benito (13), where the presence of few big hubs in the Spanish banking system is highlighted, and, again, the distribution is highly skewed, and it has become more skewed during the last decades.

We construct a Monte Carlo framework for an interbank market characterized by the above empirical features via what is called a *fitness algorithm* (De Masi et al. (28)). With a particular choice of such a function as a generating mechanism for our network, we can make sure that our artificial banking sector also displays a power law degree distribution, disassortative behavior and heterogeneity in the banks' sizes. In particular, in interbank markets characterized by a power law in the size distribution, the default of a single small or medium-sized bank will not affect the stability of the entire system: as one might expect, the losses are easily absorbed by the banks which have deposits on the liability side of the failing bank's balance sheets, and no domino effect occurs. The situation changes when the initially defaulting bank is one of the hubs of the system. In this case the propagation of the shock proceeds like the propagation of a circular wavefront in the water: starting from an initial node, the shock will hit at the same time nodes that are directly linked to the source. Moreover, each time a new node is hit by a wave, it also will become a source itself, expanding the range of nodes that will potentially be affected by the shock. Those are the kind of network effects we are interested in. Note that the results reported so far in the literature using network approaches in order to study domino effects in interbank markets have mostly used either random network models or networks constructed from aggregate data via a maximum entropy principle (cf. Upper (67), for an overview). Both approaches are very likely to underestimate the extent of a contagious spread of disturbance due to the very homogeneous level of activity and connectivity in such artificial networks. In contrast, the above stylized facts show strong heterogeneity for the levels of activity (size of the balance sheets, as well as the extent of connectivity, namely the degree distribution). In addition, the pronounced negative assortativity is also not covered by random networks or those constructed from entropy principles. Moreover, random networks are characterized by a binomial degree distribution (see, for example, Caldarelli (24)), and so no major hubs exist in such a system. Using power law degree distributions, the process of propagation of endogenous shocks could bring about different results, and should in principle give a more realistic picture of the underlying phenomena.

In the following, section 2 introduces the generating mechanism for realistic (along certain important dimensions) interbank markets, section 3 provides a summary of the main properties of the networks produced by our model, and section 4 introduces the mechanism for the propagation of the shocks and shows the result from the Monte Carlo simulations. Section 5 finally concludes.

2.2 Generating mechanism for a scale-free banking system

We consider an interbank market (IbM) composed of n financial entities linked together by their claims on each other. It seems natural to use network theory in order to represent and study such a system: each bank in the IbM will be represented as a node in the network, and the information of the loans among banks will be included in the edges of the network. These edges are directed and weighted, the weight of the link starting from node i and pointing to node j being the total amount of money that bank i lends to bank j. In order to proceed a modest step towards a more realistic representation on the interbank market, we will construct our toy financial system in a way to represent the documented empirical features highlighted in the introduction. Following Nier et al. (60), we use the scheme represented in Figure 2.1 in order to represent the balance sheets of the bank. The assets A_i of each bank ($i = 1, 2, \ldots, n$) are partitioned into interbank loans l_i and external assets e_i:

$$A_i = l_i + e_i \tag{2.1}$$

The liabilities I_i of each bank are partitioned into the internal borrowing b_i, customers' deposits d_i, and the net worth η_i:

$$I_i = b_i + d_i + \eta_i \tag{2.2}$$

Solvency requires that the difference between a bank's assets and its liabilities be positive, that is:

$$\eta_i \equiv (l_i + e_i) - (d_i + b_i) \geqslant 0 \tag{2.3}$$

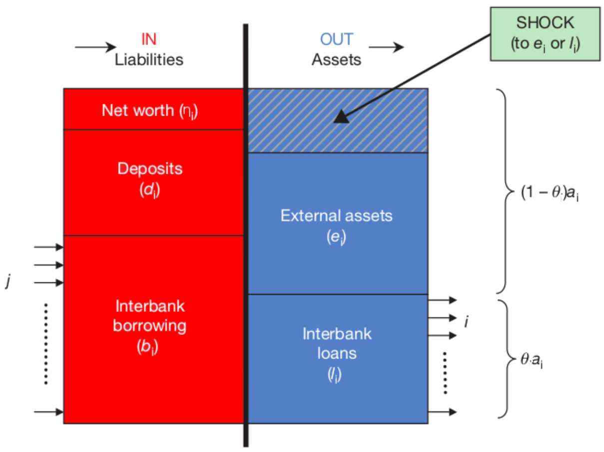

Figure 2.1: The balance sheets of each bank i belonging to the IbM.

If relationship 2.3 is not fulfilled, bank i becomes insolvent. Note that we could instead impose a minimal capital requirement and intercept the bank's operations if its capital falls below a threshold. For most purposes that would leave our results qualitatively unchanged as it would just lead to a linear rescaling of the balance sheet.

Following Nier et al. (60), we impose the following relations, that hold for all the banks belonging to the IbM:

$$e_i = \theta A_i \tag{2.4}$$

$$l_i = (1-\theta)\, A_i \tag{2.5}$$

$$\eta_i = \gamma A_i \tag{2.6}$$

This enables us to characterize the evolution of the balance sheet of the banks using the common pair of parameters θ and γ. Unlike Nier et al. (60) who investigate a banking sector with banks of equal size of balance sheets and interbank liabilities, we try to mimic some of the documented dimensions of heterogeneity in the banking sector.

The empirical properties of real interbank networks that we attempt to reproduce are the disassortative behavior and power law in the degree and size distributions. To this end, we arrange the nodes on a scale free network according to the following algorithm:

1. we start with an assumption on the distribution of the size of the banks. Using A_i as parameter indicating the size of a bank, we assume that $\rho(A_i) \propto A_i^{-\tau}$ (and $A_i \in [a, b]$) so that the sizes distribution will follow a power law, and in the following we will use $\tau = 2$. We note that since this formalism defines the size distribution over a finite range, the numbers a and b defining the absolute range of bank sizes will also be of some relevance.

2. once we have drawn the n-element set $\{A_i\}$ i.e. the distribution of the total external assets of the banks, we compute the external assets e_i, the interbank loans l_i and the net worth η_i, according to equations 2.4 - 2.6.

3. we use now the size parameter A_i as the *peculiarity* of the node. This basically means that we add interbank liabilities to the system in relation to the sizes of each pair of potential trading partners. In order to build up networks in this way, we use a *probability function* $P(A_i, A_j)$: this function provides the probability that a bank i (characterized by total external assets A_i) lends money to bank j (characterized by total external assets A_j). In most real IbMs, a pool of small and medium-sized banks usually lend money to the biggest banks of the system, which in turn redistribute liquidity to external financial markets or within the IbM itself (Iori (47), Cocco et al. (27), Lux and Fricke (55)). The choice of an appropriate probability function allows to reproduce those important empirical observations.

In the following, we will use the three following alternative probability functions for the generation of links:

$$P_1(A_i, A_j) = \left(\frac{A_i}{A_{max}}\right)^{\alpha} \cdot \left(\frac{A_j}{A_{max}}\right)^{\beta} \tag{2.7}$$

$$P_2(A_i, A_j) = c \cdot (A_i + A_j) \tag{2.8}$$

$$P_3(A_i, A_j) = \theta(A_i + A_j - z) \tag{2.9}$$

where A_{max} denotes the size of the balance sheet of the biggest bank in the system, α, β and z are constants, and θ is the classic Heaviside step function. Section 2.3 will present the main topological properties of networks produced by functions (2.7), (2.8) and (2.9). With any of these probability functions, we can build the $n \times n$ probability matrix $P \in M_{n\times n}$, with entries $p_{ij} = P_s(A_i, A_j) \in [0, 1]$, and $s = 1, 2, 3$ [1];

4. the next step consists in constructing the adjacency matrix A of the network, according to the rule:

$$a_{ij} = \begin{cases} 1, & \text{with probability } p_{ij} \\ 0, & \text{with probability } (1 - p_{ij}) \end{cases}$$

   In contrast to a standard random network with constant connectivity, the probabilities p_{ij} are drawn from one of the probability functions of eqs. (2.7) to (2.9). In this way we reproduce the systematic tendency of accumulation of links at larger entities and the disassortative nature of empirical banking networks[2];

5. we also assume that banks loan money to other banks according to their peculiarity; since loans are supposed to produce returns, it seems natural to assume that financial entities will have more intense links with banks with high peculiarity

[1] We note here that random networks are a particular case of our generating algorithm; in fact, each function with the form $P(A_i, A_j) = p$ will generate random networks characterized by a density p.

[2] It is possible, especially for symmetric probability functions, to have situations where $a_{ij} = a_{ji} = 1$. Since loops are not allowed in our model (they would mean that bank i and j are both borrower and lender of each others), we have to use a criterion for the elimination of one of the edges. A possible choice is to randomly eliminate one of the two links $i \to j$ or $j \to i$; however, other choices are possible as well, if the aim is to enforce the disassortative behavior of the networks (see section 2.3).

(balance sheet size). Including this notion in the probability functions we can compute the load l_{ij} (the volume of credit) on the link between bank i and bank j as:

$$l_{ij} = \frac{l_i p_{ij}}{\sum_{j \in \Omega_i} p_{ij}} \tag{2.10}$$

where Ω_i denotes the set of nodes for which $a_{ij} = 1$;

6. in the last step, we compute the internal borrowing b_i as:

$$b_i = \sum_j l_{ji} \tag{2.11}$$

and the customers' deposits d_i as:

$$d_i = (e_i + l_i) - (\eta_i + b_i) \tag{2.12}$$

Deposits are, thus, the residual in the construction of the balance sheets of banks that is adjusted in a way to guarantee consistency. While this leads to a certain degree of heterogeneity of the size of deposits across banks, this is not necessarily an unrealistic feature of our system.

Let us also emphasize that in the algorithm there are two levels of randomness: the first appears in step 1, in the determination of the sizes of the nodes, while the second appears in step 4, in the realization of the probability matrix. Thus, for a fixed sequence of the sizes $\{A_i\}$, several different realizations of the network are possible.

2.3 Topological properties and the probability function

The representation of the financial system in our model depends on the choice of the probability function. In the following, we will show in detail how the topological structure of the network is determined by functions (2.7), (2.8) and (2.9). One of the main features of these kind of networks is the presence of power laws in the degree distributions of both *in-* and *out-degree*. In particular, it is easy to see that the relations between the probability function and the degree distributions are [1]:

$$P(k_{in}) = \rho\left[F_{in}^{-1}\left(\frac{k_{in}}{n}\right)\right] \cdot \frac{d}{dk_{in}} F_{in}^{-1}\left(\frac{k_{in}}{n}\right) \tag{2.13}$$

$$P(k_{out}) = \rho\left[F_{out}^{-1}\left(\frac{k_{out}}{n}\right)\right] \cdot \frac{d}{dk_{out}} F_{out}^{-1}\left(\frac{k_{out}}{n}\right) \tag{2.14}$$

where n is the number of nodes in the network,

$$n \cdot F_{in}(A_i) = k_{in}(A_i) = n \cdot \int_a^b P_s(t, A_i)\rho(t)dt \tag{2.15}$$

is the mean $in - degree$ depending on the fitness parameter A_i and

$$n \cdot F_{out}(A_i) = k_{out}(A_i) = n \cdot \int_a^b P_s(A_i, t)\rho(t)dt \tag{2.16}$$

is the mean $out - degree$. In the above equations, a and b denote respectively the lower and the upper limits for the support of the distribution of bank sizes: $A_i \in [a, b]$. With probability functions 2.7, 2.8 and 2.9, we obtain respectively:

$$P_1(k_{in}) \propto k_{in}^{-\frac{1+\beta}{\beta}} \ , P_1(k_{out}) \propto k_{out}^{-\frac{1+\alpha}{\alpha}} \tag{2.17}$$

$$P_2(k_{in}) \propto (c_1 k_{in} + c_2)^{-2} \ , P_2(k_{out}) \propto (c_3 k_{out} + c_4)^{-2} \tag{2.18}$$

$$P_3(k_{in}) \propto k_{in}^{-2} \ , P_3(k_{out}) \propto k_{out}^{-2} \tag{2.19}$$

In the same way, it is possible to see that the average degree of a neighbour is determined by:

$$\langle k_{nn} \rangle (A_i) = \frac{N}{k(A_i)} \cdot \int_a^b p(A_i, t)k(t)\rho(t)dt \tag{2.20}$$

where $k(A_i)$ is the mean *total degree* of node i, as a function of its own fitness parameter.

[1] The derivation of the following equations, well known in literature (see for example Caldarelli (24)), is also reported in the Appendix.

As we can see, with all three kinds of probability functions, the results are scale-free networks (i.e., a power-law distribution of degrees). Since eq. (2.20) involves the mean total-degree of a node, $k(A_i)$, there is no closed-form solution for this expression for the three probability functions. The disassortative behavior can, however, be confirmed via numerical integration of eq. (2.20), cf Fig. 2.2. It is apparent from eq. (2.17) to (2.19), that it will be possible to change the exact shape of the degree distributions as well as the degree of disassortative behavior by modifying the parameters of the probability functions, and the distribution of the fitness parameters. Figure 2.2 shows the degree distributions and the average neighbour degree for functions (2.7), (2.8) and (2.9), for parameters $\alpha = 0.25$, $\beta = 1$ and $z = 0.6 \cdot A_{max}$. With this choice of the parameters we get tail indices in the in-degree distribution equal to, respectively, -2, -2 and -2, and -5, -2 and -2 for the out-degree distributions. Moreover, a clear disassortative behavior is observed in all the three cases[1].

2.4 Simulation results

In this section we present results from our simulation engine. The design of the simulations will be the same for all the following experiments: the first step consists in generating a Monte Carlo realization of our banking system as explained in sec. 2.2. In the second step we destroy the largest bank: this shock is assumed to wipe out all the external assets from the balance sheet of the initially failing bank. For each simulation run, we count the overall number of defaults, as well as the number of defaults in each single phase of the shock propagation. We report the average number of defaults across all banks. In the following the number of banks will be fixed at 250, and we will use probability functions (2.7), (2.8) and (2.9) with parameters $\alpha = 0.25$, $\beta = 1$ and $z = 0.6 \cdot A_{max}$; furthermore the two limits a and b will be fixed at 5 and 100 respectively. We will investigate later how those limits affect the resilience of the system. Of course, other choices are possible both for the parameters and for the probability functions.

[1] In order to reinforce the disassortative behavior, one could use a criterion for the elimination of the loops different from the one described in footnote 2. In particular, if both the edges $i \to j$ and $j \to i$ are present in the network, one could eliminate the one starting from the biggest node of the two: this mechanism would contribute to mimicking real interbank network structures, where mostly small banks lend money to big banks, as described in the introduction.

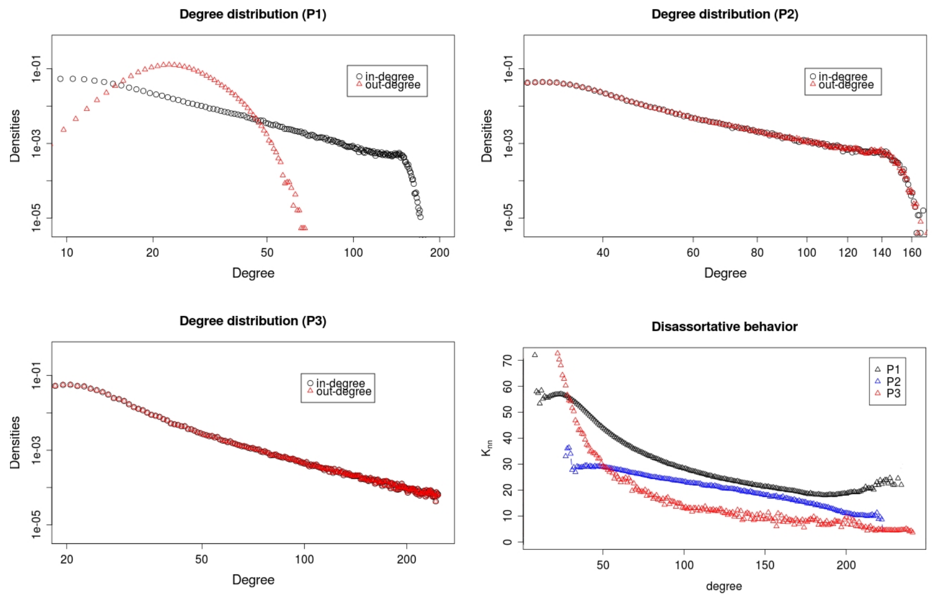

Figure 2.2: The first three panels show the *in-* and *out-degree* distributions for the three probability functions (2.7), (2.8) and (2.9). The last panel shows the mean neighbour degree as a function of the *total degree* of the nodes. The curves in the last panel are decreasing with the degree itself, indicating that big nodes are connected to a multitude of small and medium-sized nodes, which themselves are connected with only a (relatively) small number of hubs.

In the following, we will initially use as our exemplary case probability function (2.7): for systems produced by equation (2.7) we will vary only one parameter at a time, and we will study how this changes the domino effects. At the end of the section we will show for all the functions (2.7), (2.8) and (2.9) the results obtained by varying simultaneously the percentage of net worth η and the percentage of interbank borrowing θ. Moreover, in section 2.4.4 we present a comparison between the result obtained with scale free networks and the results obtained with random networks and networks generated via a maximum entropy principle. Section 4.5 shows how the absolute size of the largest hub affects the contagion process.

2.4.1 Transmission of shock

Here we study the consequences of an idiosyncratic shock hitting one of the banks in the system, and elaborate on how the aftereffects (usually the number of defaults) depend on the structural parameters of the system. There are several ways in which a shock can propagate through a financial system. First, propagation will occur through the direct bilateral exposure between banks (namely, financial entities holding in their balance sheets liabilities of other entities and incurring, for endogenous reasons, solvency problems, will transmit their losses to their creditors), correlated exposure of banks to a common source of risk (banks holding correlated portfolios can increase the probability of multiple and simultaneous failures), effects arising from endogenous fire-sales of assets by entities in distress, and informational contagion. We will focus here on the first of those mechanisms, noting that idiosyncratic shocks are a clear starting point for studying knock-on defaults due to interbank exposure.

In our subsequent analysis, the shock starts form one bank, and it consists in wiping out a certain percentage of its external assets (the *source* of the shock). Let p_i be that percentage, and let s_i be the size of the initial shock:

$$s_i = p_i \cdot e_i \tag{2.21}$$

This loss is first absorbed by the bank's net worth η_i, then its interbank liabilities b_i and last its deposits d_i, as the ultimate *sink*. That is, we assume priority of (insured) customer deposits over bank deposits which, in turn, take priority over equity (net worth). If the bank's net worth is not big enough to absorb the initial shock, the bank defaults and the residual is transmitted to creditor banks through interbank liabilities. And in case these liabilities are not large enough to absorb the shock, some of the losses have to be absorbed by depositors. Formally, if $s_i > \gamma_i$, then bank i defaults. If the residual loss $(s_i - \gamma_i)$ is less than the interbank borrowing b_i of the failed bank, then all residual loss is transmitted to creditor banks. Otherwise, if $(s_i - \gamma_i) > b_i$, then all of the residual cannot be transmitted to creditor banks and depositors receive a loss of $(s_i - \gamma_i - b_i)$. Creditor banks receive an amount of the residual shock proportional to their exposure to the failed bank. In turn, this loss is first absorbed by their net worth. If their net worth is not big enough to completely absorb the shock, it will be transmitted first to their creditors bank, and possibly also to their depositors. The part that is transmitted through the interbank channels may cause further rounds of contagious defaults, and in this way the shock spreads through the network. The transmission continues spreading through the system until the shock is completely absorbed or, alternatively, the system has completely failed. In the following, we will consider always the worst situation, namely that all the external assets of one bank are wiped out: $p_i = 1$. For our analysis of the mechanical short-run effects of a shock this is not an unrealistic assumption. Partial recovery of claims to defaulted entities requires certain legal proceedings that can be extremely time consuming. Over short horizons, the *de facto* situation is that no payment can be enforced on a defaulted claim.

2.4.2 Bank capitalization

In this first experiment we investigate the effects of banks' net worth on the resilience of the entire banking system; the parameter θ will be fixed at 0.8, so that each bank will invest 20% of its total assets in the interbank market, and the remaining 80% in some external markets. We will let the parameter η vary from 0 to 0.1 [1]. Figure 2.3 shows the result: we report both the total number of defaults (black bold line), and the number of defaults in the first four phases of the propagation of the shock. The thin vertical bars represent the standard deviation of the black line across our 200 replications of the simulations.

As one could expect, when the percentage of net worth tends to zero, the total number of defaults increases to 250: in particular, a threshold value ($\eta = 0.0143$ in the picture) exists below which the system fails completely, and below $\eta = 0.008$ it breaks down within only two rounds. This is a demonstration on the so called *small-world* effect: the diameter of this kind of networks is roughly about two when measured from the largest bank belonging to the system, and so in only two rounds the shock will have reached almost any bank of the IbM. At the other end, when the percentage of net worth is beyond an upper threshold value, no defaults are reported and no domino effects set in.

Interestingly, the shape of the line describing the total number of defaults is far from linear. Starting from the value $\eta = 0.1$, we can observe that below the value $\eta \cong 0.05$ the first defaults appear, and inspection shows that these are typically small banks connected to the initially failing bank. As η decreases further, we observe a sharp increase in the number of defaults, and this growth stops at the value $\eta \cong 0.02$ where the curve enters a *plateau*: at this point, all the banks belonging to the first *shell* around the initially failing bank have failed, and the banks which are not directly connected to the first failing unit have enough net worth to survive the shock. As the

[1] Remember that by mere rescaling η could also be interpreted as the excess over the required minimal capital requirement.

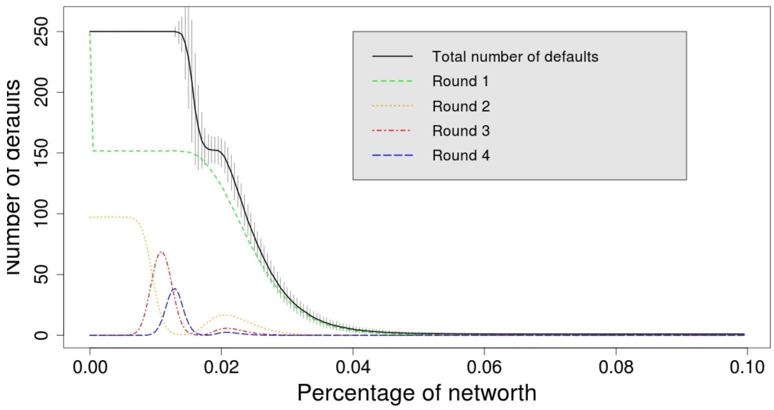

Figure 2.3: Number of defaults as a function of the percentage of net worth η, for probability function (2.7). The other parameters are fixed at: $\theta = 0.8$, $a = 5$, $b = 100$. The picture shows both the total number of defaults (bold black line) together with the standard deviation of the mean value (thin gray line), and the number of defaults occurring during the first four phases of the propagation of the shock.

net worth decreases further, also the banks outside the first shell are no more able to absorb the perturbation, and the total number of defaults sharply moves up to 250.

It is interesting to have a look at the number of defaults in the different rounds. In the first round (dotted line in Figure 2.3), banks that fail are directly connected to the initially shocked bank, and when the dotted line reaches its *saturation* at $\eta \cong 0.018$ the complete first *shell* (composed on average of 153 units) has failed. We note that the saturation point of the number of defaults in the first round does not coincide exactly with the *plateau* of the total number of defaults: the explanation is that the largest banks in the first shell need more than one hit to fail, and so they populate the failures of higher rounds. The reason for this is that for larger banks the overall number of credit relationships to other banks is larger too (by assumption, following observed empirical regularities), and so for them the failure of the largest bank will lead to a proportionally smaller loss than for the smaller client banks of the defaulted entity. When the percentage of net worth decreases, these defaults occur already in earlier rounds, up to a point in which all banks of the first shell are affected in the first round of defaults.

It is worthwhile to highlight here the ability of the system to confine the shock in the first shell if the value of η is higher than some benchmark (approximately 0.018 in our example). Even if contagion defaults occur after the first failure these are limited to banks inside the first shell, i.e. to those banks with direct exposure towards the source of the disruption.

2.4.3 Interbank exposure

In this section we are going to explore how the number of defaults is affected by the percentage of interbank exposure as a function of total assets, namely how the parameter θ affects the resilience of the system. An increase in interbank assets produces, as an immediate result, an increase in the weight of each edge, and so an increase of the channels through which the shock can propagate. This effect can potentially increase the number of defaults in the system, as the amount of losses transmitted to creditor banks will increase as well. On the other hand, an increase in interbank exposure implies a reduced relative exposure to external markets, and since here we are considering, as initial source of the shock, the external assets, this second effects could cushion banks against systemic risk.

The design of the simulations will remain the same as in the first experiment: we generate a realization of the system and we shock the biggest bank, wiping out all its external assets. Subsequently we count the number of defaults. We will show the mean value of those numbers for each round, and the standard deviation for the total number of defaults. In this section, the percentage of net worth η is fixed at 0.025, while the percentage of external assets on total assets, θ, varies from 0.5 to 1 (when θ is equal to one no interbank assets are present in the bank balance sheets). Fig. 2.4 shows the result.

First, we note that when θ tends to 1 the number of defaults tends to zero: in this case the banks' balance sheets contain only external assets, and so the channels for the propagation of the shock become smaller and smaller, until θ assumes the value 1 and there are no more links in the network, and no domino effects are possible. In Fig. 2.4 we can also note a threshold value at $\theta \cong 0.78$: at this value, the contagion effects reach their maximum while both more or less intense interbank linkages reduce the number of knock-on defaults (due to a higher degree of rik sharing on the left and fewer links for contagion on the right). At the other extreme, when θ tends to 0, the banks become completely isolated from any external market, and so in our model, where the initial source of the shock comes from the external assets of the largest bank of the system, the

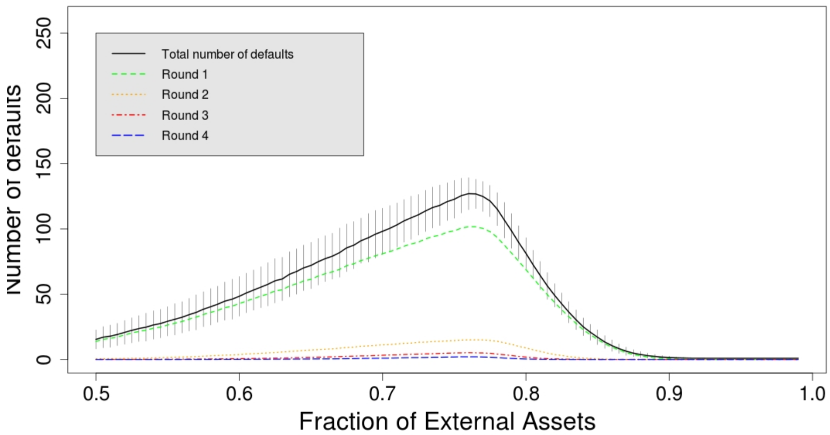

Figure 2.4: Number of defaults as a function of the percentage of external assets θ, i.e. $1-$ the percentage of interbank exposure θ, for probability function (2.7). The other parameters are fixed at: $\eta = 0.025$, $a = 5$, $b = 100$. The picture shows both the total number of defaults (bold black line) together with the standard deviation of the mean value (tiny grey line), and the number of defaults occurring during the first four phases of the propagation of the shock.

number of defaults tends to zero as well. Note that this exercise does not leave the size of the internal shock unaffected. Clearly, when external assets decline in their absolute size (from right to left) there should be a decrease of contagious defaults. Nevertheless, despite this lack of normalization of the shock, the behavior of the system is distinctly non-monotonic.

2.4.4 Results with other network generators

So far we have always used eq. (2.7) as the probability function generating the networks. Although eq. (2.7) correctly reproduces the disassortative behavior and power law degree distributions, it is interesting to see in how far other functional forms generating systems with the same qualitative features reproduce the above results or not. We are going to present, therefore, also the results obtained for the other two functions, namely equations (2.8) and (2.9). In this section we display results in the bidimensional space (η, θ), and for each pair of these two parameters we use colors to indicate the number of defaults. Figure 2.5 shows the results for the three probability functions discussed in section 2.3.

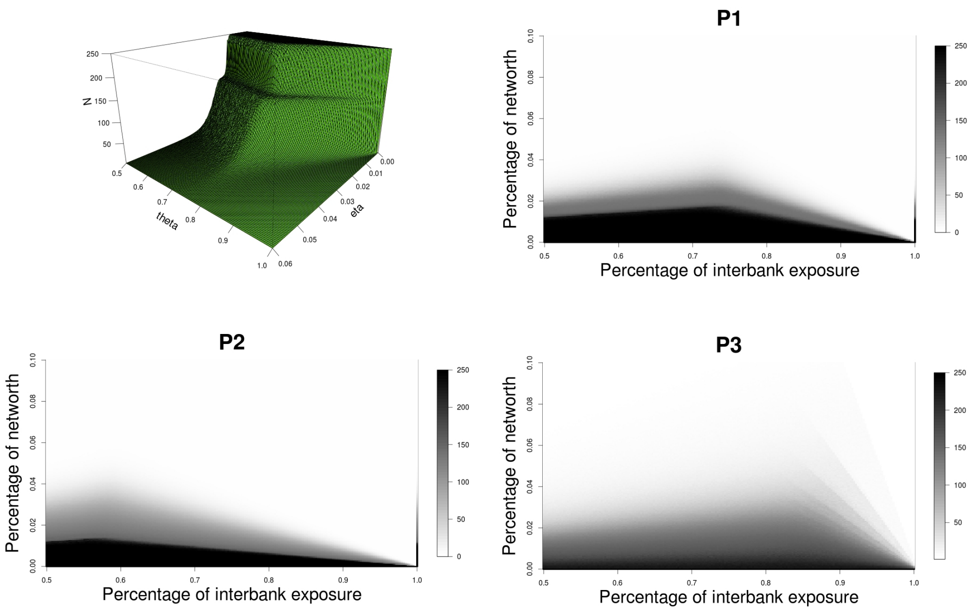

Figure 2.5: In the top left, a a $3D$ plot shows the total number of defaults as a function of the two parameters η and θ for probability function P_1: in the figure one again detects the *plateau* that already appeared in Fig. 2.3. The other three colored maps represent the same information for the three probability functions P_1, P_2 and P_3. In all these maps one observes a non-monotonic behavior of defaults in the percentage of interbank exposure. The color code indicates the number of banks in default.

As one can see from the Figure, the behavior of the systems in the presence of a perturbation is qualitatively the same in all the three cases. In particular, it is again possible to observe a threshold value for the percentage of interbank exposure θ, beyond which the trend in the total number of defaults reverts itself. Different versions of our generating mechanisms for interbank connections do, however, affect the location of the level of interbank exposure leading to the largest level of fragility of the system as well as the quantitative importance of defaults in higher rounds.

As we had already highlighted in the introduction of this paper, most empirical and simulation-based approaches of interbank markets use as topology for the underlying bank network a random network or a maximum entropy principle. Random networks are characterized by a constant probability p for each edge to exist in the network. The maximum entropy principle, on the other hand, assumes a maximum of dispersion of interbank loans (see Upper and Worms (68) for more details on this kind of networks). We want to compare here the differences in term of contagion effects when the same set of banks is connected through different underlying network structures.

In the following, we will compare the number of defaults in scale free networks, random networks and networks generated via maximum entropy principles, for varying capitalization of the system. For the scale free network case, we use as benchmark case the system generated through function (2.7): again, the limits (a, b) are set to $(5, 100)$ and the parameter θ is fixed to 0.8.

For the random network case, we will simply use the probability function:

$$P(A_i, A_j) = \begin{cases} p, & \text{if } i \neq j \\ 0, & \text{if } i = j \end{cases} \tag{2.22}$$

with p equal to 0.1, 0.2 and 0.3[1] We note here that with the value $p = 0.1$, the (mean) number of edges in the system generated with function (2.22) is equal to the (mean) number of edges in system generated with function (2.7):this is equivalent to random reshuffling the links (and their weights) among all the banks.

We cannot define a probability function that generates networks according to the maximum entropy principle. For a consistent comparison with the scale free scenario, we proceed in the following way: first we generate a weight matrix W using the fitness algorithm described in section 2.2 (with probability function given by eq. (2.7)), then we compute the sum of the rows and the sum of the columns of that matrix: they are, respectively, the total amount of interbank borrowing and the total amount of interbank lending for each bank. The problem is then to determine a new weight matrix W^* such that (i) the sum of the rows and the columns are the same as for W, and (ii) the dispersion of the new bilateral exposures w^*_{ij} is maximized. This problem can be easily solved numerically using the RAS algorithm (see Censor and Zenios (26) for technical details). The result is a banking system populated by banks having exactly the same balance sheets as in the scale free network case, but now connected in a way that maximizes the entropy of the new weighted matrix W^*.

Figure 2.6 shows the results. As in the previous simulations, we again shock the largest bank in the system by wiping out all its external assets. The figure shows the total number of defaults after the propagation of the shock terminates (for better visibility, we do not report in this graph the standard deviations). We note immediately from the figure that the scale free scenario is the most critical in terms of number of

[1]This will simply generate random networks with different densities.

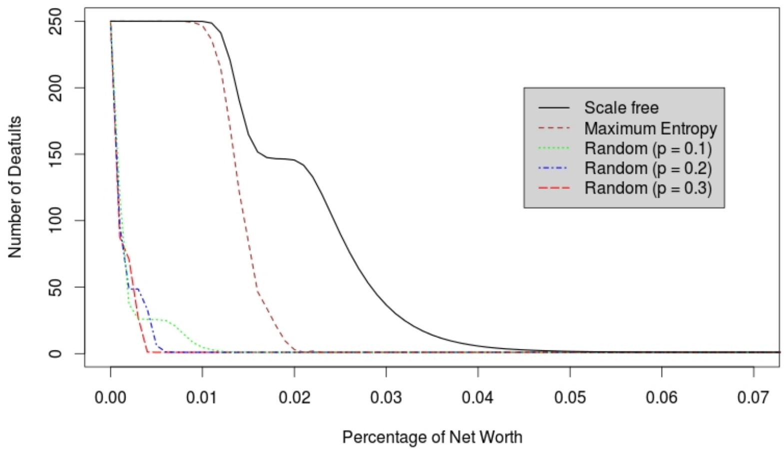

Figure 2.6: Number of defaults as a function of the percentage of net worth for different kinds of network topologies: scale-free networks, networks designed according to the maximum entropy scenario and three random network scenarios with different probability for the existence of links (the random networks generated with $p = 0.1$ have the same (mean) density as in the scale free case).

defaults. The random network scenario (no matter what the probability p is) always underestimates the effect of a targeted attack: the large pool of small and medium-sized banks now has a larger number of outcoming links randomly directed to all the other banks in the system, and, for each bank, the weight on those links is the same (in contrast to the scale free scenario, where the larger the peculiarity of the node, the larger the weight on the links pointing to it). This effect dramatically reduces the threshold value for the percentage of net worth necessary for triggering chains of defaults.

We note moreover that also the maximum entropy scenario underestimates the effects of a targeted attack, albeit to a smaller extent in comparison to the random networks. We see that the classical *plateau* that we have seen in all the other cases now disappears: the reason is that the systems built via the maximum entropy principle are fully connected[1], and so the distinction between different shells is not applicable here, i.e. all banks belong to the first shell.

[1] Note that the result is not equivalent to use a random network with probability $p = 1$, since the weights on the links are significantly different, affecting so the way a shock can propagate in the system.

2.4.5 The size of the hubs

In this section, we analyze the behavior of the networks when changing the size of the largest bank in the system. Using our simulation engine, this can be achieved simply by expanding the interval from which we draw the fitness parameters of nodes. In particular, we leave the lower boundary a of that interval constant (in our experiments it will be (and it was) fixed to 5), and increase the upper limit b. Since the fitness parameters are drawn from a power law distribution most of the sampled values will be located in a short subset at the left end of the interval. As an example, we can imagine to sample the fitness parameters from a power law on the interval $[5, 1000]$. If the exponent is 2 it is easy to see that more than 95% of the draws will lie in the interval $[5, 100]$, and that 99.5% of the values will lie in the interval $[5, 500]$. So the result of increasing the upper limit of the interval $[a, b]$ is the introduction of a very small number of very big banks. The presence of those banks has some intuitively plausible effects on the resistance of the system to shocks. Consider, for example, the probability function of eq. (2.7), with $\alpha = 0.25$ and $\beta = 1$. When A_{max} increases, the probability of a link involving two small banks or two medium-sized banks decreases: hence, more edges will point to the few hubs of the networks. Furthermore, since the edges in our model are weighted by the same probability function (see eq. 2.10), most of the interbank loans will be loaded on the edges pointing to these hubs.

After these preliminary considerations, we now investigate the behavior of the network when bigger hubs are introduced in the interbank system. We will show results for two particular values for the percentage of (excess) net worth η, namely $\eta = 0.1$ and $\eta = 0.01$. These choices permit us to study the system in two limiting cases: in the first case, as demonstrated in the previous sections, the system is relatively well cushioned against systemic risk, while in the second case the system is very *weak*. The parameter θ will be fixed at the value 0.8. Furthermore, for each realization of the system, we will again shock the largest bank by wiping out all its external assets from its balance sheet.

Fig 2.7 shows the results for the case $\eta = 0.1$. As a first observation, we note that as the value of the upper limit b exceeds the threshold value $b \cong 230$, first round effects start. We should emphasize that, in the previous experiments, at $(\eta, \theta) = (0.1, 0.8)$ no defaults were reported in our system. Figure 2.7 shows that occurrence or not of

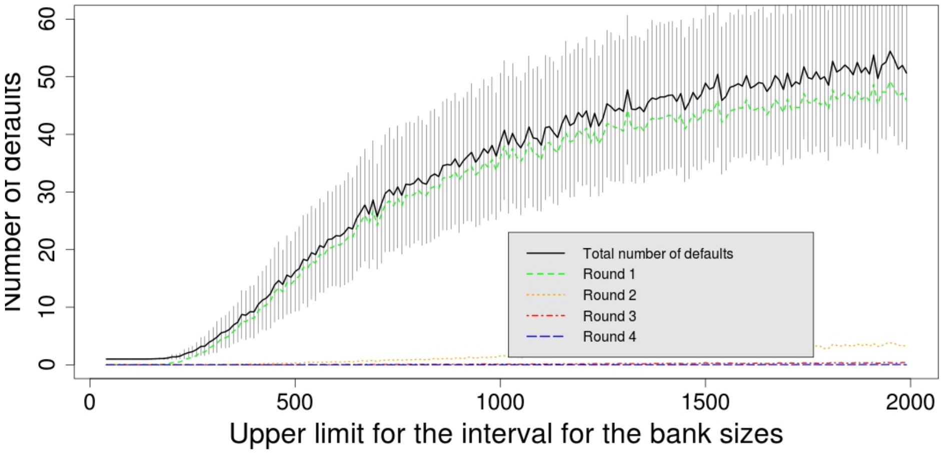

Figure 2.7: Number of defaults as function of the upper limit of the interval for banks' sizes used in the Monte Carlo simulations. The black bold line denotes the total number of defaults, together with its standard deviation (light gray bars); colored lines represent the next rounds. ($\eta = 0.1$, $\theta = 0.8$).

contagious defaults also depends on the parameter b. In particular, we can see that the number of defaults in the first round sharply increases in the range $[230, 700]$. That happens because most of the banks are now linked to the hubs and moreover these links become increasingly more loaded (higher in volume) as the parameter b increases. As a consequence, when the largest bank defaults, the first shell is no longer able to absorb the resulting losses.

Figure 2.8 shows the result in the case $\eta = 0.01$, $\theta = 0.8$. For this pair of parameters we know that the systems is extremely vulnerable against systemic risk, and in particular in a few rounds the whole IbM usually had failed after a shock. As one can see from Figure 2.8, these results change as well if larger hubs are present in the system: as the size of the biggest bank becomes larger, the pool of small and medium-sized banks effectively stops dealing among themselves, and so the channels through which a shock can propagate beyond the (relatively large) pool of trading partners of the largest hub do vanish. We can see moreover that as the upper limit b increases, the second round (yellow line in Figure 2.8) assumes basically the same importance as the first round. At this point in the system there are few big hubs (strongly) interconnected, and when the biggest of them fails (producing the default of all banks in its first shell) the other

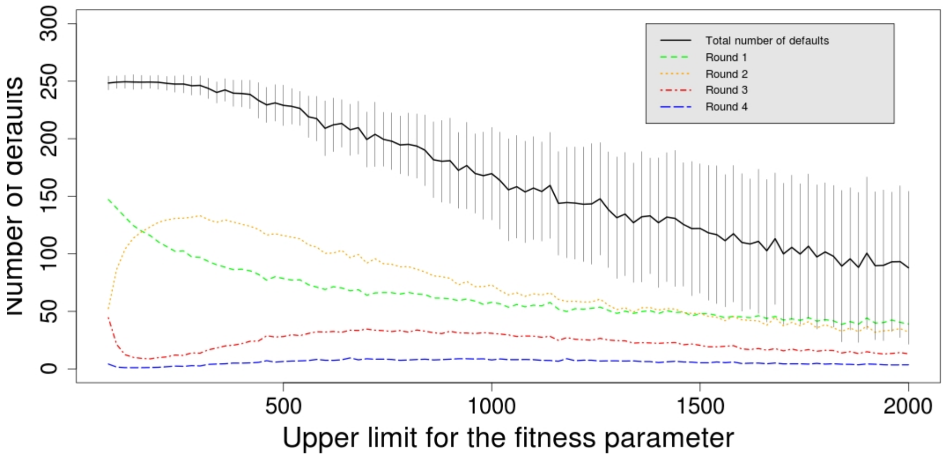

Figure 2.8: Number of defaults as function of the upper limit of the interval for banks' sizes used in the Monte Carlo simulations. The black bold line denotes the total number of defaults, together with its standard deviation (light gray bars); colored lines represent subsequent rounds. ($\eta = 0.01$, $\theta = 0.8$).

hubs will be failing in due course. When these secondary hubs fail, their first shells will fail as well, and the result is a high number of defaults in the second round. As the upper limit b increases further, networks will become very sparse, and the number of defaults decreases due to lower overall connectivity of the system.

2.5 Conclusion

This paper has investigated the behavior of a scale-free interbank market, characterized by a disassortative structure, in case of targeted attacks. The networks have been constructed according to a *fitness* algorithm, where the size of each node is used as a kind of peculiarity index for the bank itself: the higher the index, the higher the probability that other banks will lend money to it. For appropriate choices of the probability function, the networks are described by a decreasing mean neighbour degree distribution, i.e. disassortative mixing. The results are networks composed of a large pool of small and medium-sized banks which invest money in interbank loans to the biggest banks, which in turn invest this liquidity into non-financial assets and also redistribute part of it in the interbank market.

In this framework, we have investigated how the percentage of net worth and the percentage of interbank assets (on total assets) affects the spread of an idiosyncratic shock. The results show a shell structure in the propagation of losses: banks belonging to the first shell (i.e. creditor banks of the defaulted entity) fail mostly before the others, and it is possible to distinguish between defaults of the different shells in the cascade of events. Moreover, in all three types of probability functions we investigated, a hump-shaped dependency of the number of defaults on θ was observed, indicating higher robustness of networks with very few and very many links. The intuitive explanation is that if banks invest more money in the interbank market than in other external markets, the risk for endogenous shocks decreases and, moreover, banks are more able to absorb potential losses.

As it turns out, the role of the hubs is ambiguous in these networks: when the size of the hubs increases, the pool of small and medium-sized banks tends to withdraw from dealing among themselves, and to start lending and borrowing mostly from and to the hubs. Given our probability functions, the hubs are also highly connected among themselves. The results of this change in the network structure on the resilience of the system is linked to two antagonistic phenomena: on one hand, the number of channels for the shock propagation decreases as the hub sizes increase. Due to the smaller number of connections in the pool of small and medium sized banks, on the other hand, the same pool of banks concentrates their bilateral links to a few very big banks, that assume a central position in the entire system. In our model, the results from an endogenous shock are ambiguous and depend on the state of the system in terms of its capital base: for a *strong* system ($\gamma = 0.1$) the total number of defaults increases if the biggest bank meets insolvency problems, for *weakly* capitalized system ($\gamma = 0.01$), the number of defaults decreases with the size of the largest unit.

We also found that random networks or networks constructed on the base of a maximum entropy principle lead to fewer contagious defaults than our scale-free networks, under otherwise identical conditions. It is important to note that this implies a potentially tremendous underestimation of contagion risk, if due to a lack of detailed knowledge, stress tests are conducted with the simple algorithms for random network creation or maximum entropy allocation of interbank credit.

3

Contagion Risk in the Interbank Market: A Probabilistic Approach to Cope with Incomplete Structural Information

3.1 Introduction

Systemic risk refers to the likelihood of a large portion of the financial system - potentially, the entire system - to jointly fail after an idiosyncratic shock, leading to a major disruption of capital allocation and risk transformation throughout the economic system. The consequences of systemic events on the real economy have been dramatically revealed during the last financial crisis, directing the attention of academics and politicians towards new methodologies to study complex financial systems and the sources for systemic risk.

The probability of a large portion of the financial system to fail is governed by several direct and indirect connections among the individual financial institutions (hereafter, banks). Examples of direct connections are credit lines, interbank lending and derivative contracts. Indirect connections consist of spillover effects that one distressed institution can induce on any other, examples being fire sales and liquidity spirals Brunnermeier (21). A link between two financial institutions always involves the transfer of a certain amount of risk between the banks' balance sheets. Because of the very nature of the financial system, the idiosyncratic risk of each institution is shared among its direct and indirect counterparties, which transfer some of the risk to their own counterparties, and so on. The result is a system in which the materialization of the risk in one bank can induce losses to spread among a large number of financial institutions, although they might not be directly connected with the bank in distress themselves.

In reality neither the banks themselves nor any other party might be able to exactly quantify the magnitude of risk that could be transmitted via the interbank network. This uncertainty could be completely removed if one had all the necessary information regarding interbank claims. However, this is often not possible, for various reasons. First, banks are not forced by law to report all of their connections to other banks[1]. Second, some components of the interbank network are evolving extremely fast, resulting in a practical impossibility to keep track of all prevailing interbank links[2]. Third, most of the transactions are still conducted in over-the-counter trades. In all such cases, a probabilistic representation reflecting this uncertainty could be very helpful to assess contagion risk.

The aim of this paper is to develop a probabilistic framework for the estimation of the probability of systemic events in a banking network of which only some key statistics and statistical regularities are known. Our work continues the recent line of research on the determinants and the modeling of systemic risk in stylized models of the topology of the interbank financial market. The pioneering work of Allen and Gale (4) has first demonstrated the relevance of the structure of interbank linkages for the stability of the financial system in analytically solvable models with a few banks only. Subsequently, more general network approaches have been developed. Nier et al. (60) have studied a random network structure for interbank liabilities. They demonstrate how the resilience of the whole system to idiosyncratic shocks is affected by the topological features of the system, such as the connectivity of the nodes. Alternative network structures have been studied by Iori (47), Bluhm et al. (18) and Georg (35), among others. May and Arinaminpathy (56) provide an analytical formulation of the results

[1] And also if it were the case, this information would be available to regulators, but not to the single institutions, for which the problem would therefore persist.

[2] Examples are the overnight interbank network and the derivative network.

of Nier et al. (60) using a mean-field approach, offering more general insights into the connections between complexity and stability. Another related analytical approach is Gai and Kapadia (34) who use a stochastic framework based on the generating function methodology to the analysis of network structures as presented, e.g., in Newman (58). Glasserman and Young (38) derive theoretical bounds for the magnitude of contagion under different assumptions on the network structure and the heterogeneity of banks. The basic contribution of our approach to this nascent analytical literature is that we will focus on capturing certain stylized facts of the interbank market that are not captured yet in previous approaches. Our work is most closely related to May and Arinaminpathy (56), but we relax two of the assumptions that are crucial in the derivation of their analytical solution, homogeneity in bank sizes and the Erdös-Rényi topology for the interbank network. We expand this line of research by providing a analytical and semi-analytical solutions for more general cases, where both the interbank network topology and the bank size distribution can take any form.

In order to apply our framework, we develop an algorithm aimed at generating financial systems capturing certain empirical “stylized facts” of interbank markets[1]. One pervasive finding in empirical data is disassortativity of link formation via interbank credit. In network theory, if high-degree vertices have a tendency to attach to low-degree ones, the resulting graph is said to display *disassortative mixing* or *disassortative behavior*. A simple way to identify such a structure consists in studying the distribution of the average degree of the neighbours of the vertices belonging to the network. In the case of disassortative mixing, this distribution should be a decreasing function of the degree of the nodes. Disassortative mixing has indeed been found to be a typical feature of many real networks, examples including the internet, the World Wide Web, protein interactions and neural networks (Caldarelli (24)). Interestingly, essentially all interbank markets investigated so far seem to be characterized by disassortative behavior, as documented by Boss et al. (19) for the Austrian interbank market, Soramäki et al. (65) for the US Fedwire network, De Masi et al. (28) for the Italian interbank market, and Imakubo and Soejima (43) for the Japanese interbank market. Therefore, it seems important to include this well-established stylized fact in

[1] As in the case by Nier et al. (60) and May and Arinaminpathy (56), our networks are static since the single nodes are not allowed to change their behavior during the spread of the shock, but just absorb the propagation of losses.

the study of artificial financial networks, since this particular structure could affect the ability of a system to absorb shocks.

Another feature that is often present in real networks is a characteristic power law distribution of the degrees (the number of connections across the units constituting the network). A power-law distributions of degrees also is the feature characterizing so-called *scale-free networks*. Scale-free networks are characterized also by the presence of hubs, namely nodes with a degree that is much higher than the mean degree of the other nodes. Therefore, in a scale-free network, there is a high probability that many transactions take place through one of the high-degree nodes of the network. The presence of such hubs makes a system in general more prone to a break-down in case of targeted attacks. This feature is the downside of their high connectivity that might contribute to an efficient channeling of flows providing short paths between any two nodes belonging to the system. Again, in real interbank money markets scale-free degree distributions have been frequently reported. Examples are Inaoka et al. (45) and Imakubo and Soejima (43) for the Japanese interbank market, and Boss et al. (19) for the Austrian interbank market, while there exist divergent results for the Italian interbank market (Iori (47), Finger et al. (33)).

We also believe that it is important to consider a realistic size distribution when studying the interbank network. As with firms size distributions in general (Luttmer (54)), the distribution of the (balance sheet) sizes of banks is skewed to the right and at least close to a fat-tailed power-law distribution. As reported by Ennis (32) and Janicki and Prescott (49) for U.S. banks, the banking system is characterized by a large number of small banks and a few large banks, and the size distribution seems to be close to lognormal with a Pareto-distributed tail. A study on the evolution of the banking system in a European country can be found in Benito (13), where the presence of few big hubs in the Spanish banking system is highlighted, and, again, the distribution is found to be highly skewed, and has become more skewed during the last decades. Glasserman and Young (38) show how theoretical bounds on network effects depend on the heterogeneity of bank sizes and the distribution of links with both kinds of heterogeneity being crucial determinants for the extent of contagion effects.

We take the above three stylized facts into account in the design of our artificial banking system. In particular, we construct a Monte Carlo framework for an interbank market characterized by the above empirical features via what is called a *fitness* *algorithm* (De Masi et al. (28)). With a particular choice of such a function as a generating mechanism for our network, we can make sure that our artificial banking sector displays a power law degree distribution together with disassortative link formation. As an immediate consequence, in an interbank market characterized by a power law in the size distribution, the default of a single small or medium-sized bank will mostly not affect the stability of the entire system: as one might expect, their losses are easily absorbed by their mostly large lenders, and typically no domino effect occurs. The situation changes when the initially defaulting bank is one of the hubs of the system. In this case the propagation of the shock proceeds like the propagation of a circular wavefront in the water: starting from an initial node, the shock will hit at the same time all nodes that are directly linked to the source. Moreover, each time a new node is hit by the wave, it also will become a source of shock propagation itself, expanding the range of nodes that will potentially be affected by the shock. Those are the kind of network effects we are interested in.

Note that the results reported so far in the literature using network approaches in order to study domino effects in interbank markets have mostly used either random network models or networks constructed from aggregate data via a maximum entropy principle (cf. Upper (67), for an overview). Both approaches are very likely to underestimate the extent of a contagious spread of a disturbance due to the very homogeneous level of activity and connectivity in such artificial networks (as demonstarted, for example, by Montagna and Lux (57)). In contrast, the above stylized facts show strong heterogeneity for the levels of activity (size of the balance sheets, as well as the extent of connectivity, namely the degree distribution). In addition, the pronounced negative assortativity is also not covered by random networks or those constructed from entropy principles. We might, therefore, expect a higher risk of contagion effects in models that share the above stylized facts.

The paper is organized as follows: Section 3.2 introduces the basic ideas of our probabilistic framework to measure systemic risk. Section 3.3 shows the algorithm we will use to generate interbank markets, demonstrating its ability to reproduce the above stylized facts. Section 3.4 applies the general probabilistic approach to this framework. Section 3.5 provides simple examples of contagion processes, and explains how the framework can be used to measure the systemic importance of single institutions.

Section 3.6 uses more realistic shocks to perturb the banking system, by introducing correlation between banks' assets. Section 3.7 concludes.

3.2 The probabilistic framework

To assess financial stability we need a framework capable to measure the likelihood of systemic events. As our starting point, we consider the joint distribution of the equity levels of all the banks in the system. We denote by:

$$\Phi\left(\eta_1, \eta_2, \ldots, \eta_N\right) \tag{3.1}$$

the joint distribution of equity levels η_i, for a financial system composed of N banks $i = 1, 2, \ldots, N$[1].

In assessing the financial stability of the system, we are interested in studying how the distribution Φ evolves after a shock hits the system. The uncertainty on the level of equity of banks can be due to two reasons. First, there could be incomplete information regarding the structure of the financial system. In this case, a pre-determined shock will generate several scenarios for the evolution over time given the initial configuration of the system: assigning a probabilistic weight to each of them will result in a joint distribution for the equity levels. Second, the shock itself could be described as a draw from of a stochastic variable. Even if the structure of the financial system were completely known, one would need to investigate the resulting scenarios through a probabilistic perspective. The known data on current balance sheet sizes would then be used as initial condition, and ignorance on the composition of the balance sheet and the existing interbank links would constitute the source of uncertainty.

Let us indicate with S a shock hitting the system at time $t = 0$. This shock can assume several forms: it can be a deterministic shock to a single institution, e.g. the default of a certain amount of its loan portfolio, it can be a probabilistic shock to a set of banks, specifying a correlation structure among the single shock components which reflect the correlation among their investments. Independently from its form, the shock

[1] We will specify later a complete structure for the banks balance sheets. In the present section, the framework we introduce is independent of the shape and composition of assets and liabilities, as well as of the possible direct and indirect mechanisms that propagate the shock from one institution to the other.

will generally change the initial configuration of banks' equity levels, and we indicate with:

$$\Phi(\vec{\eta}|S) = \Phi\left(\eta_1, \eta_2, \ldots, \eta_N; S\right) \tag{3.2}$$

the distribution of the equity levels conditional on the shock S. In all that follows, we will refer to eq. (3.2) as the Φ-*function* of the financial system conditional on the shock S. From the joint distribution 3.2 it will be possible to quantify the probability of systemic events after an exogenous shock S, taking into account the incomplete structural information on the financial system. We explore in the following several examples for the use of our framework.

We start by considering the case where the shock S consists in wiping out a certain percentage of assets λ from bank i_0; the shock S can be therefore represented by the N-dimensional vector $\vec{s} = (0, 0, \ldots, \lambda_{i_0}, \ldots, 0) = s_{i_0}$. The function $\Phi(\vec{\eta}|\vec{s})$ includes all the information regarding the losses suffered by the other banks after the default of bank i_0, and can therefore be used to develop measures for its systemic importance. The expected number of defaults $\langle \bar{N}|s_{i_0}\rangle$ is computed as:

$$\begin{aligned}\langle \bar{N}|s_{i_0}\rangle = \langle\sum_{i=1}^{N}\left(1-\theta(\eta_i)\right)|\vec{s}\rangle = \sum_{i=1}^{N}\langle\left(1-\theta(\eta_i)\right)|\vec{s}\rangle = \\ = \sum_{i=1}^{N}\int_{-\infty}^{+\infty} d\eta_1 \int_{-\infty}^{+\infty} d\eta_2 \ldots \int_{-\infty}^{0} d\eta_i \ldots \int_{-\infty}^{+\infty} d\eta_N \Phi(\vec{\eta}|\vec{s})\end{aligned} \tag{3.3}$$

where we indicated with $\theta(\cdot)$ the classical Heaviside function. The mean number of defaults computed in eq. (3.3) is a first indicator of the systemic importance of a financial institution. In fact, it quantifies the spillover effects coming from the default of bank i_0. Nevertheless, the above expression can underestimate systemic importance since it ignores the events populating the tails of the distribution Φ, as well as a possible correlation structure among banks' balance sheets. To overcome this problem, another choice could be to compute the probability to observe a certain number $\bar{N}$ of defaults given the defaults of bank i_0, that is $Pr\left[\bar{N}|s_{i_0}\right]$, which can be computed as:

$$Pr\left[\bar{N}|s_{i_0}\right] = c \cdot \sum_{\Pi} \int_{-\infty}^{0} d\eta_1 \cdots \int_{-\infty}^{0} d\eta_{\bar{N}} \cdots \int_{0}^{\infty} d\eta_N \Phi(\vec{\eta}|s_{i_0}) \tag{3.4}$$

where Π represents all possible permutations of the indexes i, c being a normalization factor:

$$c = \left(\frac{\bar{N}!}{N!(N-\bar{N})!} \right)^{-1} \tag{3.5}$$

The quantity expressed in eq. (3.4) can be seen as the systemic value at risk conditional on the initial shock S.

The shock S can also be described by a set of stochastic variables. Let's consider therefore a vector of random variables $\vec{\Lambda} = (\Lambda_1, \Lambda_2, \dots, \Lambda_N)$. The distribution of the i-th component Λ_i could, for instance, be extracted from the profit-loss distribution of banks. Moreover, a correlation structure among the N variables can be specified and it will play a fundamental role in assessing the probability of joint failures in the system, i.e. systemic events. Given the distribution $\Phi(\vec{\eta}|\vec{\Lambda})$, another interesting quantity one may want to compute is the extreme q-quantile of the distribution of the number of defaults following the stochastic shock $\vec{\Lambda}$. If we call $\phi(\bar{N}|\vec{\Lambda})$ the distribution of the number of defaults conditional on the shock $\vec{\Lambda}$, that is:

$$\phi(\bar{N}|\vec{\Lambda}) = Pr\left[\bar{N}|\vec{\Lambda}\right] \tag{3.6}$$

the extreme q-quantile of this distribution, N_q, defined as:

$$\int_0^{N_q} dx \phi(x|\vec{\Lambda}) = (1-q) \tag{3.7}$$

measures the fatness of the tail of the joint distribution where systemic events are happening.

The above set of measures to detect systemic importance of institutions and to assess systemic risk can be further enriched depending on the particular scenarios one wants to analyze, and on the available data. In the following, we concentrate on one particular mechanism of contagion among financial institutions, which is direct interbank exposure through bilateral loans. For this mechanism of contagion, we are able to analytically compute some of the above quantities, while others can be easily computed through numerical algorithms. We highlight again that, due to the generality of the framework we introduced, including other forms of interbank contracts is straightforward, at least from a computational point of view. The goal of the paper is to provide a framework based on statistical tools and basic assumptions on the contagion mechanism to capture "probabilities" of contagious events based upon empirically plausible distributional assumptions for the observed structural features of the financial network. In order to test our approach on a simulated interbank market, we introduce in the next section an algorithm which (i) is able to reproduce the most common features of real interbank lending networks; (ii) allows to include eventual uncertainty one has on the structure of the banking system; and (iii) is easy to implement and calibrate. Then, we show how to compute the quantities expressed above, and how they can play a role in assessing systemic risk.

3.3 The structure of the banking network

We consider an interbank market (IbM) composed of N financial entities linked together by their claims on each other. Each bank in the IbM will be represented as a node in the network, and the information of the loans among banks will constitute the edges of the network. These edges are directed and weighted, the weight of the link starting from node i and pointing to node j being the total amount of money that bank i lends to bank j. The structure of our model will be set up in a way to represent certain documented empirical features. Following Nier et al. (60), we use the scheme in Fig. 3.1 to represent the balance sheets of banks. The assets A_i of each bank ($i = 1, 2, \dots, N$) are partitioned into interbank loans l_i and external assets e_i:

$$A_i = l_i + e_i \tag{3.8}$$

The liabilities I_i of each bank are partitioned into interbank borrowing b_i and customers' deposits d_i:

$$I_i = b_i + d_i \tag{3.9}$$

Solvency requires that the difference between a bank's assets and its liabilities be positive, that is:

$$\eta_i \equiv (l_i + e_i) - (d_i + b_i) \geqslant 0 \tag{3.10}$$

where we denote bank i's net worth by η_i.

If relationship (3.10) is not fullfilled, bank i becomes insolvent. Note that we could instead impose a minimal capital requirement and intercept the bank's operations if its capital falls below a certain threshold. For most purposes this would leave our results qualitatively unchanged as it would just lead to a linear rescaling of the balance sheet.

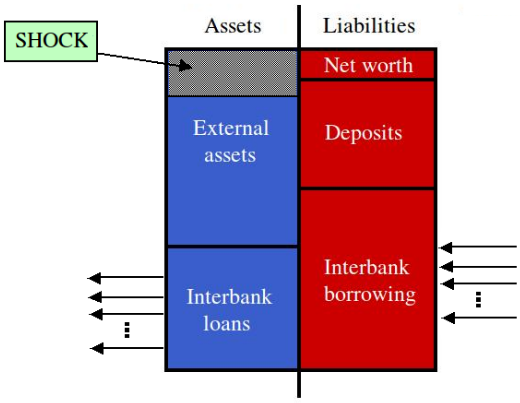

Figure 3.1: The balance sheet structure of each bank i belonging to the IbM.

However, our analytical representation of an insolvency cascade is facilitated by a zero threshold for the default of a financial institution.

Following Nier et al. (60), we impose the following relations, that hold for all banks belonging to the IbM:

$$e_i = \theta A_i \tag{3.11}$$

$$l_i = (1 - \theta) A_i \tag{3.12}$$

$$\eta_i = \gamma A_i \tag{3.13}$$

i.e., external assets, interbank loans and net worth are determined (initially) as fixed functions of total assets. This enables us to characterize the evolution of the balance sheet of the banks using the common pair of parameters θ and γ. Unlike Nier et al. (60) who investigate a banking sector with banks of equal size of balance sheets and interbank liabilities, we, however, try to mimic some of the documented dimensions of heterogeneity in the banking sector via the distribution of banks' size and that of the links between banks.

The empirical properties of real interbank networks that we attempt to reproduce are the disassortative behavior and the power law in the degree and size distributions. To this end, we arrange the nodes on a scale free network according to the algorithm presented in Montagna and Lux (57), and reported in Section 2.2. The basic idea of the algorithm is to draw the sizes of the N banks composing the system, A_i, from a power-law distribution:

$$\rho(A_i) \propto A_i^{-\tau} \tag{3.14}$$

where $A_i \in [a, b]$. Afterwards, we generate an interbank networks of claims by mean of a *probability function* $P(A_i, A_j)$: this function provides the probability that a bank i (characterized by total external assets A_i) lends money to bank j (characterized by total external assets A_j). It has typically been found in empirical data of interbank credit relations that a pool of small and medium-sized banks mostly lend money to the largest banks of the system, which in turn redistribute liquidity to external financial markets or within the system itself (Iori *et al.* (2008), Cocco *et al.* (2009), Fricke and Lux (2012)). The choice of an appropriate probability function allows to reproduce those important empirical observations. In this paper, like in Montagna and Lux (57), we will use the following alternative probability functions:

$$P_1(A_i, A_j) = d_1 \cdot \left(\frac{A_i}{A_{max}}\right)^{\alpha} \cdot \left(\frac{A_j}{A_{max}}\right)^{\beta} \tag{3.15}$$

$$P_2(A_i, A_j) = d_2 \cdot (A_i + A_j) \tag{3.16}$$

$$P_3(A_i, A_j) = d_3 \cdot H(A_i + A_j - z) \tag{3.17}$$

where A_{max} denotes the size of the balance sheet of the largest bank in the system, α, β and z are constants, and $H(x)$ is the Heaviside step function. d_1, d_2 and d_3 can be used to adjust the density of the networks. Section 2.3 presents the main topological properties of networks produced by functions (3.15), (3.16) and (3.17). With any of these probability functions, we can build an $N \times N$ probability matrix $P \in M_{N \times N}$, with entries $p_{ij} = P_s(A_i, A_j) \in [0, 1]$ determining the probability for the link between i and j, and $s = 1, 2, 3$;

3.4 Single Shocks and Network Risk

We now combine the probabilistic framework introduced in Sec. 3.2 and the algorithm introduced in Sec. 3.3 to asses how the financial stability of the banking system is affected by the main parameters of the model. The shock S in this section will consist in wiping out a percentage of the external assets of the largest bank in the system, so it can be written as $\vec{s} = (0, 0, \ldots, \lambda_{i_0}, \ldots, 0) = s_{i_0}$, where i_0 is the largest bank. In this scenario, the only uncertainty is due to the missing information regarding the structure of the banking system, represented by the probability functions introduced in Sec. 3.3. In particular, we will use function (3.15) to generate our interbank networks, and we will explore how the parameters γ and θ affect the stability of the banking system.

When the largest bank in the system fails, the other banks can suffer losses in two ways. The first way is through direct contagion. In fact, the initial loss is first absorbed by the bank's net worth η_{i_0}, then by its interbank liabilities b_{i_0} and last its deposits d_{i_0}, as the ultimate *sink*. That is, we assume priority of (insured) customer deposits over bank deposits which, in turn, take priority over equity (net worth). If the bank's net worth is not large enough to absorb the initial shock, the bank defaults and the residual is transmitted to creditor banks through interbank liabilities. Creditor banks are assumed to receive an amount of the residual shock proportional to their exposure to the failed bank. Those banks will have to book losses in their equities[1].

The second way banks can suffer losses is indirect contagion through network effects. In fact, in case the direct creditors of the initial failing bank are not able to absorb the losses, they will fail and transmit losses to their own creditors. The process continues until the losses are completely absorbed by the system or, alternatively, the whole system has failed.

It seems natural when studying the loss propagation process to formally introduce a discrete event index t describing the different phases of the propagation of the shock. We call that index the *round* of propagation. We start from a situation in which the system is in a stationary state with positive net worth of all banks, and at a certain point $t = 0$ we subject one bank, i_0, to a shock by wiping out a fraction λ_{i_0} of its external assets[2]. At event time $t = 0$ no other banks will incur any losses, but part of

[1] We disregard partial recovery of the defaulted loans as this will happen only much later during bankruptcy proceeding and would be of little relevance to the unfolding short-run dynamics.

[2] We note here that restricting ourselves to the case of a single shocked unit does not restrict the generality of our approach. In fact, simultaneous deterministic shocks to different banks at the same time can be represented as the convolution of multiple Φ-functions.

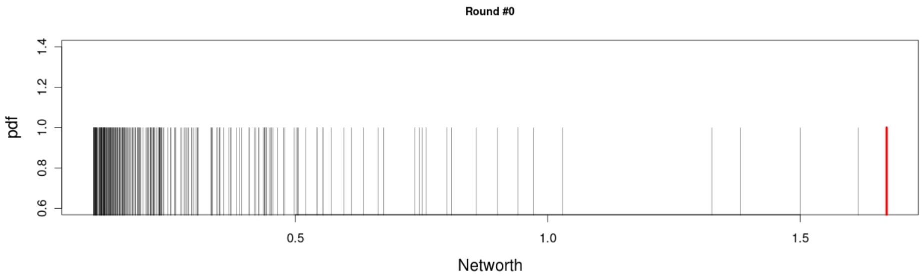

Figure 3.2: The figure schematically shows the Φ-function at round zero, i.e. eq. (3.18). At time $t = 0$ all the banks have a well-defined non-stochastic net worth η_i, represented in the figure by a vertical line of length 1, i.e. the probability for each bank to have net worth η_i to be exactly 1. The red line represents the largest bank in the IbM. The distribution of banks size has been drawn from a power-law distribution with tail parameter equal to 2.

the assets of the initially shocked bank have been destroyed, and so we can write:

$$\Phi^{t=0}(\eta_1, \eta_2, \dots, \eta_n | s_{i_0}) = \delta\left(\eta_{i_0} - \left(\eta_{i_0}^0 \cdot \frac{\gamma - \lambda_{i_0}\theta}{\gamma}\right)\right) \cdot \prod_{i=1, i\neq i_0}^{N} \delta(\eta_i - \eta_i^0) \tag{3.18}$$

where $\delta(x)$ is the Dirac delta, and η_i^0 are the net worths of the banks before the shock starts propagating. If we apply now eq. (3.3) we obtain:

$$\bar{N}^{t=0} = \begin{cases} 1, & \text{if } \gamma \leq \lambda_{i_0}\theta \\ 0, & \text{otherwise} \end{cases} \tag{3.19}$$

and so the perturbation can start propagating only if the shock is large enough[1]. Fig. 3.2 shows an illustration of the function $\Phi^{t=0}$ and the initially shocked bank i_0 (red line). Note that, initially, the net worth of each bank is known with certainty, i.e. all values have probability 1 (vertical axis).

We can now move on to the next round; at time $t = 1$ the variables η_i are still independent (and hence uncorrelated), and it is possible to factorize the Φ-function as in the previous case:

$$\Phi^{t=1}(\eta_1, \eta_2, \dots, \eta_n | s_{i_0}) = \delta\left(\eta_{i_0} - \left(\eta_{i_0}^0 \cdot \frac{\gamma - \lambda_{i_0}\theta}{\gamma}\right)\right) \cdot \prod_{i=1, i\neq i_0}^{N} \Phi_i^{t=1}(\eta_i | s_{i_0}) \tag{3.20}$$

[1] If $N_0 = 0$, the first bank is able to absorb the shock and no contagion effects will be registered in the system.

where $\Phi_i^{t=1}(\eta_i|s_{i_0})$ represents the marginal distribution of the net worth of bank i at time $t=1$. In the probabilistic determination of eq. (3.20) the stochastic representation of our ignorance of the details of interbank credit connections comes in. We assume that these connections are well represented by the probability function $P(A_i, A_j)$ introduced in Sec. 3.3 that replicates important stylized facts of empirical data. In the Appendix we show that $\Phi_i^{t=1}(\eta_i|s_{i_0})$ consists of two parts: with probability p_{ii_0} bank i will be affected in the first round of aftereffects after the initial shock, while with probability $1-p_{ii_0}$, it will still remain unaffected at this stage (it is sufficiently remote from bank i_0). The first case, then, leads to a loss due to the defaults of bank i_0 on some of its interbank loans. In the absence of exact knowledge this effect is stochastic (to the outside observer or to the supervisory authority). We show in the Appendix that the size of the loss can be approximated by a Normally distributed random variable. The complete expression can be written as:

$$\Phi_i^{t=1}(\eta_i|s_{i_0}) = P_i^I \cdot \frac{b(\gamma,\theta)(a(\gamma,\theta)-\eta_i)^{-2}}{\sigma_1^i\sqrt{2\pi}} exp\left\{-\frac{1}{2}\left(\frac{\frac{b(\gamma,\theta)}{a(\gamma,\theta)-\eta_i} - m_1^i}{\sigma_1^i}\right)^2\right\} + (1-P_i^I)\delta(\eta_i - \eta_i^0) \quad (3.21)$$

where $a(\gamma,\theta)$ and $b(\gamma,\theta)$ are functions of the percentage of net worth and of the weight of the first term, $P_i^I = p_{ii_0}$ is the probability for bank i to belong to the first shell of banks connected to i_0. Explicit equations for m_1^i and σ_1^i are presented in the Appendix, and both completely depend only on the topological features of the network and in the case of our probability functions (3.15) through (3.17) on the size of the balance sheet of the banks. We compute in the Appendix the mean value and the standard deviation for $\Phi_i^{t=1}(\eta_i|s_{i_0})$, and we show that its variance tends to zero when the entries of the probability matrix p_{ij} tend to 0 or 1, namely when the network becomes deterministic.

Fig. 3.3 shows an example of the marginal distributions $\Phi_i^{t=1}(\eta_i|s_{i_0})$ for a single bank, and the blue area highlighted in the figure is the probability for that bank to fail. The marginal Φ-function expressed in eq. (3.21) represents what can be defined as *first round effects*. In fact, banks subject to the potential losses in this first stage of the propagation are only the direct counterparties of the initial failing bank i_0. In the other stages of the shock propagation, instead, all the banks can potentially be subject to losses because of the network of interbank contracts, and we call them *higher round*

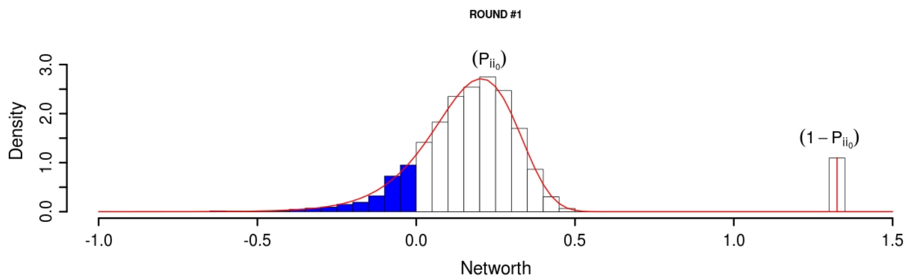

Figure 3.3: The picture shows one of the marginal distribution functions described by eq. (3.21). Each of these distributions are composed by a Dirac delta centered on η_i^0, indicating that with probability $(1 - p_{ii_0})$ bank i is not linked to bank i_0 directly, and so its net worth will rest unchanged at time $t = 1$. The second component gives a contribution of the propagation of the initial shock if a link exists to bank i_0 which happens with probability p_{ii_0}.

effects. In general, a closed form solution for the Φ-function describing higher round effects is hard to obtain. Although different types of approximations are possible[1], we prefer to generate random variables according to the joint distribution Φ^t and compute numerically the integrals in eqs. (3.3), (3.4) and (3.7)[2].

Figure 3.4 shows the temporal evolution from $t = 1$ (round 1) to $t = 2$ (round 2) of one of the marginal distributions $\Phi_i^t\,(\eta_i|\, s_{i_0})$. We immediately note from the graph that also the contribution linked to $(1 - p_{ii_0})$ spreads out, due to possible connections of second order (i.e. credit expanded to the creditor banks of the initially defaulting one). This fact actually reflects the topology of the networks generated by probability function (3.15): the small diameter of these scale-free networks imposes that in two steps a node can mostly reach every other nodes, if the initially shocked bank is one of the biggest of the system. If we again consider the marginal distributions, we can split them up into three components, so that for round 2 we can formally write:

$$\Phi_i^{t=2}(\eta_i|s_{i_0}) = P_i^I \cdot \Phi_i^{t=2,I}(\eta_i|s_{i_0}) + P_i^{II} \cdot \Phi_i^{t=2,II}(\eta_i|s_{i_0}) + (1 - P_i^I - P_i^{II}) \cdot \delta(\eta_i - \eta_i^0) \tag{3.22}$$

where P_i^I is the probability for bank i to belong to the first shell with respect to the initially defaulting bank i_0, that is $P_i^I = p_{ii_0}$, and in general P_i^l is the probability for

[1]One possible approach consists in assuming the variables to be independent, factorize the function Φ and compute it as in the first round. Another possibility is to use a mean field approximation to derive approximate solutions to the first moments of the distribution.

[2]In the Appendix we show how to compute those variables.

bank i to belong to the lth shell, $l = I, II, III, \dots$, with respect to bank i_0[1]. The contribution linked to $(1 - P^I - P^{II})$ is a Dirac delta since in two rounds there is no way for the shock to hit banks belonging to the $3rd$ (or higher) shell. In the pink distribution of Fig. 3.4, representing a possible outcome of eq. (3.22) this contribution vanishes simply because with the underlying parameters $P_i^I + P_i^{II} \simeq 1$. In general, higher-order defaults can occur over many rounds.

Note that in the limit $t \to \infty$[2] the system will converge in probability to a steady state, defined by the Φ-function $\Phi^\infty(\eta_1, \eta_2, \dots, \eta_N|s_{i_0})$. Decomposing the overall distribution into the effects emanating from different "shells", we can write the stationary distribution as:

$$\Phi_i^\infty(\eta_i|s_{i_0}) = \sum_{l=1}^{\infty} P^l \cdot \Phi_i^{\infty,l}(\eta_i|s_{i_0}) \tag{3.24}$$

With a finite diameter d of the network it can be reduced to:

$$\Phi_i^\infty(\eta_i|s_{i_0}) = \sum_{l=1}^{d} P^l \cdot \Phi_i^{\infty,l}(\eta_i|s_{i_0}) \tag{3.25}$$

since P^l is equal to zero for each l equal or higher than d. Note that for any of the l components in eq. (3.25) a long-lasting sequence of aftereffects can result since any possible defaults would lead to the possibility of subsequent defaults in the next period of events whose losses are exceeding their (remaining) equity level and so on. So, in principle, along the time dimension, the sequence of events and, therefore, flow of probability between different states, evolves for much longer than along the dimension of shells. Typically, however, the macroeconomic statistics emerge after a relatively small number of iterations. This holds particularly for the number of defaults as these are binary counts that only change if losses exceeds threshold value, and so, higher-order knock-on effects would at some period not trigger any more defaults. We will see that the additive components of eq. (3.24) play a fundamental role in understanding

[1] It is easy to see that :

$$P_i^l = (1 - P_i^I)(1 - P_i^{II}) \cdots \left(1 - P_i^{l-1}\right) \cdot \left[1 - \prod_{j_1=1, j_1 \neq i}^{N} \cdots \prod_{j_l=1, j_l \neq i}^{N} \left(1 - p_{ij_1} P_{j_1}^{(l-1)} \cdots p_{j_{l-1}j_l} P_{j_{l-1}}^{II} P_{j_l}^{I}\right)\right] \tag{3.23}$$

which is the probability for node i not to belong to shells $1, 2, \dots, l-1$, multiplied by the probability for at least one l-length path to exist connecting node i and node i_0.

[2] Numerically we saw from the simulations that a good approximation is typically obtained for $t \cong 20$, and after $t \cong 7$ rounds one obtains about 95% of all defaults observed in the simulations.

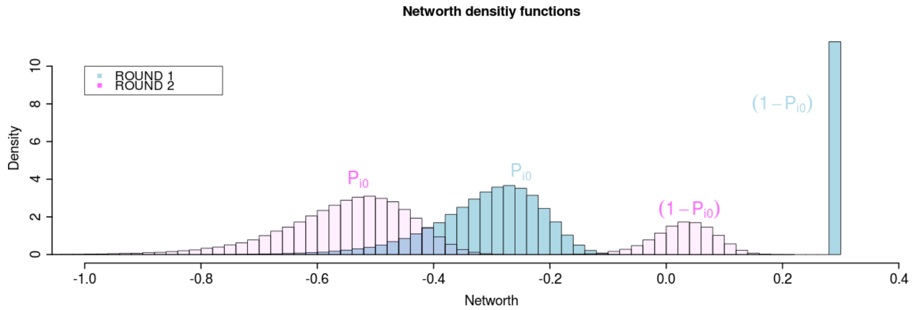

Figure 3.4: The figure shows the temporal evolution of the marginal Φ-function from round $t = 1$ (cyan distribution) to round $t = 2$ (pink distribution), for a particular bank i. At $t = 2$, due to the small diameter of the present network, also the contribution linked to $(1 - p_{ii_0})$ spreads, adding a second contribution to the probability for bank i to fail.

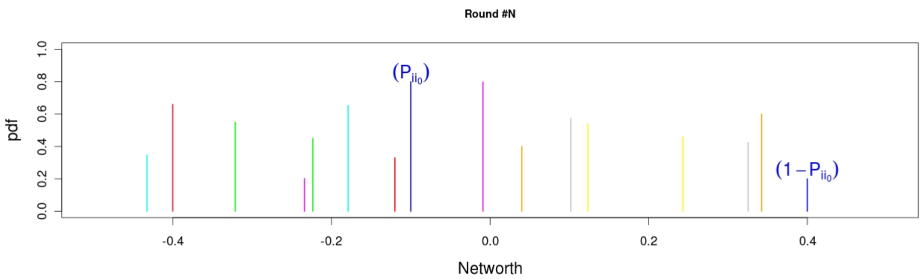

Figure 3.5: The figure shows a possible final equilibrium state for the system; in particular, different colors represent the marginal distribution of different banks belonging to the IbM, after the shock has been absorbed. Still for each node the Φ-function can be decomposed into two components depending on whether they have been hit immediately after the shock or at a later stage. This is illustrated by the two different entries for each bank (each color).

the results from the simulation engine, and they are directly related to the network structure through the coefficients P^l.

Figure 3.5 shows a possible final equilibrium state for the system. In particular, the mean values of the $d = 2$ components of the marginal Φ-functions (3.25) are plotted for some banks[1]. We note here the differences in information contained in the Φ-function and in the number of defaults obtained via eq. (3.3): although a bank might have a positive mean value in one (or both) of the two contributions that appear in eq. (3.25), the probability for that bank to fail might nevertheless not be zero. This effect is not caught by eq. (3.3), but it is correctly quantified via the Φ-function, that contains all the information regarding the state of the system.

[1]Note that in the framework generated by eq. (3.15) $P_i^I + P_i^{II} \simeq 1$.

In the following subsection, we explore how the main parameters affect the stability of the banking system under the failure of the largest bank.

3.5 Computational Experiments

3.5.1 The role of bank capitalization

In our first computational experiment we investigate the effects of banks' net worth on the resilience of the entire banking system. The parameter θ will be fixed at 0.8, so that each bank will invest 20% of its total assets in the interbank market, and the remaining 80% in some external assets. We will let the parameter η vary from 0 to 0.1 [1]. In all that follows, the number of banks will be fixed at $N = 250$. The design of the simulations will be the same for all the following experiments: the first step consists in generating one Monte Carlo realization of our banking system as explained in sec. 3.3. In the second step we destroy the largest bank: this shock is assumed to wipe out all the external assets from the balance sheet of the initially failing bank. For each simulation run, we count the overall number of defaults, as well as the number of defaults in each single phase of the shock propagation. We report the average number of defaults across all banks. We will use probability functions (3.15) with parameters $\alpha = 0.2$, $\beta = 1.2$. Furthermore the two limits a and b will be fixed at 5 and 100 respectively[2]. Fig. 3.6 shows the result of the pertinent Monte Carlo simulations: we report both the total number of defaults (black bold line), and the number of defaults in the first four phases of the propagation of the shock. The thin vertical bars represent the standard deviation of the black line across our 200 replications of the simulations.

As one could expect, when the percentage of net worth tends to zero, the total number of defaults increases to 250: in particular, a threshold value ($\eta = 0.0143$ in the figure) exists below which the system fails completely, and below $\eta = 0.008$ it breaks down within only two rounds. This is a demonstration of the so called *small-world* effect: the diameter of this particular network is roughly about two for the largest bank belonging to the system, and so in only two rounds the shock will have reached almost any bank of the IbM. At the other end, when the percentage of net worth is beyond an upper threshold value, no defaults are reported and no domino effects set in.

Interestingly, the shape of the line describing the total number of defaults is far

[1] Remember that by mere rescaling η could also be interpreted as the excess over the required minimum capital requirement.

[2] Montagna and Lux (57) investigate how these limits affect the resilience of the system.

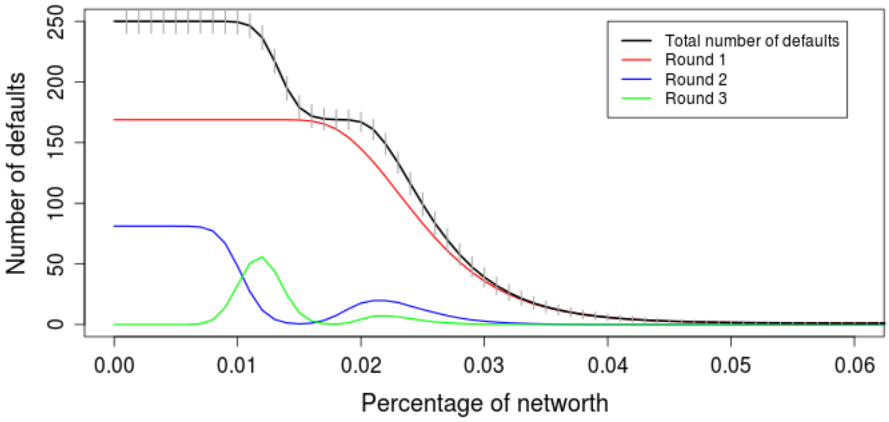

Figure 3.6: Number of defaults as a function of the percentage of net worth η, for probability function 3.15. The other parameters are fixed at: $\theta = 0.8$, $a = 5$, $b = 100$. The picture shows both the total number of defaults (bold black line) together with the standard deviation of the mean value (small gray bars), and the number of defaults occurring during the first four phases of the propagation of the shock.

from linear. Starting from the value $\eta = 0.1$, we can observe that below the value $\eta \cong 0.05$ the first defaults appear, and inspection shows that these typically happen for small banks connected to the initially failed bank. As η decreases further, we observe a sharp increase in the number of defaults, and this growth stops at the value $\eta \cong 0.02$ where the curve enters a *plateau*. Inspection of the defaults per round of propagation shows the reason for this non-linearity: at the level of net worth of the plateau, all the banks belonging to the first *shell* around the initially failed bank have failed, and the banks which are not directly connected to the first failing unit have enough net worth to survive the subsequent aftereffects of the shock. When the net worth decreases further, also the banks outside the first shell are no more able to absorb the perturbation, and the total number of defaults sharply moves up to 250.

It is interesting to look in more detail at the number of defaults in the different rounds. In the first round (red line in Figure 3.6), banks that fail are directly connected to the initially shocked bank, and when the red line reaches its *saturation* at $\eta \cong 0.018$ the complete first *shell* (composed on average of 153 units) has failed. We note that the saturation point of the number of defaults in the first round does not coincide exactly with the *plateau* of the total number of defaults: the explanation is that with slightly higher equity levels the largest banks in the first shell need more than one hit to fail, and so they populate the failures of higher rounds. The reason for this is that for larger banks the overall number of credit relationships to other banks (by assumption, following observed empirical regularities) is higher on average and so for them the failure of the largest bank will lead to a proportionally smaller loss than for the smaller client banks of the defaulted entity. When the percentage of net worth decreases, these defaults occur already in earlier rounds, up to a point in which all banks of the first shell are affected in the first round of defaults.

The theoretical counterpart of the shapes appearing in Fig. 3.6 can be provided by the analytical framework of Sec. 3.4. In particular, we can compute the number of expected defaults due to first round effects by inserting eq. (3.1) in (3.3). In the top left panel of the figure, a comparison between the simulation results and the results obtained via eqs. (3.20) and (3.21) for the effects in the first round is shown. In the second and third panels (upper right-hand side and lower left-hand side) we represent the contributions, respectively, from the first shell during the second round, and from the second shell during the second round. The results are now obtained via a numerical algorithm (see Appendix for more details), which provides the advantage that these two contributing factors can be clearly distinguished from each other. In particular, the hump in the number of defaults in the second round is caused by banks from the first shell that have survived the first round of knock-on effects but are too fragile to survive the second wave of losses in round 2. In a similar way it is possible also to compute all effects in the other rounds.

3.5.2 Interbank exposure

In this section we are going to explore how the number of defaults is affected by the percentage of interbank exposure as a function of total assets, namely how the parameter θ affects the resilience of the system. An increase in interbank assets produces, as an immediate result, an increase in the weight of each edge, and so an increase of the channels through which the shock can propagate. This effect can potentially increase the number of defaults in the system, as the amount of losses transmitted to creditor banks will increase as well. On the other hand, an increase in interbank exposure implies a reduced relative exposure to external markets, and since here we are considering, as initial source of the shock, a loss in value of external assets, this second effect could reduce the systemic risks from defaults of single banks.

The design of the simulations will remain the same as in the first experiment: we generate a realization of the system and we shock the biggest bank, wiping out all its external assets. Subsequently we count the number of defaults. We will show the mean value of those numbers for each round, and the standard deviation for the total number

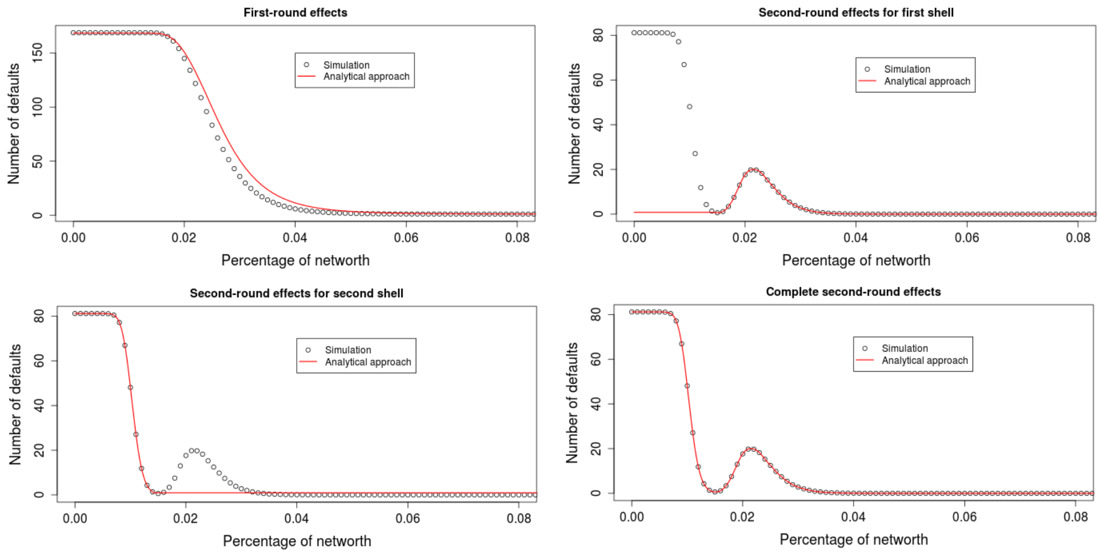

Figure 3.7: In the four panels we show the expected number of defaults as a function of the percentage of net worth γ, for the first two rounds. In particular, the first panel (top-left) contains a comparison between the simulation result and the probabilistic approach varying the percentage of net worth; the red line is computed combining eqs. (3.21) and (3.3). The slight difference in the two lines is due to the application of the Central Limit Theorem in the computation of eq. (3.21) (see Appendix), and it will tend to zero as the number of nodes increases. The second and third panels (top-right and bottom-left) highlight the role of different shells in the spread of the shock. In particular, the two contributions linked to eq. (3.22) are compared with the simulation results. The last panel (bottom-right) shows a comparison between the simulation results and the analytical approach for the second round.

of defaults. In this section, the percentage of net worth η is fixed at 0.025, while the percentage of external assets on total assets, θ, varies from 0.5 to 1 (when θ is equal to one no interbank assets are present in the bank balance sheets). Fig. 3.8 shows the result.

Overall results are similar to those reported for similar experiments in Nier et al. (60).First, we note that when θ tends to 1 the number of defaults tends to zero: in this case the banks' balance sheets contain only external assets, and so the channels for the propagation of the shock become smaller and smaller, until θ assumes the value 1 and there are no more links in the network, and no domino effects are possible. We can also note a threshold value at $\theta \cong 0.78$: at this value, the contagion effects reach their maximum while both more or less intense interbank linkages reduce the number of knock-on defaults (due to a higher degree of risk sharing on the left and fewer links for contagion on the right). At the other extreme, when θ tends to 0, banks become

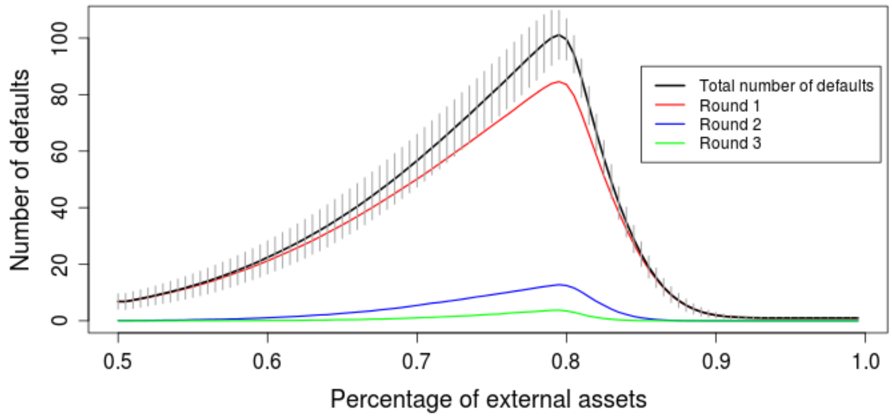

Figure 3.8: Number of defaults as a function of the percentage of external assets θ, i.e. $1-$ the percentage of interbank exposure θ, for probability function (3.15). The other parameters are fixed at: $\eta = 0.025$, $a = 5$, $b = 100$. The picture shows both the total number of defaults (bold black line) together with the standard deviation of the mean value (small gray bars), and the number of defaults occurring during the first four phases of the propagation of the shock.

completely isolated from any external market, and so in our model, where the initial source of the shock comes from the external assets of the largest bank of the system, the number of defaults tends to zero as well. Note that this exercise does not leave the size of the internal shock unaffected. Clearly, when external assets decline in their absolute size (from right to left) there should be a decrease of contagious defaults.

A comparison with the analytical solution is shown in Fig. 3.9. The trend in the number of defaults can be easily understood by studying the properties of the Φ-function (3.21). In fact, as we show in the Appendix, the parameter b_i appearing in the distribution of η_i include the expected losses coming from the loan to the initial failing bank. These losses monotonically decrease as the percentage of external assets over total asset increases, since the initial failing bank is less exposed to idiosyncratic external shock. Interestingly, here the second-round effects exhibit basically the same pattern as those observed in the first-round of knock-on effects.

3.6 Correlated Shocks and Systemic Risk

In the computation of the Φ-functions we have so far assumed that the initial shock to the system was a percentage of the external assets wiped out from the balance sheets of a bank in the network. In reality the banks' balance sheets shocks are also random events,

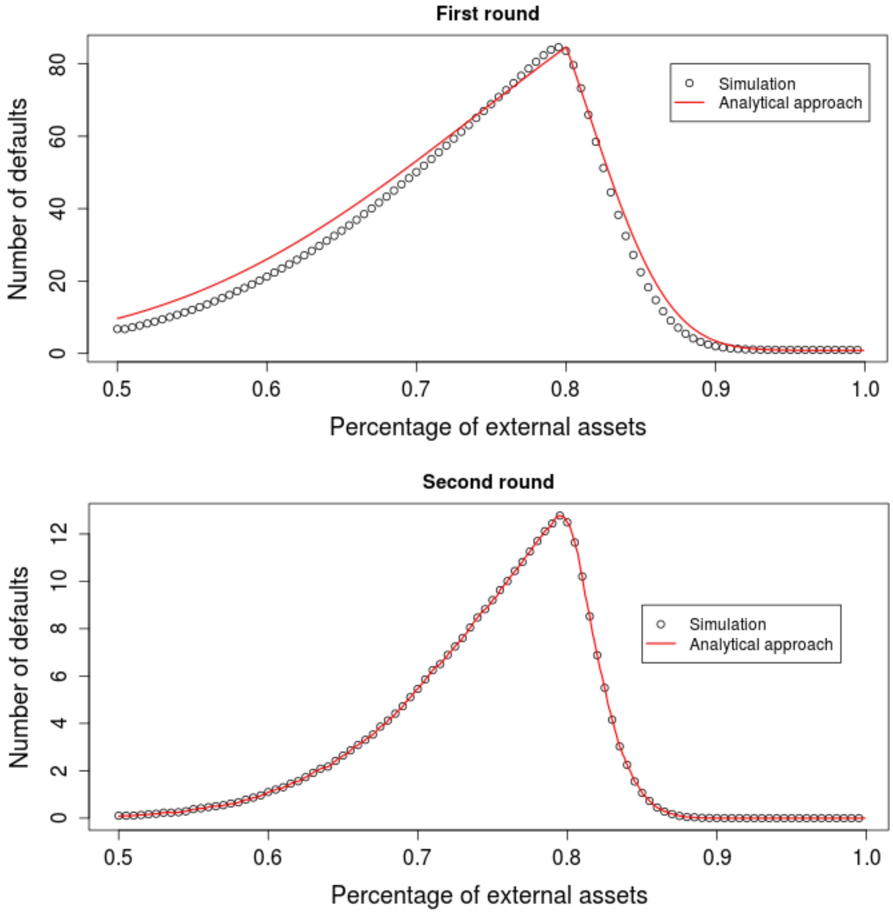

Figure 3.9: Simulations and analytical results for the number of defaults with varying percentage of external assets.

and in order to assess the financial stability of a banking system one should combine the information regarding banks profit/loss distribution with structural information on the interbank network. In our probabilistic framework, this can be captured by assigning a distribution for the initial shocks to the external parts of banks balance sheets. Here we present a simple example for correlated shocks, and we later discuss the importance of interbank credit on the propagation of idiosyncratic risk in the network.

As a suitable candidate for the loss distribution of the loan portfolio we adopt the formulation of Vasicek (1987)[1]:

$$v(\Lambda_i;p,\tau) = \sqrt{\frac{1-\tau}{\tau}} exp\left(-\frac{1}{2\tau}\left(\sqrt{1-\tau}G^{-1}(\Lambda_i) - G^{-1}(p)\right)^2 + \frac{1}{2}\left(G^{-1}(\Lambda_i)\right)^2\right) \tag{3.26}$$

where $0 \leq \Lambda_i \leq 1$ is the percentage losses of the loan portfolio, according to the notation introduced in Sec. 3.2 , p and τ are parameters of the distribution, and we indicate with $G(\cdot)$ the Normal standardized cumulative distribution function. As shown by Vasicek, eq. (3.26) characterizes the loss distribution of a large portfolio under the assumption of individual loan values following a logarithmic Wiener process. In this setting, banks' shocks are drawn from the probability distribution function (3.26), but for the time being we assume no lending relationships exist among the institutions. Hence, according to the notation introduced in Sec. 3.3, we set $\theta = 1$. Moreover, we introduce a correlation ρ among the shock variables Λ_i:

$$cor(\Lambda_i, \Lambda_j) = \delta_{ij} + (1 - \delta_{ij})\rho \tag{3.27}$$

The correlation, of course, leaves the marginal distributions for the single shocks unchanged. We set the net worth of each bank equal to the α-quantile of the distribution (3.26), meaning that the probability of default of each single institution is α, and we use in the example below $\alpha = 0.05$. Our first goal is to show that, also if there is no contagion process, the probabilistic framework introduced in Sec. 3.2 can still be usefully applied to understand and quantify the financial stability of the system. In fact, for a given level of correlation ρ, we can study the Φ-function of the system when a vector of stochastic shocks hits the system. The shock S takes here the form of a vector of random variables $\vec{\Lambda}$, where each component has a distribution described by eq. (3.26), and the correlation among the variables is defined by eq. (3.27). We want to study the function $\Phi(\vec{\eta}|\vec{\Lambda})$ to analyze the systemic risk in the system.

We compute again the expected value of the number of defaults after a shock hits the system and the q-quantile of the distribution of the number of defaults, as defined in eqs. (3.3) and (3.7). When the correlation among banks' balance sheets is increasing, keeping the marginals constants, the expected number of defaults computed as in eq. (3.3) remains constant. Nevertheless, as the correlation increases the probability to have tail events (i.e. the probability to have large number of defaults) increases as well.

Figure 3.10 shows different measures representing the stability of the system as a function of the correlation among banks' balance sheets, for the example discussed

[1] In all what follow we use the parameters p and τ equal respectively to 0.1 and 0.2 in eq. (3.26).

above. In particular, the average number of defaults (computed according to eq. (3.3)), the $5th$ quantile of the distribution $\phi(\bar{N}|\vec{\Lambda})$ (computed according to eq. (3.7)), and the maximum and the median of the same distribution are plotted. As one can see from the figure, the expected number of defaults remains unchanged (the mean is not affected by the correlation). Nevertheless, the risk for tail events increases dramatically with the correlation. In the right side of the figure, we plot the distribution of the number of defaults for the two cases $\rho = 0$ and $\rho = 0.5$, to show how the overall distribution of outcomes changes.

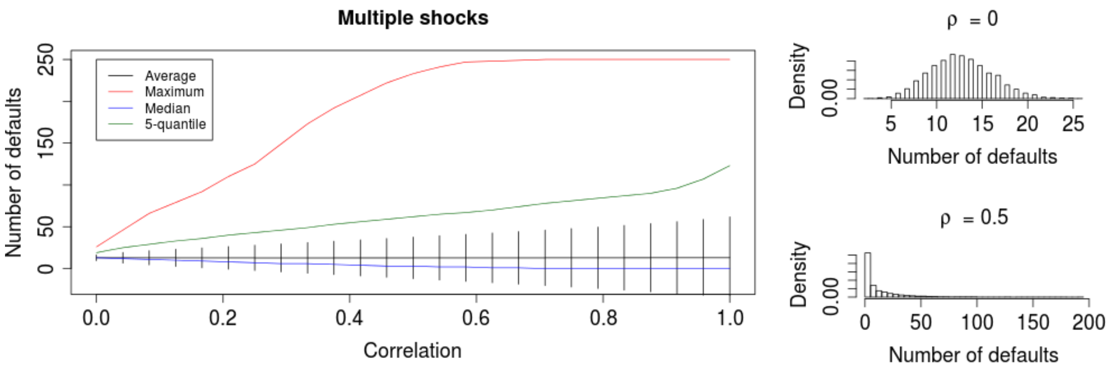

Figure 3.10: Systemic risk measures in a banking system without interbank credit. On the left, some systemic risk statistics are plotted as functions of the correlation between banks' balance sheets. In particular, the mean number of defaults (eq. (3.3)) is seen to be constant, while the extreme $5th$-quantile of the distribution of the number of defaults (eq. (3.7)) and the maximum number of defaults are seen to increase. On the right, the distribution of the number of defaults is shown for two values of the correlation ρ.

We now expand the example above by allowing again for interbank loans. The shock S assumes the same stochastic form $\vec{\Lambda}$ described in the previous section, and again we are interested in varying the correlation ρ among the shocks experienced by individual banks. The parameter θ, i.e. the fraction of external assets over total assets, will now be fixed at 0.8. The equity of the banks will be determined as the regulatory minimum: it consists of the sum of the lower $5th$ quantile of the distribution of portfolio losses expressed in eq. (3.26) and a fraction γ of their interbank assets, we use $\gamma = 0.02$. This scenario roughly reflects the standard Basel requirements, where investments are weighted according to their risk, and interbank loans have a fixed risk weight independently of the counterparty's identity.

The results are shown in the same fashion as in the previous case. While, again, the mean value $\langle \bar{N}|S \rangle$ remains constant, the probability for systemic events increases. A numerical comparison illustrates the differences: for a value of the correlation ρ

equal to 0.2, the maximum number of defaults is 108 for the case without interbank connections, and 195 for the case where interbank loans are present. Equivalently, the last $5th$ quantile moves from 39 in the first case to 51 in the second case. Despite the apparently moderate level of correlation of portfolio risk, the probability of systemic events is drastically increasing in the presence of interbank connections.

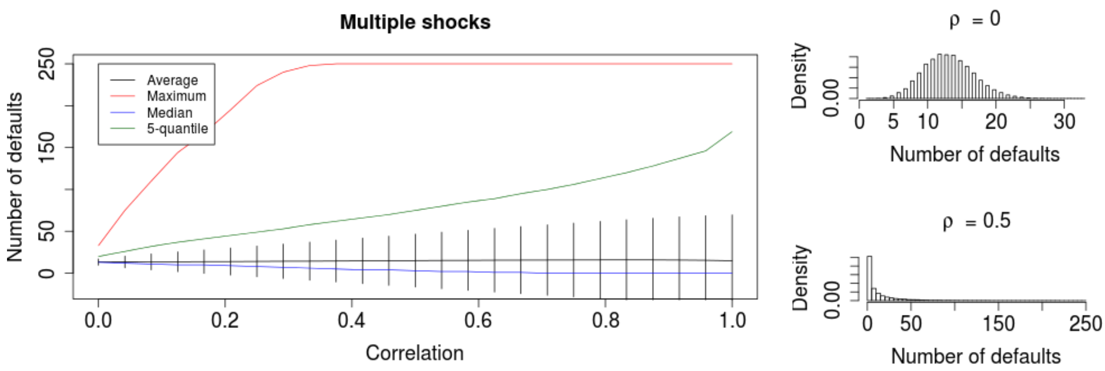

Figure 3.11: Systemic risk measures in a banking system where interbank loans are present. On the left, some systemic risk statistics are plotted as functions of the correlation between banks' balance sheets. In particular, the mean number of defaults (eq. (3.3)) is seen to be constant, while the extreme $5th$-quantile of the distribution of the number of defaults (eq. (3.7)) and the maximum number of defaults are seen to increase. On the right, the distribution of the number of defaults is shown for two values of the correlation ρ.

3.7 Conclusion

We have introduced an analytical formulation for the assessment of systemic risk through interbank contagion, and we tested our framework on a simulated financial system. The latter is generated with an algorithm that reproduces the main important topological features of a real banking system, which are the disassortative link formation and the power law behavior of the degree distribution. Moreover, heterogeneity in bank sizes is also taken into account, playing an important role for the stability of the banking system. The results are networks composed of a large pool of small and medium-sized banks with a dominating pattern of disassortative link formation forming credit connections between dissimilar partners.

In this framework, we have investigated how the percentage of net worth and the percentage of interbank assets (on total assets) affects the spread of an idiosyncratic shock. The analytical apparatus allows to decompose the overall number of expected contagion effects both in terms of the sequence of events and the banks' location within the network: banks belonging to the first shell (i.e. creditor banks of the defaulted entity) fail mostly before the others, and it is possible to distinguish between defaults of the different shells in the cascade of events.

The analytical formulation of the problem is based on the concept of Φ-functions. The Φ-function describes, in a discrete event framework, the evolution of the state of the system. The computation of an explicit closed form for Φ is possible only for the first round effects. Nevertheless, approximations or numerical methods can be used for higher rounds. These results, moreover, can be easily generalized to other forms of interbank contracts.

When allowing for correlation among banks' investments the probability of systemic events increases sharply even if each single unit perfectly follows the micro prudential regulation. The tails of systemic events are furthermore made fatter by direct contracts among the financial institutions, like in our example of interbank loans. In times where portfolio correlation increases, the correct assessment of the propagation of small probability events becomes crucial to assess systemic risk.

We note that the computation of the state function would not get much more complicated when using different values of θ and η for each bank, and so it can be in principle used in order to asses the systemic impact of each bank on the entire system. For example, using eq. (3.7), it is possible to determine the risk that a regulator is willing to run in case of the default of a particular entity, for different parameters θ and η (or, eventually, heterogeneous vectors $\overrightarrow{\theta} = (\theta_1, \theta_2, \ldots, \theta_N)$ and $\overrightarrow{\eta} = (\eta_1, \eta_2, \ldots, \eta_N)$ if, for example, different capital requirements depending on different systemic impact level were imposed). In terms of the systemic impact of a default, eq. (3.3) provides the expected number of triggered defaults in case of insolvency of a particular entity: the implementation of this expression using empirical data can help in quantitatively identify institutions that are too-big-to-fail and too-interconnected-to-fail. Overall, the framework of Sec. 3.3 is sufficiently flexible and general to accommodate whatever knowledge is available on the structural details of the interbank market. With complete knowledge of all links and exposures, the exact extent of knock-on effects could be determined as well as the identity of defaulting units. If we only know some boundary conditions (like the distribution of balance sheet sizes) and have an informed guess on others (link distribution and and distribution of mutual exposures in our present application), expected knock-on effects, quantiles, value-at-risk and other interesting quantities can be computed numerically. We note here that the lack of analytical results for higher rounds is not a major obstacle as the closed-form solutions can easily be replaced by their numerical counterparts.

4

Multi-layered Interbank Model for Assessing Systemic Risk

4.1 Introduction

During the financial crisis that emerged in 2008 a large part of the global financial system came under stress with severe repercussions on the real economy. The sequence of events which unfolded from the summer of 2008 forced public sectors to intervene in order to restore financial stability. The costs associated with those interventions put pressure on many European public finances during the following years, and such costs highlighted the importance to have stable financial systems.

A robust financial system should not amplify the propagation of idiosyncratic (or "local") shocks to other parts of the system and ultimately to the real economy. In this paper, systemic risk exactly refers to the possibility that the financial system is in a configuration which makes it particularly prone to global breakdowns in case of an initial, local shock. The reasons driving the system to such unstable and fragile configurations are probably rooted in the duality among local and global properties of the financial system. Indeed, as a matter of fact, each financial institution takes actions with the aim of maximizing its own profits and interests, while the impact of those actions on the stability of the system as a whole are hardly taken into account. Moreover, as we will show in this paper, also if banks were willing to minimize systemic risk when they take decisions, they would need to have sufficient information regarding the financial situations of the other banks, including the exposures each bank have on all the others. As an example, one can consider the direct exposures in an interbank market. If one bank wants to evaluate the riskiness associated with a loan to another bank, it should be able to know the exposures of its counterparty, whom probability of default depends on its own counterparties, and so on. No bank is able to peer so deeply into the interbank credit network to evaluate the probability of defaults due to contagion effects. As a direct consequence, this kind of risk cannot be priced in financial markets, and its evolution over time is, at least, not understood.

A crucial role in ensuring financial stability is therefore played by information. If the ultimate goal is to reduce systemic risk, it is necessary to have a global view of the financial system in order to identify and monitor possible sources and channels of contagion. A robust framework for monitoring and assessing financial stability, and for managing it with interventions able to prevent the system from entering into critical configurations, must be able to evaluate the continuously evolving structure of the financial system. Another important lesson emerging from the recent financial crisis that we try to account for in this paper is that the possible sources of systemic instability are multiple. For instance, direct bilateral exposures can create domino effects and propagate idiosyncratic (or local) shocks to the wides (global) financial system. In addition, forced firesales of financial assets can lead to strong asset price declines and can transmit losses through banks with common exposures and overlapping portfolios. Furthermore, news about a firm's assets can signal that others with similar assets may also be distressed and thus create widespread market uncertainty. Moreover, the sudden interruption of a service provided by a bank to the financial system can constitute a threat in case other banks are not able to immediately substitute it.

Against this background, the aim of this paper is to study systemic risk in highly interconnected financial systems. A natural way to represent and study an interbank market is network theory, nowadays commonly used in finance. In order to encapsulate the different kinds of possible connections among banks, we use a multi-layered network model. A multi-layered network is a system where the same set of nodes belong to different layers, and each layer is characterized by its own *kind* of edge (representing a particular kind of financial connection), by its own topology (so each node may have different neighbors in different layers), and its own rules for the propagation of eventual shocks. This holistic view of the financial system should enable us to study systemic risk in a more encompassing perspective, than typical single-layered network structures focusing on individual segments.

On top of the multi-layered system we put an agent-based model where agents can interact with each other through the network structure. The standard approach in the literature to study systemic risk using network theory is to assume passive banks as nodes in the network[1]. Those kinds of models are good at estimating the resilience of particular network structures against shocks, but they lack real dynamic effects, since shocks propagate through the system without incorporating the (likely) reaction of banks to those shocks. The introduction of agents enable us to investigate specific network structures in combination with a plausible bank behavior. In particular, in our model banks will only adjust their balance sheets when endogenous or exogenous shocks bring their liquidity or their risk-weighted capital ratio below the minimum requirements. In fact, if we assume that prior to the shock the system was in equilibrium, banks would just try to keep the same structure of their balance sheets also during the propagation of the shock. The failure of a financial institution usually implies several repercussions on the system. As already highlighted, the liquidation of a failed bank can push prices down, its counterparts can book losses from direct bilateral exposures, the financial services provided by the bank cannot always be replaced, at least not immediately, and the combination of such reactions can significantly amplify shocks and lead to dangerous spirals which could potentially collapse substantial parts of the financial system (Brunnermeier (21)). The complete dynamics of such events is difficult to capture with analytical models and from this perspective an agent-based model is more suitable, since it enables studying also systems out of equilibrium.

The agent-based model combined with the multi-layered network is subsequently used to design measures for the systemic importance of each bank in the system. Those measures rely on information regarding direct and indirect interbank connections, which can be inferred from network theory, and banks balance sheet information. The basic notion is that standard network centrality measures alone cannot explain the systemic importance of individual financial institutions, since the high level of heterogeneity in banking systems can bring central capitalized nodes to stabilize the system, whereas only network measures would just judge nodes depending on their centrality. Instead, it is necessary to combine information regarding the balance sheet structure of institutions with measures of centrality in order to understand the impact of each bank failure on the system.

This paper is organized as follows: section 4.2 reviews the main literature linked to our work, highlighting both the contributions in the multi-layered network theory and the agent-based interbank models; section 4.3 introduces the multi-layered interbank market and explains how the structure is calibrated on a real dataset; section 4.4 explains the model we use for investigating systemic risk; section 4.5 presents details

[1] A pioneering work in this direction was initially proposed by Nier et al. (60), while a summary of the results coming from this branch of literature can be found in Upper (67).

about the implementation of the model and the results from our simulation engine; section 4.6 introduces our measures for the systemic importance banks, and shows how the measures can be used to monitor systemic risk in the system; section 4.7 concludes and provides some policy implications.

4.2 Literature Review

In the past years, especially after the last financial crisis, a large amount of studies have emerged analyzing the financial system, and in particular the banking sector, from a network perspective. An early, seminal contribution to this literature is Allen and Gale (4). Starting from the model of Diamond and Dybvig (30), the authors introduce an interbank liquidity market which enables banks to insure each other against liquidity shocks. Although in normal conditions such an interbank market can improve the stability of the financial system, in case a large shock hits one of the banks, the bank may fail and induce losses to its counterparties. These losses can subsequently potentially cause other defaults, therefore creating a domino-effect. The authors show that when the underlying network structure is complete (each bank is connected to all the others) the system is much more resilient due to risk sharing, while incomplete networks are much more fragile since banks find it more difficult to diversify their portfolio structure against idiosyncratic shocks.

Nier et al. (60) show in their work how the topological features of the interbank network can be related to the financial stability of the system. Surprisingly, the results highlight that the higher the risk-sharing among banks, the higher the size of the domino effect (up to a certain threshold value for the connectivity between banks) in case of a shock hits one of the banks in the system. Furthermore, they show that increasing the level of capitalization will reduce the number of defaults in case a shock hits the system, and this effect is strongly non linear. Other studies concerning the interbank network, e.g. Gai and Kapadia (34), clearly show the dualism of interbank connections: on one side, they are necessary in order to pool idiosyncratic risk of single institutions and improve the efficiency of the banking sector. On the other side, interbank connections turn to be channels for the propagation of local shocks through the whole system. In Iori et al. (46) a dynamic model of the banking system, where banks can interact with each other through interbank loans, is used to show the stabilizing role of the interbank lending. Lengnick et al. (53) develop an agent-based model of a monetary economy, composed of three types of agents, i.e. banks, households and a central bank. The model endogenously allows for the creation of credit relationships among banks (the interbank market) and between banks and households (the credit market). They analyze how the formation of the interbank market endogenously creates systemic risk, and in particular it stabilizes the economy in normal times, but amplifies contagion during crises. A summary of the results coming from this branch of the literature can be found in Upper (67).

From a supervisory and macroprudential viewpoint, it is therefore necessary to measure and monitor the stability of the banking system as a whole, in parallel to the situation of the single financial institutions. In this respect, different measures of systemic risk have been developed, and a taxonomy of these measures is provided for example in Bisias et al. (16). In this non-exhaustive review of the interbank contagion literature we focus only on measures based on network analysis and systemic financial linkages. In Eisenberg and Noe (31) a recursive algorithm to find the clearing payment vector that clears the obligations of a set of financial firms is provided. In addition, the authors provide information about the systemic risk faced by each institution. In Battiston et al. (8) a measure based on network feedback centrality is introduced, the so-called *DebtRank*; this measure is used to analyze a dataset concerning the FED emergency loans program to global financial institutions during the period 2008-2010. The results show how, at the peak of the crisis, all the largest institutions served by the FED program became systemically important at the same time. In Hałaj and Kok (41) an approach to generate interbank networks with realistic topologies is presented. Furthermore, the authors expand the Eisenberg and Noe (31) algorithm to include fire-sales effect. Delpini et al. (29) study the Italian electronic trading system (e-MID) with tools borrowed from statistical physics to find the key players on a liquidity overnight market. Interestingly, the drivers of the market (ie the nodes which are crucial for the functioning of the interbank market) are often not the *hubs* neither the largest lenders in the system. We highlight that in all these contributions, results are always restricted to contagion or spillover effects related to one particular segment of the interbank market, which usually is the interbank claims banks have on each other.

The branch of the literature closer to our contribution is probably the one concerning dynamic interbank models. These discrete-time models usually allow to include some realistic microeconomic behavior for the banks on top of the network structure. An example can be found in Bluhm et al. (18). The authors study systemic risk in a banking system where financial institutions are linked to each other through interbank lending, and firesales by one institutions affect the capital of all the others, since the price of the (mark-to-market) assets in the secondary market is endogenous in the model, and driven by the liquidity needs of the banks. The authors also introduce a gametheoretical approach to identify the contribution of each bank to systemic risk, and use this measure to develop an optimal charge to reduce financial instability. Georg (35) develops a dynamic banking system where banks are allowed to optimize their portfolios of investments and they receive random fluctuation in their deposits. With this agent-based model, the author shows how the topology of the interbank market affects the stability of the system. In particular, he shows that contagion effects are larger in random network than in scale-free network, the classical structure of real world networks. He also investigates the role of the central bank in the interbank market, and in particular how the level of collateral which is accepted by the central bank affects financial stability. The results show that an abundant provision of liquidity by the central bank leads to a reduction of the liquidity banks exchange with each other on the interbank market. Ladley (52) develops a model of a closed economy composed of households which can deposit their funds in a banking system and require loans for their private investments, and banks which learn through genetic algorithm how to better allocate their resources in order to maximize their expected returns. Since banks can lend also among each other, bad investments taken by households can trigger domino effects among the banks in the system. Banks in the model are subject to regulation, and the aim of the model is to qualitatively show the link among regulation, interbank network structure, and the likelihood of a contagion. The results show that for high levels of connectivity the system is more stable when the shock is small, while the spillover effects are amplified in case of larger initial shocks. Hałaj and Kok (42) similarly introduce an agent-based model where banks optimize their risk-adjusted returns. The model is used to study the emergence of network structures when adjusting some key (macro-prudential) policy parameters.

Despite the huge number of contributions in network theory aimed at the identification of *important* nodes in a graph, a lot of work still has to be done for what regards multi-layered (ML) networks which are the topic of this paper. In different fields, from telecommunication engineering to sociology, ML system are a natural representation of the reality. Examples are the Open Systems Interconnections (OSI) model, used to abstract the real internal structure of a communication system into different functionality layers, or the several ML social network model which encapsulate in different layers the different natures of possible social connections among people. Financial systems are another example of multi-layered network, given the several kinds of connections that can exist among banks balance sheets. Recently, Gómez et al. (39) showed that a diffusion process, modeled as a flow traveling on the network from node to node, can be extremely amplified in case the same set of nodes is connected through multiple layers.

The linear equations they propose in order to analyze the model are hardly applicable to cases when the nodes have a non trivial internal structure and the contagion mechanisms change from layer to layer, but the results clearly claim the necessity to study ML systems from a different perspective than their single-layered counterparty.

We contribute to the literature in two main dimensions. First, we study how different segments of the interbank markets, and the related risks arising from them, interact with each other in an holistic view of the financial system. Second, we introduce a new measure for systemic importance institutions which embodies information regarding both the network structure of the multi-layered financial system, which can be extracted with classical tools borrowed by network theory, and the balance sheets of the banks.

4.3 Multi-Layered Financial Systems

A natural way to study highly interconnected systems is network theory. Network theory provides a rich set of tools to assess the centrality (or systemic importance) of the members of a network of nodes. In this paper, each node in the network represents a bank; importantly each node will be equipped with a non-trivial internal structure, representing the banks' balance sheets. This is crucial, since abstracting from a realistic internal structure for the node means to disregard the realistic and interesting effects linked to limited liabilities and capital absorption. Moreover, a key aspect of this paper is to analyze the interconnectedness between banks in a multi-dimensional space. Banks in reality are connected through several kinds of relationships, directed and undirected, with different maturities. In order to encapsulate this level of complexity, we use a multi-layered instead of a single-layered network. We formally denote a *multi-layered* network by a triple $\mathfrak{G} = (V, \mathbf{W}, L)$, where V is a set of nodes, common to all the layers, L is a set of labels indicating the different layers, $\mathbf{W} = \left(W^1, W^2, \ldots, W^l\right)$ is a set of matrices, with the same cardinality of L, representing the network topologies in the different layers.

In this study, we concentrate in particular on three layers, which represent three different kinds of dependencies among banks that were reveled to be fundamental during the last financial crisis: (i) long-term, direct bilateral exposures, reflecting the lending-borrowing network; (ii) short-term direct bilateral exposures, reflecting the liquidity network; and (iii) common exposures to financial assets, measuring the network of overlapping portfolios[1]. Consequently, we will label layers l_1 and l_2 for the long-term

[1] It should be noted that several other layers can be added to the multi-layered framework, for

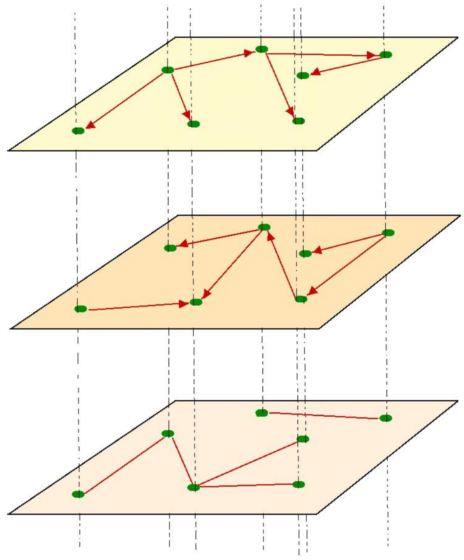

Figure 4.1: An example of triple-layered network, where the same set of nodes belong to each of the three layers, each characterized by its own topology. The first two layers contain directed networks, meanwhile the last one is undirected. The different neighbors in the different layers give the multi-layered networks completely different system dynamics during shock propagation, since the number of affected nodes can drastically be increased due to the multi dimensional structure of the system.

and short-term bilateral exposures, respectively, which are weighted and directed, and the layer l_3 for the common exposures which is an undirected and weighted network[1].

In layer l_1 a link from node i to node j represents a long-term loan from bank i to bank j, and the load W^1_{ij} on the edge represents the amount of the loan. If bank i defaults, losses in this layer are transmitted through the counterparty channel: the creditors of bank i are directly affected, since its failure can potentially results in the inability of the bank to pay back (partially or totally) its outstanding loans. The losses thus incurred would directly affect the capital of the creditor banks. Layer l_1 therefore embodies interbank counterparty risk; differently from the case in which banks lend to isolated firms, when the borrower is a bank that immerses in a network of credit relationships, its probability of defaults depends also on its own counterparties, which in turn depends on the conditions of their debtors, and so on. Interbank counterparty risk therefore is more complicated to estimate than risks related to non-bank counterparties, especially because banks usually do not have the complete information about the full network of exposures.

For what concerns layer l_2, the 2007-9 financial crisis illustrated that the short-term

example the layers representing the network of collaterals and the network of derivatives exposures. Obviously, the inclusion and calibration of other layers require more data, not available to us, that would increases the correctness of the results.

[1]The kind of network arising in layer l_3 depends on the definition used to compute the amount of overlapping securities portfolios. Different definitions can bring to directed and weighted networks as well.

interbank funding market can play a crucial role in the propagation of shocks. Even well-capitalized financial institutions, which heavily rely on some form of short-term debt for financing their balance sheets, can get into trouble when the liquidity in the interbank markets suddenly disappears. This happens if banks start (for whatever reason) to hoard liquidity instead of making it available on the market. The introduction of layer l_2 aims at capturing this funding risk. A link from node i to node j represents a short-term loan from bank i to bank j. The risk for bank j is that the debt will not be rolled over, and therefore layer l_2 embodies funding risk. We note the necessity to use different layers in order to encapsulate different maturities in the interbank connections, which bring to different contagion mechanisms during a shock propagation.

The third layer l_3 is meant to reflect the situation where two banks invest in the same financial product(s). This would imply that their balance sheets can be correlated, in the sense that asset price induced problems of one bank can increase the probability of financial stress of the other bank. Losses can induce one or more banks to firesale that particular financial product, and the resulting decline in its price will affect the balance sheets of the indirectly connected banks which hold the same asset marked to market. Layer l_3 aims at reproducing such interdependencies among banks' balance sheets, and therefore embodies the liquidity risk banks face. A link between bank i and bank j exists if the two have some common mark-to-market assets in their balance sheets, and the load on the edge represents a measure of the strength of the correlation among them. In this layer, as already highlighted, shocks are transmitted through an indirect channel.

Funding risk and liquidity risk are instead intrinsically related to each other. Funding risk refers to the condition for which a bank is suddenly unable to raise liquidity, in this framework exemplified by the short-term interbank market. This can happen for several reasons: bad news about the financial institution leads to a deterioration of its creditworthiness, a common hoarding behavior by banks due to the fear of bad times ahead, or a real deterioration of the quality of the assets of the bank. If the bank is used to fund its assets through short-term loans, the inability of the bank to roll over its debt can force it to firesale some of its financial assets, which would have negative implications on the price of those assets. When assets prices fall down, deteriorating balance sheets may force firms which face capital ratio requirements to adjust their portfolios, perhaps by trying to hoard liquidity and capital. This mechanism can create liquidity spirals which amplify shocks (Brunnermeier (21)).

4.4 Model for the Interbank Network

The model described in this section will be used for the analysis of systemic risk in this paper, and it is designed to capture important features of a real financial system. The system is composed of N interconnected financial institutions (hereafter, banks) and M financial securities. Banks' balance sheets are here composed of securities e_i, long-term interbank loans l_i^l, short-term interbank loans l_i^s, cash c_i, and other assets including all the other banks activity that will not be used in our model, o_i^a; i.e. total assets can be expressed as follow: $a_i = e_i + l_i^l + l_i^s + c_i + o_i^a$. Liabilities include long-term interbank borrowing b_i^l, short-term interbank borrowing b_i^s, deposits d_i, and other liabilities not used in the model, o_i^l. i.e. total liabilities can be expressed as: $l_i = b_i^l + b_i^s + d_i + o_i^l$. The balance sheets equality holds:

$$a_i = l_i + eq_i \tag{4.1}$$

where we call eq_i the equity of bank i. The securities portfolio of each bank are composed of a certain number of financial securities s_μ, $\mu = 1, 2, \ldots, M$. So we can formally write $e_i = \sum_{\mu=0}^{M} s_\mu^i \cdot p_\mu$, where p_μ is the price of the security μ and $s_\mu^i \geq 0$ is the amount of security μ in the portfolio of bank i. Banks' portfolios are assumed to be marked to market, and the price of the securities is endogenously determined in the model. The financial system can be mapped through the three weighted matrices described in section 4.3: W^1 describes the long-term interbank exposures, W^2 the short-term interbank exposures and W^3 the common exposures among banks.

Banks have to keep their risk-weighted capital ratio above a certain threshold value, and they have to fulfill a liquidity requirement. The risk-weighted capital ratio is computed as:

$$\gamma_i = \frac{a_i - l_i}{w^{ib} \cdot (l_i^l + l_i^s) + \sum_{\mu=0}^{M} w^\mu \cdot s_\mu^i p_\mu + CRWA_i} \tag{4.2}$$

where w^{ib} represents the weight for interbank assets, fixed here at 0.2, and w^μ are the weights for the financial assets, which are inferred from our data set; $CRWA_i$ represents the part of the risk-weighted assets which is not used in our model, and therefore is a constant. The first constraint banks have to fulfill is:

$$\gamma_i \geq \bar{\gamma} \tag{4.3}$$

where $\bar{\gamma}$ is the minimum capital requirement. The second constraint banks have to fulfill is:

$$c_i \geq \beta \cdot (d_i + b_i^s) \tag{4.4}$$

where β is the parameter representing the liquidity buffer.

In this model, a bank can suffer losses for two reasons: (i) some of its counterparts fail and are unable to pay back the debt, or (ii) the price of some of its securities declines. The price of each security is endogenously determined in the model, and it is described by the following equation:

$$p_\mu = p_\mu^0 \cdot exp\left\{\frac{-\alpha_\mu \cdot \sum_i^N sell_\mu^i}{\sum_i^N s_\mu^i}\right\} \tag{4.5}$$

where $0 \leq sell_\mu^i \leq s_\mu^i$ is the amount of security μ sold by bank i, and α_μ is a positive constant representing the deepness of the market for that security.

If the bank's capital ratio in eq. (4.2) becomes lower than $\bar{\gamma}$ after it books some losses, the bank can increase it in two ways: reducing its short-term interbank exposure, or selling securities. Since the cheapest way of increasing the risk-weighted capital ratio is to reduce interbank exposures, as long as $l_i^s > 0$ each bank first prefers to follow this way[1]. Similarly, if the bank has to raise liquidity in order to fulfill the requirement expressed in eq. (4.4), it will first withdraw liquidity from the short-term interbank market, and if this is not enough, it will liquidate part of its portfolio. If a bank is not able to fulfill the capital requirement, it defaults. When a bank defaults, it is first liquidated, so all its securities are sold (if any) and it withdraws all its funds from the short-term interbank market, and then it tries to pay back its creditor banks. The default of a bank involves three risks for the other banks: (i) counterparty risk, associated with the possible losses from the long-term interbank market, (ii) funding risk, associated with the possibility of losing funds from the short term interbank market, and (iii) liquidity risk, associated with firesales of marked to market financial securities.

[1] In this model, withdrawing funds from the short-term interbank market is the cheapest way to raise liquidity, since it does not involve any capital losses like the ones associated with firesales. Nevertheless, in reality a bank might prefer to sell assets if the market is deep enough to absorb the sales without resulting in large depreciation of the value of the assets. In any case, the dynamics reproduced in this model represents a possible series of events in case banks stop trusting each other inducing them to hoard liquidity rather than retain funds in the interbank market.

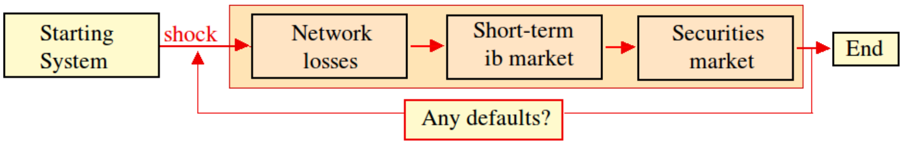

Figure 4.2: The Figure represents the dynamics of the model. Starting from the system at equilibrium, we shock it, usually by letting default one or more banks at the same time. Subsequently, the sequence of events in the shaded area of the figure is iterated till the number of defaults stops increasing; at the beginning of each (short-term financial) period, banks book losses coming from the default of their creditors during the previous period, if any; in a second step, they decide the percentage of debt to roll-over to their borrowers in the short-term interbank market; in the last step, banks which have liquidity needs liquidate part of their securities holdings.

4.4.1 Model Dynamics

The model dynamics is reported in Fig. 4.2. Starting from a particular configuration of the multi-layered network $\mathfrak{G}$ of banks with heterogeneous balance sheets, we shock the system and then repeat the same sequence of events, representing a short-term financial period, until when the cumulative number of defaults stops increasing.

At the beginning of each period, banks book eventual losses from the interbank market due to the bankruptcy of their debtors in the previous period. Those losses immediately affect the capital of banks, and therefore their risk-weighted capital ratio described in eq. (4.2). If a bank's risk-weighted capital ratio remains above the threshold value $\bar{\gamma}$, then it will not react to the losses. Otherwise, it will first try to reduce its short-term interbank exposures. Indeed, during each period, banks have to decide which percentage of the short-term debt they want to roll-over to their debtors. This choice depends both on the internal needs of banks, due for example to losses coming from the long-term interbank market, which causes a reduction of the risk-weighted capital ratio of the bank under the threshold value $\bar{\gamma}$, or due to the fact that its own funding from other creditors bank is reduced, forcing it to withdraw money from the short-term market. This loop is properly described by the following map:

$$\vec{f} \cdot \vec{l^s}^\intercal = min\left(\vec{r} + max\left(W^2\vec{f} - \vec{c_{buf}}; 0\right); \vec{l^s}^\intercal\right) \tag{4.6}$$

where $\vec{f} = (f_1, f_2, \ldots, f_N)$ is the percentage of funds withdrawn by each bank from the short-term interbank market ($f_i \in [0,1]$, $i = 1, 2, \ldots, N$); $\vec{r} = (r_1, r_2, \ldots, r_N)$ is the amount each bank wants to withdraw for liquidity and capital reasons; $\vec{l^s} = (l_1^s, l_2^s, \ldots, l_N^s)$ is the total short-term exposure of each bank; and $\vec{c_{buf}} = (c_{buf,1}, c_{buf,2}, \ldots, c_{buf,N})$

is the total amount of cash each bank has out of its liquidity buffer, if any: $c_{buf,i} = max\left[c_i - \beta(d_i + b_i^s); 0\right]$. The capital and liquidity needs are computed in order to restore the required level of cash and risk-weighted capital ratio according to the bank's constraints. We have from equation (4.4):

$$r_i^{liq} = min\left(l_i^s; \frac{\beta(d_i + b_i^s) - c_i}{1+\beta}\right) \tag{4.7}$$

which is larger than zero as far as $c_i < \beta \cdot (d_i + b_i^s)$. If $c_i \geq \beta \cdot (d_i + b_i^s)$ the banks has no liquidity needs to fulfill, and therefore $r_i^{liq} = 0$. In the same spirit, we compute the amount to withdrawn due to the risk-weighted capital ratio constraint; from equation (4.3) we have:

$$r_i^{cap} = min\left(l_i^s - r_i^{liq}; \frac{\gamma_i(CRWA_i + \sum_{\mu=0}^{M} w^\mu \cdot s_\mu^i p_\mu) + \gamma_i w^{ib} \cdot (l_i^l + l_i^s - r_i^{liq}) - eq_i}{\gamma_i w^{ib}}\right) \tag{4.8}$$

r_i^{cap} is larger than zero as far as $\gamma_i < \bar{\gamma}$. If $\gamma_i \geq \bar{\gamma}$, then $r_i^{cap} = 0$. The final amount to withdraw will be so $r_i = r_i^{liq} + r_i^{cap} \in [0, l_i^s]$. All in all, equation (4.6) simply states that each bank withdraw funds from the short-term interbank market only in case it has to fulfill its liquidity or risk-weighted capital ratio requirement, and in case other banks decide to withdraw their funds from its liabilities and the cash it has is not enough to pay back those creditors.

Once banks decide about how much to withdraw from the interbank market, they may still need to sell securities in order to pay back eventual creditors and to restore the required levels of liquidity and capital buffers. As described by eq. (4.6), banks first use their available liquidity to pay back creditors, and if this is not enough they withdraw funds from the short-term interbank market. In case they still need liquidity, they have to liquidate some securities. We can indicate with $Z \in \mathbb{R}_{N\times M}$ the matrix whose entries $Z_{i\mu} \geq 0$ indicate how many securities of kind μ bank i has to sell in order to fulfill its needs. Since the securities prices are adjusting according to eq (4.5), we use a modified version of the map introduced by Eisenberg and Noe (31) in order to compute both matrix Z and the clearing vector $\vec{p}$ which resolves the system. We have:

$$\vec{p} = min\left[\vec{l}; \Pi^\intercal \cdot \vec{p} + \vec{c} + Z \cdot \vec{v}\right] \tag{4.9}$$

where we denoted with Π the matrix with the relative obligations among banks, that is:

$$\Pi_{ij} = \frac{w_{ji}^2 f_j}{\sum_j w_{ji}^2 f_j} \tag{4.10}$$

The vector $\vec{l}$ represents the total obligations of the banks towards the other institutions, that is:

$$l_i = \sum_j w^2_{ji} f_j \tag{4.11}$$

and $\vec{v}$ is the vector indicating the value of each security, according to eq. (4.5).

In turn, the matrix Z is computed as the sum of three components, which are the liquidity needs driven by obligations towards other banks in the system, the liquidity needs driven by the requirement expressed in eq. (4.4), and the liquidity needs driven by the capital requirement expressed in eq. (4.3). In more details, they can be formalized as follows: suppose there is only one security in the system, the generalization to the case of several securities is then straightaway; in this case, the matrix Z becomes a vector, again composed by three parts; the first part is:

$$Z^{ib} = min\left[max\left[0; \frac{\vec{l} - \vec{c} - \Pi^{\intercal} \cdot \vec{p}}{p_\mu}\right]; \vec{s}\right] \tag{4.12}$$

where we indicated with $\vec{s} = (s_1, s_2, \ldots, s_N)$ the amount of securities each bank still have in its portfolio. This is the component driven by the credit line reduction in the short-term interbank market.

The second components is:

$$Z^{liq} = min\left[\frac{max\left[0; \vec{c} - \alpha(\vec{d} + \vec{b^s})\right]}{p_\mu}; \vec{s}\right] \tag{4.13}$$

This component takes into account for the liquidity requirements of banks.

Eventually, there is the component due to the necessity of fulfilling capital requirements, which is larger than zero if also by withdrawing all their funds from the short-term interbank market they still need to increase their risk-weighted capital ratio:

$$Z^{cap} = min\left[\frac{w^{ib}\vec{l^{ib}} + w^{\mu}p_\mu - \frac{\vec{eq}}{\bar{\gamma}}}{w^{\mu}}; \vec{s}\right] \tag{4.14}$$

The sum of these three components represents the total amount which appears in eq. (4.9) : $Z = Z^{ib} + Z^{liq} + Z^{cap}$. The generalization to the case of multiple securities is simply derived as follow: each bank tries to sells the first type of security in its portfolio; if the bank sell all those securities, it moves to the second type of security, and so on, up to the point when it fulfills its liquidity needs. Alternatively if its liquidity needs cannot be fulfilled, the bank will have to sell all its securities.

After the payment vector $\vec{p}$ is computed, banks which are not able to pay back their creditors or to fulfill their Risk-Weighted Capital Ratio (hereafter RWCR) are declared in default, they are liquidated and eventual losses are transmitted through the long and short-term interbank market at the beginning of the next period. The dynamic is repeated till the cumulated number of defaults, namely the sum of the number of defaults in each short-term financial period, stops increasing. It should also be noted here that in our framework a bank can default for two different reasons: first, it can be unable to fulfill liquidity or capital requirements, second, it may be illiquid and become unable to pay back its debtors.

In the model, bank's actions directly affect the link weights in layers l_2, by withdrawing liquidity from the short term interbank market, and l_3 by selling securities and thus reducing the portfolio overlap with other institutions. On the other hand, layer l_1 only changes when defaults occur. The model does not allow the banks to create new links in the three layers. This represents a crisis period with banks hoarding liquidity instead of making it available on the short-term interbank market. Since the scope of the paper is to investigate the financial resilience of the network structures observed in real interbank markets, we abstract from modeling micro founded network generating mechanisms, but instead we sample the multi-layered networks from a distribution calibrated on real data, as shown in the next section. We also note that the three layers are characterized by different time scales in reality: layer l_3 changes rapidly, layer l_2 somewhat slower, and layer l_1 evolves the slowest. This issue has to be addressed in future research where bank decisions may feed back into the network topology, potentially leading to different dynamics at the systemic level. The results of our simulations can thus be seen as a lower bound for system stability, where banks act under distress.

4.4.2 Data Set

Our dataset consists of a sample of 50 large EU banks. For each bank, we include information about capital, short-term and long-term interbank borrowing, deposits, short-term and long-term interbank loans, aggregate securities holdings[1], and cash. The distinction between short and long-term interbank assets reflects the maturity of the loan which can be below or above three months. We also know the RWCR of banks, from which we can reconstruct the mean weights for the financial securities of each bank. The data sources are the banks' annual financial reports, and Bureau van Dijk's Bankscope; the balance sheets data refer to the end of 2011. Figure 4.3 shows the

[1] As securities holdings, we use the sum of *Securities Held for Trading*, *Securities Held at Fair Value* and *Available for Sale Securities*.

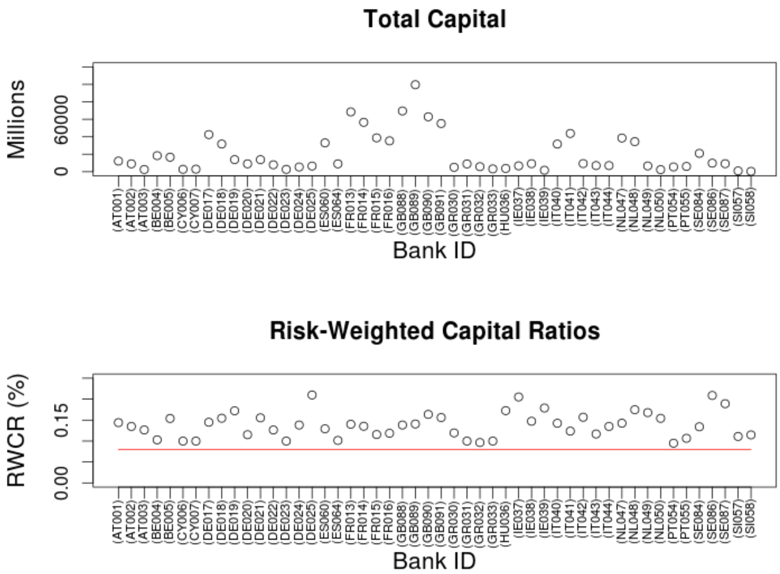

Figure 4.3: In the upper panel, the equities of the 50 banks in our sample, in millions. In the bottom panel, the Risk-weighted Capital Ratio of the banks; the horizontal red line represents the standard Basel capital requirement of 8%. The figure highlight a high level of heterogeneity in the sample, both in term in total equity and in term of Risk-weighted Capital Ratio.

total capital across the banks in the sample, and their Risk-Weighted Capital Ratios, revealing a high level of heterogeneity. The horizontal red line in the lower panel of the figure represents the standard Risk-Weighted Capital Ratio requirement equals to 8%, as specified in the Basel standards. The aggregate short-term interbank exposures in the system amount to about €1.2tn and the aggregate long-term interbank assets amounts to €900bn.

We do not have data on individual banks' bilateral exposures, neither on the details of financial securities portfolios. Instead, we use this uncertainty as degree of freedom of the model, in order to investigate which multi-layered network structures are particularly prone to a systemic breakdown. In principle, every possible network in each of the three layers represents a plausible configuration for the multi-layered network structure; in order to focus only on the interbank networks which are the most probable in the real financial system, we extract the network topologies for the short and long-term interbank exposures according to a probability matrix, with the only restriction that each bank is exposed to other entities at most for the 20% of its total interbank assets. A probability matrix P^G is a matrix which entries p_{ij}^G specify the probability of existing of the directed link $i \to j$, representing a loan from bank i to bank j. The probability matrix is built upon the European Banking Authority (EBA) disclosures on the geographical breakdown of individual banks' activities as disclosed in the context of the EU-wide roll stress test. The methodology is based on Hałaj and Kok (41), and networks in layers l_1 and l_2 are generated as follow: banks are randomly extracted from the sample, and for each bank we sequentially generate links according to the probability matrix; for each link, a random number from a uniform distribution on $[0, 1]$ is extracted, indicating what percentage of the residual interbank assets of the first bank is deposited in the interbank liabilities of the second. Formally, for the jth link generated in layer l_1 from bank i we have:

$$l^1_{ij} = \epsilon_{ij} \left(l^l_i - \sum_{k=1}^{m} l^1_{ik} \right) \tag{4.15}$$

where $\epsilon_{ij} \sim U(0, 1)$, and $\{l^1_{i1}, l^1_{i2}, \ldots, l^1_{im}\}$ are the links in layer l_1 starting from node i generated in the previous m steps of the algorithm. A similar expression can be written for layer l_2. The amount in eq. (4.15) is properly truncated to take into account the limited liabilities of the borrowing bank, and the constraint that each bank is exposed to no more than 20% of its total interbank assets to each other bank. This constraint excludes network realizations where a bank lends all its interbank assets to a single counterparty, a situation hardly met in reality.

In contrast, the network in layer l_3 is randomly generated, since we do not have sufficiently granular data or statistics concerning the securities portfolio structures of the banks in the sample. We only have information about individual banks' aggregate amount of securities. This random network generation is conducted by first choosing the number M of securities to use in the simulations, and subsequently building a random bipartite network between the N nodes and the M securities: in this network a link from a bank i and a security μ means that the bank has in its portfolio that particular security, and the amount of the shares is represented through the weight of the edge. Each link in this bipartite network has the same probability p to exist. In the baseline setting we assume that, for each bank, all the out-coming links have the same weight. Starting from this random bipartite network, there are different ways to build the network of the overlapping portfolios, and an example is:

$$W^3_{ij} = \sum_{\mu=1}^{M} \frac{s^\mu_j}{s^{tot}_j} \cdot \left[max \left[1; \frac{s^\mu_i}{s^\mu_j} \right] \right] \tag{4.16}$$

In this setting, the weight of the directed link from bank i to bank j is the proportion of the portfolio of bank i that overlaps with the portfolio of bank j.

We note that the topology of the multi-layered network is the only degree of freedom in the simulations, since banks' balance sheets are always kept fixed and calibrated according to our data. Therefore, all the degrees of randomness would be completely removed in case of full knowledge of direct bilateral exposures for the long-term interbank market, exposures on the short-term interbank market, and more granular information on banks' portfolios.

4.4.3 Topological properties

The networks in layers l_1 and l_2 generated with the algorithm proposed in the previous section have link weights which depend on the order of drawn linkages. For a given bank i, the first drawn link (i, j) would on average carry 50% of bank i's interbank assets (before the truncation due to counterparty's liabilities and limited exposures), the second drawn link 25%, and so on. Since we do not have data for a proper calibration of link weights, we are implicitly assuming that banks trade more loan volumes with their more frequent counterparties. We note that, if the number of simulations is large enough, several different scenarios will be generated, including situations where nodes have many linkages of similar size. Moreover, the use of a probability matrix to randomly generate the networks in the different layers does not take into account for the possible statistical dependency of two links to exist in the same network. Again, without proper data, it can be difficult to reproduce such a correlation structure in the links formation.[1]

Networks produced in this way show some of the most common statistical regularities found in real interbank networks, as documented in Boss et al. (19), De Masi et al. (28), Lux and Fricke (55) and Bargigli et al. (5). Such regularities are heterogeneity of nodes' degree, disassortative mixing, i.e. the tendency of high degree nodes to connect with low degree nodes, sparsity, and a Jaccard similarity among different layers similar to the one found in real multi-layered interbank networks.

More in detail, Fig. 4.4 shows the total degree distributions for layers l_1 and l_2; the two graphs highlight a high level of heterogeneity in the nodes' degree, meaning that most of the nodes have very few connections, and few nodes have many connections to

[1] The network generating algorithm we use implicitly assumes independence between links. Without having data to calibrate a possible correlation structure, and without using an underlying model for the link creation mechanism based on micro behavioral rules, assuming independence seems the most neutral way to test the stability of the financial network. Nevertheless, a large number of simulations should be able to reproduce also real life situations where links are dependent random variables.

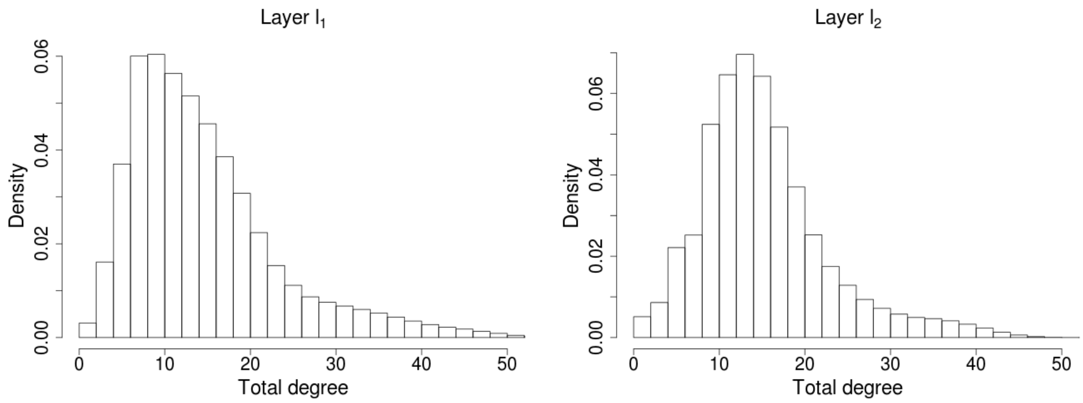

Figure 4.4: The LHS figure shows the total degree distribution of layer l_1, and the RHS figure shows the distribution for layer l_2. A clear level of heterogeneity among nodes' degree is evident in both the layers.

the other banks in the system[1].

Among others, a way to capture assortative mixing in a network is by examining the properties of the average nearest neighbor degree as function of vertex degrees, usually indicated as $\langle K_{nn} \rangle$, and defined as:

$$\langle K_{nn}(k) \rangle = \sum_{k'} P\left(k'|k\right) \cdot k' \tag{4.17}$$

where $P\left(k'|k\right)$ is the conditional probability that an edge of node degree k has a neighbor of degree k'. If the above function is increasing, the network shows an assortative mixing, since node with high degree tend (on average) to connect to nodes with high degree. Alternatively, in case function 4.17 is decreasing, the network shows a disassortative mixing, since nodes with low degree tend to connect with high degree nodes, and vice versa. Figure 4.5 shows a clear disassortative mixing in the structure of layers l_1 and l_2[2]. Finally, we report a mean density for layers l_1 and l_2 equal to respectively 14% and 12%.

We eventually introduce a measure for the similarity among the topologies in the different layers, since this measure will be used to analyze the results from the simulation engine. Generally speaking, given two networks G_1 and G_2, we use the Jaccard index $J_{12} \in [0; 1]$ to describe the similarity among the networks (see Appendix for a

[1]Also if we use the same probability matrix P^G for the two layers l_1 and l_2, the final topologies can be different due to the role played in the generating algorithm by short and long-term interbank exposures.

[2]The non monotonic trend, observed in the left panel of the figure, arises directly from the combination of the probability matrix P^G and the banks balance sheets.

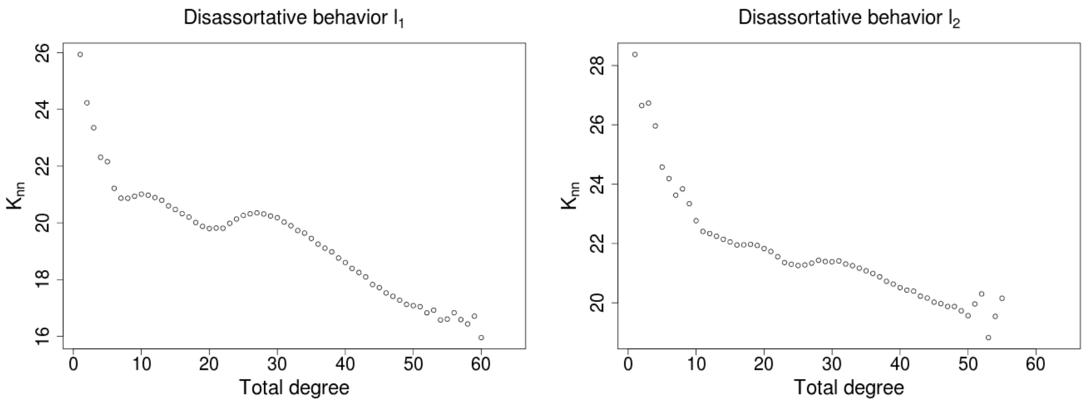

Figure 4.5: The LHS figure shows the disassortative behavior for layer l_1, while the RHS shows the same for layer l_2. As means to capture the assortative mixing is by plotting the average nearest neighbor degree as function of vertex degrees. A decreasing trend means that the network is dissortative, since nodes of high degree tend to connect to nodes of lower degree.

formal definition). This index will be equal to 0 when G_1 and G_2 have no links in common, and it will be equal to 1 when the two networks are identical. As documented in Bargigli et al. (5), values of Jaccard index for different layers in the same interbank market range roughly about between 0.1 and 0.3, depending on the kind of transaction (secured or unsecured) and on the point in time the index is measured. As comparison, we can compute the Jaccard index J_{12} among layers l_1 and l_2 of our multilayer network, the Jaccard index J_{23} among layers l_2 and l_3, and the Jaccard index J_{13} among layers l_1 and l_3. The mean values and the standard deviations of these three indexes, computed over 10^5 different multilayer network structures generated according from our simulation engine, are reported in Table 4.1. The Jaccard index J_{12} for layers l_1 and l_2 is comparable to the one found in reality. Obviously, since layers l_3 are generated from a random bipartite network, we cannot expect realistic values also for the indexes J_{13} and J_{23}, which have never been measured in reality. We will use those indexes again when we study the results of our simulation engine[1].

We stress again the the choice to use three layers for the structure of the financial system is also driven by data availability. Introducing further layers without having proper data to calibrate them, would result in the introduction of a large number of

[1]A correlation structure among the networks in the different layers could, in principle, play a very important role in assessing the financial stability of the system. Yet, since we cannot calibrate it on real data, we can still measure the correlation structure appearing from the multi-layered network random generating algorithm we use, and look for possible links with the financial stability of the simulated banking system. This task is systematically addressed in section 4.5.2.

Table 4.1: Jaccard indexes. The table reports the mean values of the Jaccard indexes J_{12}, J_{13} and J_{23} for the multilayer networks generated with the algorithm proposed in Section 4.4.2, together with their standard deviations.

J	mean	sd
J_{12}	0.27	0.03
J_{13}	0.09	0.04
J_{23}	0.10	0.04

parameters, which can drastically complicate the analysis of the results. Instead, we prefer to use layers that can be (at least partially) calibrated, and at the same time that revealed to play a fundamental role in the last financial crisis.

4.5 Simulation Results

Systemic risk in interbank markets depends on numerous factors regarding both the financial status of the members of the banking system, their balance sheets, and the disposition of the linkages among them. In this paper, we keep a defined and realistic structure of banks' balance sheets, as described in section 4.4, and we investigate how the different structures for the interconnections among the agents affect the financial stability of the whole system. This is interesting for various reasons. First, it gives indications about the impact of different network structures on financial stability; second, by using classical tools from network theory, it enables us to assess each bank's contribution to systemic risk; third, it sheds light on the role of banks' capitalization on the resilience of the system.

In the baseline specification of the model, parameters are set in a way to reproduce realistic regulatory requirements on banking systems and a plausible price elasticity for the securities market. The minimum risk-weighted capital ratio requirement is fixed, according to the Basel standard, to $\bar{\gamma} = 8\%$. The minimum required liquidity buffer is fixed through the parameter $\beta = 5\%$.

The price of all M securities is initially fixed at 1: $p_\mu^0 = 1$ ($\mu = 1, 2, \cdots, M$). The elasticity factors, α_μ, are fixed at 0.2, and the number of securities is $M = 30$. In this way, banks do not have preferences about which securities to liquidate first in case of need, and the bipartite network banks-securities, which represents banks' securities holdings, is built with a Erdös-Rényi index $p = 0.2$. We will investigate later how the number of securities and the topology of the network in layer l_3 affect the results.

In the following, we consider two forms of initial shock for the system. The first one is assumed to derive from the failure of one of the 50 banks in the sample. The failure of the bank implies the liquidation of all its securities holdings, the transmission of losses on the long-term interbank market, if any, and the withdrawn of all the funds it provides in the short-term interbank market. The risk for the system hence materializes via the lack of the funding services provided by the targeted bank, together with the risk of losses transmitted through the exposure channel and the securities market. How the system reacts to this initial shock strongly depends on the topological structure of the underlying multi-layered network. The second kind of shock is assumed to derive from the depreciation of a certain percentage of one or more securities in the system. The depreciation will immediately affect the equity and the risk weighted capital ratio of the banks which have the shocked securities in their portfolios.

4.5.1 Systemically Important Banks

The importance of a bank in a banking system does not depend only on its financial situation. In fact, contagion is a process involving two main steps: the default of one or more components of the system, which in turn depends on the financial situation of the entities, and the propagation of the shock through interbank linkages. In this paper, we are interested in this second effect, namely how the network structure can affect the stability of the system after an idiosyncratic shock hits one of the banks, and part of our task is to determine which structures are more prone to financial breakdowns.

A first result from our simulation engine is a test of the impact of each bank's failure on the whole system. For this purpose, we first shock one initial bank, we call it bank b_0, and then we let the system evolve according to the scheme in Fig. 4.2 up to when the cumulated number of defaults stops increasing. The impact of each bank on the financial stability of the system is measured through the total number of defaults it produces. This number of defaults is the random variable we want to estimate the distribution of. In fact, even if the banks' balance sheets are always the same, including also the aggregate exposures of each bank towards all the others, the degree of randomness left in the structure of the financial multi-layered system produces a level of uncertainty on the number of defaults following the bankruptcy of bank b_0[1].

In order to highlight the role of each bank in the system, we present the disentangled effects from the three layers, together with the effects coming from the complete multi-layered network's structure. To this end, we first run the simulations when all the banks are only connected through the long-term interbank market, meaning that the

[1] It should be recalled that when the bank b_0 defaults at the beginning of the simulation, it is liquidated, implying that it withdraws all its funds from the short-term interbank market, it sells all its available for sale securities, and it tries to pay back its creditors on the short and long-term interbank market.

only layers presenting some edges is l_1; the only risk present in this system is therefore the counterparty risk. Then we run the same simulations with only layer l_2 activated, meaning that the only risk present in the system is the funding risk[1]. In the third scenario, we run the simulations with layer l_3 as the only active layer[2], representing the case where the only risk banks face is liquidity risk. Finally, we present the case where all the three layers are activated simultaneously.

As a benchmark example, we start to show the dynamics of the contagion process when a particular bank defaults, for one specific configuration of the multi-layered network. In particular, the red bold line in Fig. (4.6) represents the evolution of the number of defaults when all the three layers are working together. The other lines in the graph represent all the possible other combinations of active contagion channels. Simply by eye-balling, it is easy to discern that the sum of the number of defaults in the single-channel scenarios never reaches the total number of defaults for the whole system. A deeper examination reveals that this phenomenon is actually due to spiral effects: in case only one of the three layers is active, the contagion process is dampened (see Fig. 4.6). Yet when more than one channel of contagion is present, the contagion process is much more probable, and liquidity needs of one bank can result in a capital reduction of others, which have to increase their capital ratio by withdrawing further short-term funds or by liquidating their securities portfolio.

To clarify the importance of taking into account the interactions among different layers, Fig. (4.7) reports the results for bank FR014 (as example) in a more statistical fashion. The four panels in the figure show the distributions of the number of defaults in the four scenarios described above, namely when only layer l_1 is activated (top left panel), when only layer l_2 is activated (bottom left panel), when only layer l_3 is activated (top right panel), and finally when the three layers are simultaneously activated (bottom right panel). The red line in the bottom right panel represents the quantitative convolution of the three single-layered network distributions: it basically represents the linear superimposition of the three effects, and it is interesting to compare it with the distribution for the total number of defaults in the case of three active layers. In fact, the differences among the two have to be attributed to the interaction of the

[1]In those two scenarios, each bank is assumed to have a securities portfolio which is completely independent from all the other banks' portfolio in the system. Nevertheless, price is still driven by eq. (4.5), and therefore firesales can still be costly for the banks, also if there are no contagion effects due to common exposures.

[2]In this third scenario, all the interbank assets of the institutions in our sample are supposed to be directed to an external node, and all the liabilities in the interbank market are provided by this node, which does not play any other role in our financial simulator, in the sense that it never withdraws funds and it cannot fail or transmit any losses.

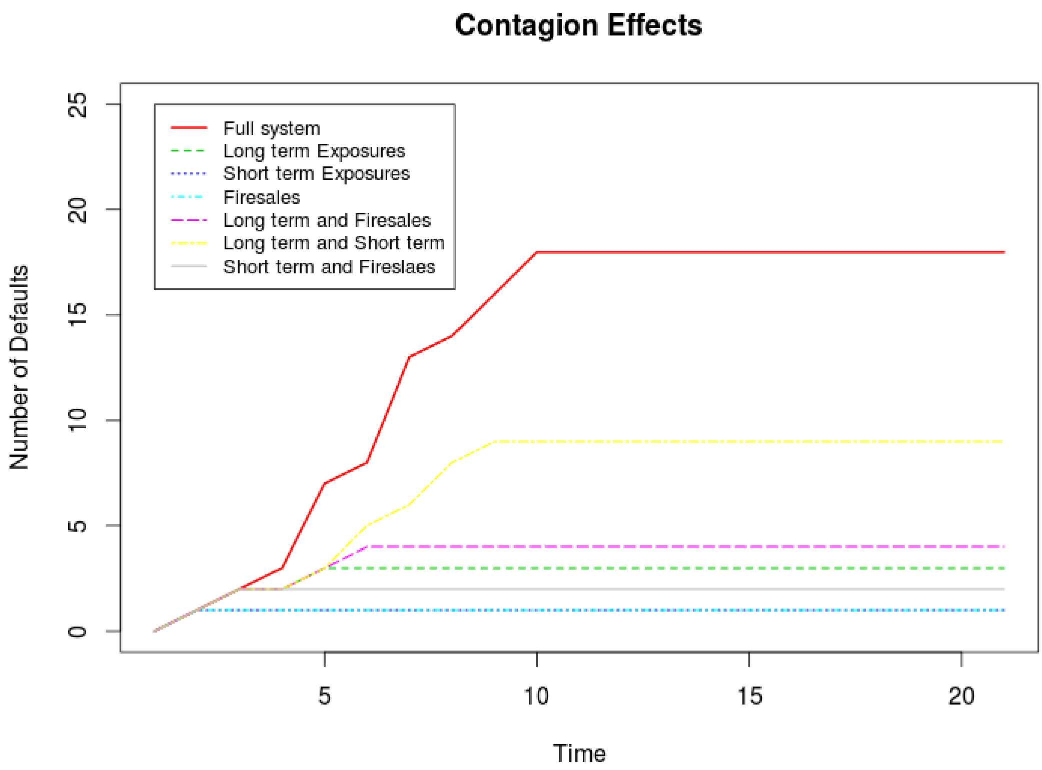

Figure 4.6: The figure shows the dynamic process when the bank fails for one particular realization of the multi graph. The horizontal axes represents the time, and the vertical axes represents the total number of defaults.

three layers.

As one can see from the figure, the default of bank FR014 results in contagion effects via only one channel, namely the short-term interbank exposures represented in the bottom left panel of the figure. Interestingly, however, the systemic importance of the bank is amplified by the presence of the other two layers in the multi-layered network. In fact, when the single layers are considered separately, the largest number of defaults is 12, reported when only layer l_2 is activated, meaning that bank FR014 is an important short-term liquidity provider. No defaults are reported when only layer l_1 is activated, and a maximum of 5 defaults can be seen when only layer l_3 is activated. Yet, when we consider the three layers working together, the largest number of defaults reported in the simulations is 42, and the distribution is much more fat tailed. As one can see from the bottom right panel of Fig. (4.7), the distribution of the number of default for the case where the three layers are simultaneously activated differs from its convolution counterpart (red line in the same panel) in the way that the three layers working together produce more mass in the tail. We will show in section 4.6 that the risk transformation process implicitly performed in banks balance sheet activities is at the core of the generation of high level of systemic risk, and this will clarify the importance to study the financial stability from a more holistic lens.

In the Appendix we report the same graphs for the most important banks in the sample. Overall, for the great majority of the banks there is no substantial contagion effects when they fail, indicating a certain resilience of the financial system against random defaults of its members. At the same time, there are a few banks whose default could have considerable contagion effects in at least one of the three layers, and this importance is extremely amplified when considering all the three layers in conjunction. The main lesson from these results is the limitations of measures of systemic risk based on single-layered networks' configurations. Single-network measures run the risk of heavily underestimating the systemic importance of banks, since they usually take into account only the counterparty risk associated with a particular segment of the interbank relations. The simulations performed with only layer l_2 activated, on the other hand, show the importance of funding risk in banking activities, as also highlighted during the last financial crisis, and how it can materialize if banks start hoarding liquidity instead of making short-term funds available on the interbank market. Moreover, the amplification of the shock due to fire sales and to non-perfectly liquid markets can greatly amplify local shocks, leading to much more dangerous configurations in which a large portion of the banking system can break down. We also note that with the selected parameters, the layer l_3 representing common exposures usually just works as amplifier for the propagation of an initial shock.

4.5.2 Systemically Important Topologies

The previous subsection showed that, given an initial defaulting bank, different topologies for the multi-layered network imply different results with respect to the stability of the financial system. And in particular, for some banks there exist critical configurations for the system such that it becomes prone to systemic breakdowns. Those configurations are the ones which populate the fat tails of the distributions of the total number of defaults highlighted in the previous subsection.

An interesting question which can be addressed with the simulation engine is weather there exist some configurations which are critical for all the banks at the same time. This is not a trivial issue. In fact, also if a topology of the multi-layered graph can make the system very vulnerable to the failure of one particular institution,

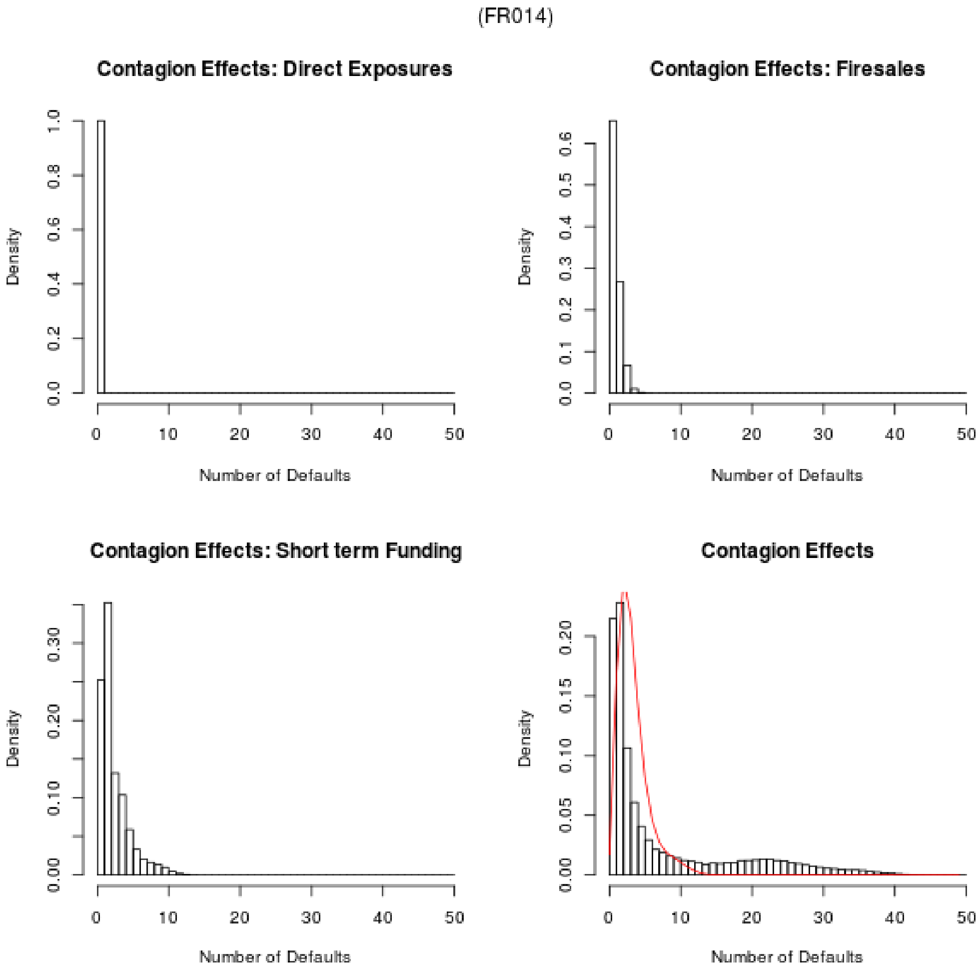

Figure 4.7: In the top left panel, the distribution of the total number of defaults when the bank FR014 defaults in our simulation engine in the first scenario, namely when the only active layer is l_1. The distribution shows the counterparty risk that the bank represents to the whole system. In the bottom right panel, the distribution of the number of defaults when the only active layer is l_2. In the top right panel the same distribution is presented for the case of layer l_3, which represents the contribution of the bank to the liquidity risk of the system. In the bottom right panel, the distribution of the total number of defaults in the case of all the three layers are active at the same time. The red line represents the quantitative convolution of the other three distributions, representing the linear sum of the three effects. Each graph is the result of 50000 realizations of the banking system.

we cannot so far say anything about the systemic importance of the other banks in exactly the same network structure. In case a very important bank for the system in terms of the financial services it provides to the other banks, assumes a central position in the network structure, systemic risk is high, since the bankruptcy of this bank can create contagion effects which affects a large number of other financial institutions. If substantial contagion occurs only in some of the simulated network structures we generate in our simulations, it means that, in those cases, the idiosyncratic risk assumed by the defaulting bank was badly distributed among the other institutions in the system. We therefore speak about systemic risk, and systemically important institutions. Moreover, the possibility that more large banks become systemically important at the same time is a much riskier situation for the entire system. Given the probability matrix P^G, we are interested in investigating the possibility of existence of systemically important topologies; formally, given a certain multi-layered graph $\mathfrak{G}$, we can compute the systemic risk associated with the structure as follow:

$$R_{\mathfrak{G}} = \frac{\sum_{i=1}^{N} d(i)}{N} \tag{4.18}$$

where we indicate with $d(i)$ the number of defaults caused by the bankruptcy of bank i, computed as the result of our simulation engine.

In order to explore the possibility and the frequency of extremely critical configuration for the banking system, we generate 10^6 multi-layered network topologies, and for each of these configurations we compute the mean value of the number of defaults produced by the initial failure of each of the 50 banks in the system, according to eq. (4.18). In this way, we associate to each network structure produced its systemic relevance, indicating the mean level of systemically importance across the banks. Obviously, since most of the banks do not produce any contagion effects upon their failure (see Appendix), the mean number of defaults will be relatively low. Figure 4.8 shows the results of this exercise. In the left panel of the picture the distribution of the systemic relevance $R_{\mathfrak{G}}$ of 10^6 multi graphs produced following the methodology described in section 4.4 is shown. It can be observed from the figure that, most of the network structures are only relevant in the case where one of the largest banks default. There exist, nevertheless, some topologies which make the financial system particularly prone to a financial breakdown. To clearly illustrate this idea, in the right-side panel of Fig. 4.8 two extreme cases are shown: in the multi network structure represented by the blue crosses, the initial bankruptcy of almost all the banks does not produce any contagion effects, a part of the case of bank 34 which triggers other 2 defaults. The systemic relevance for this structure will therefore be close to zero. By contrast, the red triangles in the same picture show a very risky configuration for the system, since the initial failure of 11 financial institutions would trigger a lot of other defaults, highlighting the financial weakness of the entire system.

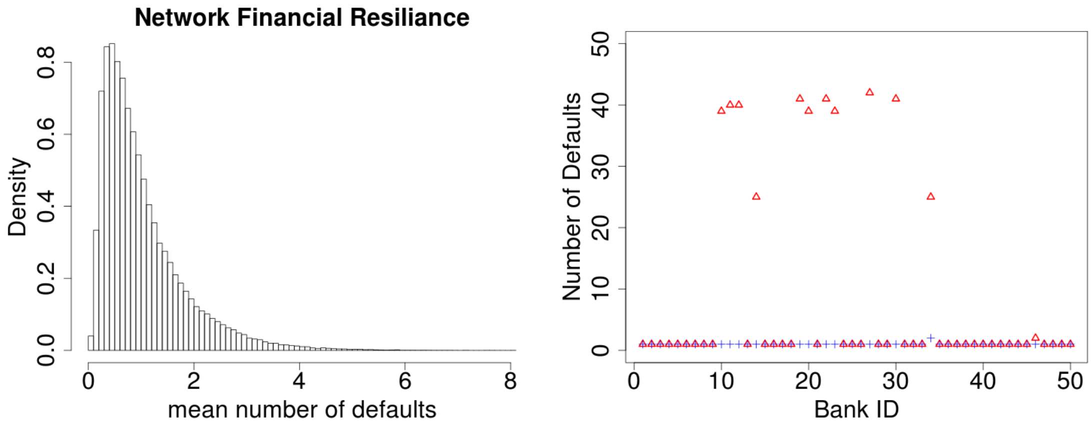

Figure 4.8: On the left panel, the distribution of the systemic relevance is plotted for 10^6 different network topologies. Each systemic relevance parameter is built by generating the same network N times, where in our case $N = 50$, and for each of this realizations we shock one of the banks in the system and we count the number of defaults: the mean value of those numbers is then used as systemic relevance for that configurations. The tail of the distribution highlights the existence of some critical configurations for the financial system. As example, we present in the right panel of the figure two cases: the network described by the blue crosses is a resilient configuration, since the defaults of all the banks does not produce any considerable effects. The network described by the red triangles, on the other, is extremely unstable, since the failure of one of the largest bank trigger a lot of subsequent defaults.

Hence, fig. 4.8 illustrates that network structures matter for the financial resilience and the proper functioning of the banking system. It should be recalled that in all the simulations the banks' balance sheets are kept constant, and therefore also the aggregate short and long-term interbank exposures. It is clear that configurations like the one in the tail of the distribution in the left side panel of Fig. 4.8 have to be avoided. In this framework, the multi-layered networks are extracted according to a particular distribution specified by the probability matrix P^G for layer l_1 and l_2 and by a random portfolios generator for layer l_3, and they are all plausible networks, in the sense that there is a certain probability for the real system to be in those configurations. In reality, however, the multi-layered network structure arises as the result of the local behaviors of a multitude of economic agents, which (supposedly) have as target the maximization of their personal interests. The experiments we performed highlights once again the necessity of having more granular data regarding banks' direct and indirect interconnections, in order to monitor the system from a global perspective and avoid it to evolve through configurations extremely prone to large breakdowns.

Consequently, it arises the problem to identify dangerous configurations. We introduced in Section 4.4.3 the Jaccard index as measure of similarity between two different networks, and we characterized its basic statistical properties for the networks generated in our simulation engine. We now study the correlation between the indexes J_{12}, J_{13} and J_{23} and the systemic relevance parameter $R_{\mathfrak{G}}$ introduced above. Fig. 4.9 shows the result. In particular, the four panels plot the Jaccard index against the systemic relevance parameter, where $J^* = J_{12} + J_{13} + J_{23}$ is used to take into account possible crossed correlations among the three layers which could potentially bring high level of systemic risk. As one can see from the figure, simple similarity measures like the one we use is not able to explain the formation of critical configurations. To solve the problem, we will introduce a numerical algorithm in section 4.6 ables to take into account the real roots of the systemic risk generated in our model, which is the intrinsic ability of banks balance sheets management to transform the several kinds of financial risks into each other.

4.5.3 The Systemic Importance of the Securities Portfolios

In the previous sections the initial shock to the financial system was always the bankruptcy of one single bank. In this section, we investigate how the system reacts when instead the shock consists of the depreciation of the value of one or more securities. It should be recalled that in the model banks are endowed with random portfolios. All the securities, moreover, are characterized by the same price at the beginning of the simulations, which for sake of simplicity is fixed to $p_\mu(0) = 1$, and the same elasticity factor $\alpha_\mu = 0.2$. In the previous subsections, the number of securities was fixed to $M = 30$[1]. Keeping fixed this initial configuration, we first investigate how the banking system absorbs a price reduction of one or more securities. Fig. 4.10 shows the results. In the left side panels the number of defaults following a certain percentage of reduction of the securities' price is shown, respectively when the price reduction affects only one security (top left panel), two securities (top right panel), three securities (bottom left panel) and ten securities (bottom right panel). In each of the graphs are reported the mean number of defaults corresponding to different shock sizes, where the solid line represents the situation when all the three layers are activated, while the dashed line represents the situation when the only active layer is l_3. It is observed that if banks were completely independent from each other in the layers l_1 and l_2, there would be very few defaults,

[1] Since the initial bipartite network is random, where a link between any bank i and any security μ has a probability to exist equal to p, it is easy to see that the corresponding network l_3 of overlapping portfolios is also random, with a Erdös' coefficient equals to $p' = 1 - (1 - p^2)^M$, where M is the number of securities.

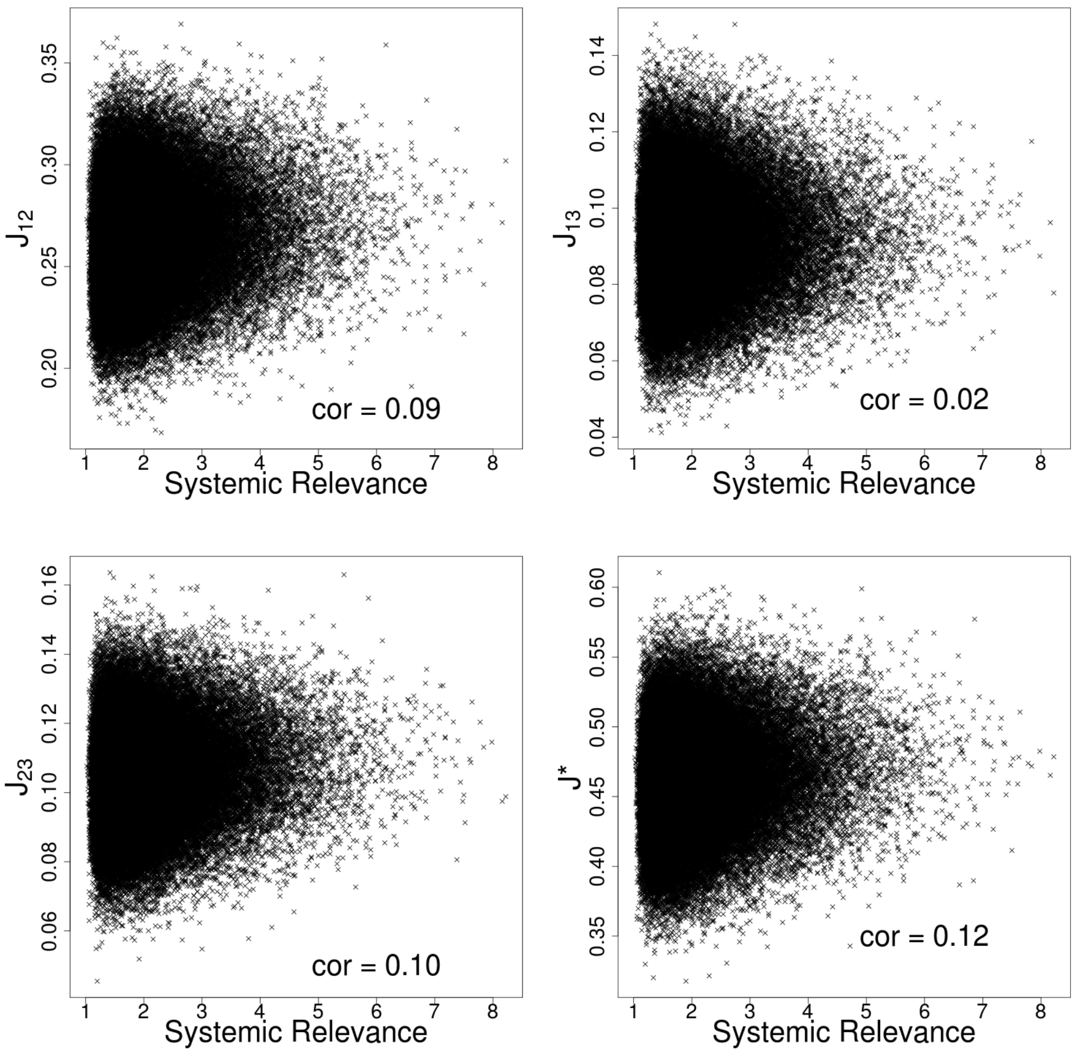

Figure 4.9: The four panels shows the correlation between the Jaccard indexes J_{12}, J_{13}, J_{23}, their sum $J^* = J_{12} + J_{13} + J_{23}$, and the systemic relevance parameter $R_{\mathfrak{G}}$. In particular, the points in each panel represent a multi-layer network structure extracted according to the algorithm presented in Section 4.4.2. For each structure, we measure its systemic relevance parameter (reported on the horizontal axes) and the Jaccard indexes (reported on the vertical axes). Correlations between the two quantities are also reported in the graph. Results are reported for 10^5 different network topologies.

especially for price shocks which are not abnormally large[1]. Consider, for example, the

[1] We report in the graphs all the possible values for a shock, so from 0% to 100% of reduction of the asset's value; of course, this is only an illustrative simulation exercise, since in reality depreciations larger than 20% are extremely rare.

case when 10 securities are shocked at the same time by reducing their value of 15%. Without any other connections among banks apart from the common exposures, the mean number of defaults is around 7. Meanwhile this number drastically increases to 38 if banks are also connected through layers l_1 and l_2. We note that since all the securities have the initial same price, and are all characterized by the same elasticity factor, in this random portfolio scenario it does not play a role which securities are shocked, since the effects are averaged out when the number of simulations is large enough. Eventually, as one can see from the figure, for values of the shock smaller than 5% no defaults are observed, indicating an adequate capital buffer level for small losses in banks' securities portfolios.

On the right-side panel of Fig. 4.10 we report the tails of the distributions of the number of defaults for a shock to the securities equal to 15%, for the cases of one, two, three and ten initial shocked securities respectively. The blue areas highlighted in the graphs represent the last fifth quantile of the distributions. In the cases of one, two and three shocked securities, the great part of the mass of these distributions is concentrated in values close to zero, highlighting a considerable financial resilience of the banking system for random assets depreciations. Nevertheless, one can see in the graphs that, also in the scenario of one security shocked by 15% of its initial value, the shock can be amplified to destroy a large part of the banking system[1]. These findings highlight that also if the initial shock derives from a depreciation of the mark-to-market banks' portfolios, the multi-layered network structure is playing the crucial role of shock amplifier.

A particular aspect related to the banks' portfolio structures should be highlighted. In all the previous results, the securities portfolios were built according to the random algorithm described in section 4.4.2. It should be noted however, that since all the securities in our framework are equivalent, banks maximize their utilities by simply allocating their funds in equal measure in all the possible available securities. In this configuration the system results in a maximum degree of overlap of banks' portfolios, which implies a fully connected (i.e. complete) network in the layer l_3. The diametric opposite of this configuration happens when banks invest all in different securities, which translates in an empty network in the layer l_3. In order to illustrate the impact that the degree of overlapping portfolios has on systemic risk, we use now a number of securities M equal to N, the number of banks. This allows for comparing situations

[1] We note that those fat tails disappear as far as the layers l_1 and l_2 are deactivated. We do not report here here also those distributions, but one can see from Fig. 4.10 that the mean values of the number of defaults is exactly zero for shocks equal to 15% (dashed lines in the left side panels), a part of the case when ten securities are shocked at the same time.

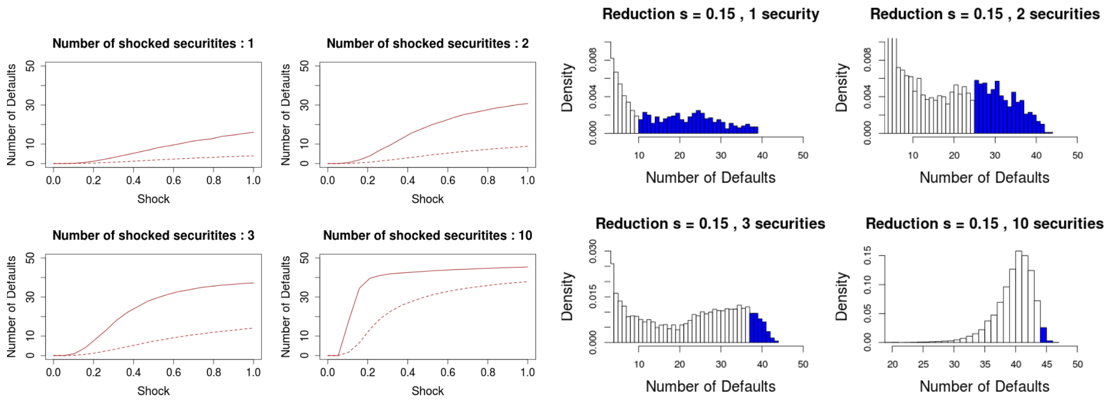

Figure 4.10: On the left side of the figure, the four panels show the number of defaults when one, two three and ten securities are shocked; the solid lines represent the number of defaults when all the three layers are active at the same time, while the dashed lines represents the same results when only the layer l_3 is activated (firesales contagion effects). On the right side, the tails of the distributions of the total number of defaults are reported, when the percentage of securities' reduction is equal to 15%; results are here reported for the case of one, two, three and ten initially shocked securities. The blue areas highlighted represent the last fifth quantile of the distributions.

ranging from banks having maximum overlapping portfolios (precisely, when all the banks equally share their funds among all the possible M securities), to situations where banks invest their funds in only one security and there are no common exposures among them. The results of this exercise are shown in figure 4.11. We assume that the shock is a reduction of the value of all the M securities in the system, respectively of 5% (black line), 7% (red line), 10% (blue line) and 15% (green line). In this way, for a given shock size, all the banks have to book the same losses (in percentage points) in all the portfolios' configuration we examine. The horizontal axes of the graph reports the number n_s of securities each bank is investing in, and the portfolios are built in a way to always minimize the degree of overlap among different banks. When n_s is equal to one, each bank has only one security in its portfolios, each different from all the others (so there is a correspondence one-to-one between the N banks and the $M = N$ securities in the system). When n_s is equal to N, each bank invest its funds in all the possible securities, and all the banks have the same portfolio structure. It is interesting to note that moving along the horizontal axes from left to right maximizes banks' portfolio diversification (and hence reduces their vulnerability to idiosyncratic risk) but at the same time minimizes financial stability (it maximizes the number of defaults, and therefore, roughly speaking, the systemic risk). Our model highlights the interesting duality between maximization of banks' utility and minimization of systemic risk, a concept already highlighted in Beale et al. (12) who argue that banks' portfolios optimization can lead to higher level of systemic risk, thereby emphasizing the necessity to supervise systemic risk from a more global perspective[1].

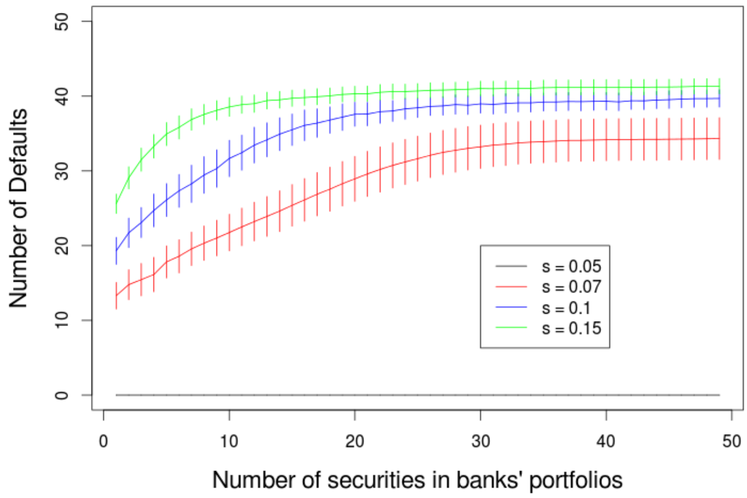

Figure 4.11: The horizontal axes represents the number of securities in banks' portfolios; banks portfolios are built in a way to minimize their overlapping. The vertical axes represent the mean number of defaults when all the securities are shocked by 5% (black line), 7% (red line), 10% (blue line) and 15% (green line). The vertical ticks represent the standard deviations computed over 10^5 simulations.

4.6 Systemic Importance Measure

A multi-graph financial structure reveals its fragility only in case a shock hits the system; part of our task is to show when the system is in a critical configuration, namely a configuration which is able to amplify a local shock to the entire financial system. We recall that, in this paper, systemic risk reflects the possibility that a single major events triggers a series of defaults among financial institutions within a short time period. Among the different methodologies developed in the last years to identify systemically important banks and their contribution to systemic risk[2], network-based measures are receiving more and more attention, although there is no a standard measure so far which can be considered universally accepted in the literature. The main reason for the

[1] See also Tasca and Battiston (66) for similar fundings.
[2] See e.g. Upper (67) and Bisias et al. (16).

inconsistency among systemic risk measures is that they rely on different microeconomic models for the specification of banks' behavior and the mechanisms through which a shock can propagate within the financial system. At the same time, network-based measures have the advantage of compressing a lot of information regarding direct and indirect bank interconnections, which appeared to be crucial during the last financial crisis. A network-based representation of the banking system is therefore crucial to understand how the single institutions share their idiosyncratic risks with the others, and to which extent this risk-pooling is dangerous for the system.

It is important to note that a comprehensive study of the systemic risk generated from the presence of interbank connections cannot rely only on the network structure of the financial system. The interconnections in an interbank market provide a way for banks to pool the unavoidable risks linked to their activities, and the interbank market should in principle play a stabilizing role for the banking system. A bank which is very connected to a major part of the others can have a crucial positive role in this scenario if its level of capitalization is large enough, as it can be able to absorb the local shocks of its neighbors. Such a bank will be considered as central in terms of spillover potential to other part of the system, but from the economic point of view its presence is beneficial for the system, since it reduces idiosyncratic risks of other institutions. Figure 4.12 clearly illustrates this notion. The panels in the figure represents a comparison between some classical network centrality measures and the number of defaults reported in our simulation engine following the bankruptcy of one bank. The number of defaults can be used as a proxy for the systemic importance of a bank in the system. Since we are dealing with a multi-layered framework, we compute four different centrality measures (which are *closeness*, *betweennes*, *eigenvector centrality* and *PageRank*) for all the three layers separately, and the same measures when the three layers are projected in a single one. As can be seen from the panels, there is basically no correlation among those network measures and the number of defaults we obtain from our simulations. This result highlights the necessity to develop more sophisticated measures to asses the systemic contribution of each institution to the financial system, and those measures have to take into account the articulated internal structure of the nodes in the network (in other words, banks' balance sheets) as well as the different mechanisms of contagion and risk-sharing present in the banking system.

This notwithstanding, considering only banks' balance sheets information to assess the level of systemic risk in the banking sector is extremely restrictive. Prior to the recent financial crisis micro-prudential supervision was based on the notion that it was sufficient to ensure the stability of the banking sector to require institutions to have

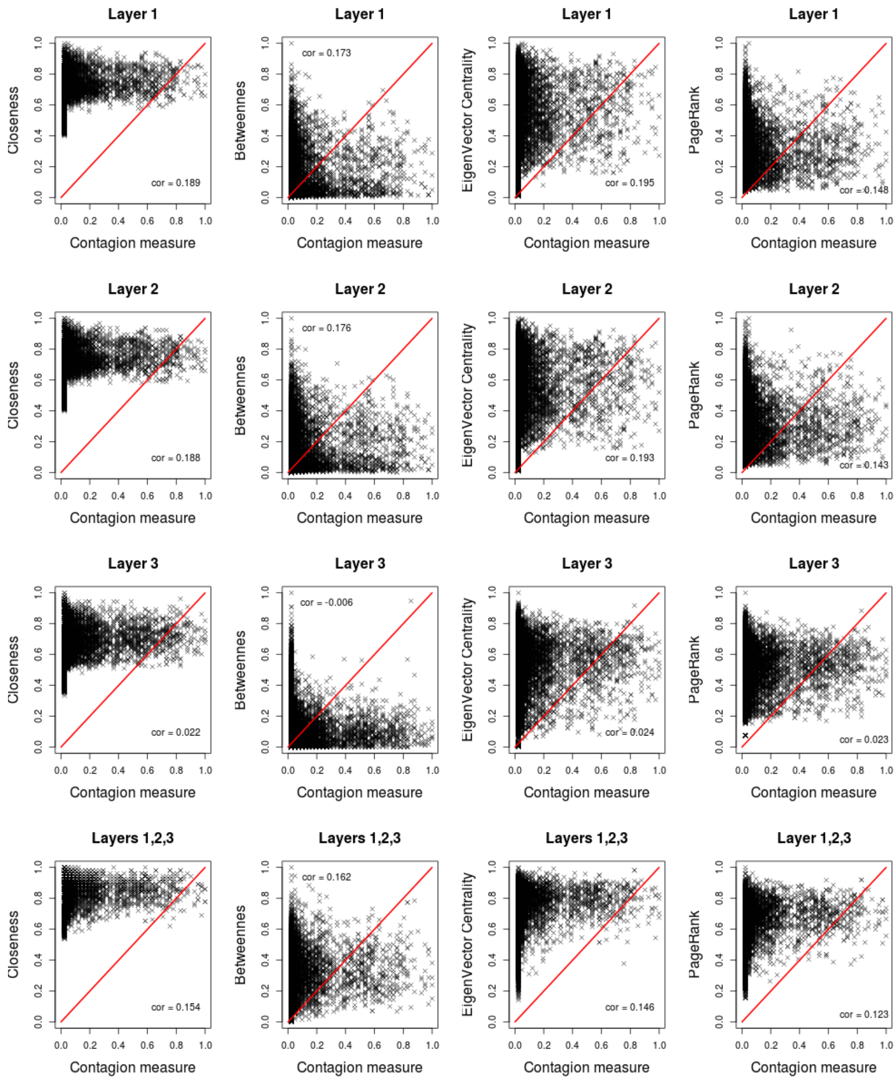

Figure 4.12: The panels show a comparison between some classical network centrality measures, and the number of defaults reported in our simulation engine following the defaults of one particular financial institution. Each tick in the panels represents a bank in a random-generated multi-layered network structure; the vertical axes represents a measure of centrality of that bank in layer l_1 (first row of panels), layer l_2 (second row of panels), layer l_3 (third row of panel) and the superimposition of the three layers (last row of panels); the horizontal axes represents the number of defaults triggered by the bankruptcy of that particular bank, according to our simulation engine. All the value are normalized to one, and the panels also show the correlation among the two indexes. Results are reported for 10^5 random replications of the system.

operate with an adequate level of capitalization. The recent financial crisis, if anything, revealed that focusing only on individual banks' soundness is a necessary but not sufficient condition for safeguarding the financial system. In fact, as we will show later, the risk-pooling mechanism, which is at the core of an interbank market, can increase the chances of multiple failures to occur following an initial shock. Since the process of contagion among financial institutions, as we already highlighted, is composed of two parts, which are an initial triggering events (for example the failure of one single institution), and the propagation of losses and distress in the financial system, the extent to which a local shock can propagate and be amplified from bank to bank greatly depends also on the structure of the banking system as a whole. To illustrate this point, figure 4.13 shows a comparison between some balance sheet-related quantities and the number of defaults following the bankruptcy of a single institution. The figure shows that classical quantities like banks' total assets, total interbank liabilities, total interbank assets and risk-weighted capital ratios do not necessarily provide useful information regarding the systemic importance of the bank, as measured by the number of defaults its bankruptcy can trigger. In particular, one can see from the picture that the failure of small-sized banks usually does not trigger too many other defaults. On the other hand, regarding large-sized banks we find mixed results in the sense that some of them trigger domino effects, while others do not. Eventually, the last panel on the right-hand side shows that there is no link between the banks risk-weighted capital ratios and their systemic importance.

To account for the fact that neither classical centrality measures nor balance sheet indicators are sufficient for assessing the systemic importance of an institution, the next subsection introduces an algorithm to derive the systemic contribution of each bank to the financial system. The framework will take into account both network and balance sheets information, with the final aim of (i) reproducing the results we obtained with the simulation engine; and (ii) visualizing the network structure in a way to highlight how the idiosyncratic risk of each bank is distributed among the other institutions, and when this risk-sharing brings the system to an unstable configuration.

4.6.1 The aggregation algorithm

The algorithm we propose in this section to study the multi-layered financial network is based on the concept of *critical link*. In each of the three layers we introduced, a link starting from node i and pointing to node j is said to be critical if the bankruptcy of bank i results in the bankruptcy of bank j. We note immediately that, without critical links in the three layers, no contagion effect is possible, although losses can be

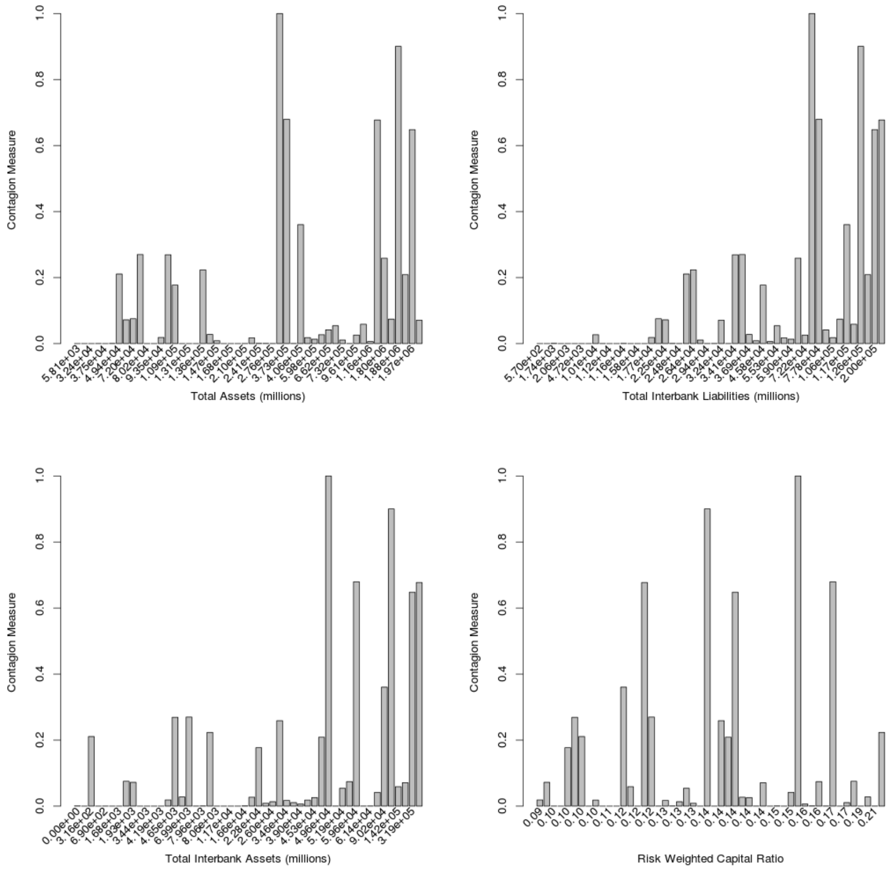

Figure 4.13: The four panels show a comparison between some banks balance sheets trait, (namely banks total assets, banks interbank liabilities, bank interbank assets, and banks risk weighted capital ratios) and a contagion index, computed as the mean value of the number of defaults triggered after the bankruptcy of the bank with that particular trait. Mean values, taken over 10^5 realizations of the multi-layered network, are here used as proxy for the systemic importance of the single institutions. The values are normalized to the maximum number of defaults reported in simulations.

transmitted to the direct neighbors of the failed bank. In fact, in case the default of a single bank does not imply any other failures, the direct and indirect counterparties of that bank were assuming an acceptable amount of risk with respect to their own capital buffer, and we speak about counterparty risk (or liquidity risk, or funding risk) but not about systemic risk. We can distinguish the conditions for a link to be critical in the three different layers. Also if the detailed approach to identify critical links is reported in the Appendix, we give here the general ideas.

Following the definition, a link in layer l_1 between bank i and bank j is critical if the default of bank j will induce losses that bank i is not able to absorb without violating the RWCR requirement. In the computation of the threshold value for the link weight, one has therefore to take into account, among other factors, the looses-given-default of bank j, the available capital of bank i, together with all the items in bank i's balance sheets which can be used by the bank to increase its RWCR. In the same spirit, a link in layer l_2 between two banks i and j is said to be critical if the interruption by bank i of the credit line to bank j will induce the failure of the borrower bank. Eventually, a link in layer l_3 between banks i and j is said to be critical if the liquidation by bank i of its whole securities portfolio will produce losses to bank j which is not able to cope with.

We stress here that a link criticality depends on the micro behavioral rules assumed to drive the banks into the dynamic model. This implies that changing the banks behavior in the model will change the threshold values for the link weights necessary to identify critical links. Nevertheless, the algorithm we propose can still be used to simplify the multi layer network structure and to identify systemic important banks and critical configurations in the financial system.

Before introducing the algorithm for the simplification of the multi-layered financial network, we need to introduce the following notation: given a square-real-matrix $A_{N\times N}$ and a set of indexes $I = \{i_1, i_2, \cdots, i_K\}$ $(0 < i_1 < i_2 < \cdots < i_K \leq N)$, we indicate with A_I the $(N-K+1)\times(N-K+1)$ square-real-matrix obtained by summing the rows and columns indicated in the set I, and by putting the row and column arising from the sum first in the new matrix. If the matrix A is the weighted matrix of a network, the reduction operation just described is the aggregation of the nodes in the set $I = \{i_1, i_2, \cdots, i_K\}$ in one single node; this new super-node has links to all other nodes that were connected to the original subset absorbed into the super-node, and the weights on the links are summed accordingly.

We can finally introduce the aggregation algorithm for the simplification of a multi-layered financial network. We start with a multi-layered structure $\mathfrak{G}$ and an initial bank b_0 for which we want to compute its systemic importance. In the first step, $s = 0$, we consider the node b_0 as the only one in the super-node, and in each step $s = 1, 2, \ldots$ we perform the following operations:

1. We build up the matrices $W^1_{I_{s-1}}$, $W^2_{I_{s-1}}$ and $W^3_{I_{s-1}}$, where I_{s-1} are the nodes belonging to the super-node the step before. We note that this is equivalent to introduce a new bank in the system, instead of the banks in the set I_{s-1}, whose balance sheet is the aggregation of the K suppressed banks' balance sheets, and whose links are the aggregation of the in-coming and out-coming links of the nodes in I_{s-1}.

2. We identify the critical links in each of the three layers l_1, l_2 and l_3 and we build up three new matrices A^1_s, A^2_s and A^3_s which entries are:

$$A^l_{s,ij} = \left\{ \begin{array}{ll} 1 & \text{if there is a critical link from } i \text{ to } j \text{ in layer } l \\ 0 & \text{otherwise} \end{array} \right\} \tag{4.19}$$

3. We find the directed tree in the unweighted, directed network characterized by the adjacency matrix $A_s = A^1_s + A^2_s + A^3_s$ starting from the super-node; the nodes belonging to this tree will constitute the set I_s, while its edges are recorded in the set C_s.

The algorithm ends when the size of the super-node stops increasing and it happens in at most N steps, since in the worst case each node is absorbed in the super-node in a different step. The first output of the algorithm is a series of sets of nodes I_s ($s = 1, 2, \ldots$) which can be used to extremely simplify the multi-layer network structure. In fact, nodes absorbed in the super-node in step s are all characterized by the following property: they will fail if all the nodes belonging to the set I_{s-1} fail simultaneously, but not if any single node in I_{s-1} fails separately. The second output of the algorithm is the series C_s of links belonging to the spanning trees starting from the super-nodes. This series of critical links helps us in the identification of critical paths in the system, namely multidimensional paths which can bring the losses from one node in the network to a remote region of the same network.

A multidimensional critical path has actually a meaning which is deeper than only being a channel for the transmission of losses through the financial system. The presence of multidimensional paths in interbank network represents a way of risk sharing that goes beyond the knowledge of the single banks. The idiosyncratic risk of one single institution is shared not only with its direct counterparties, which are aware of the risk taken, but also with other players not directly connected to the institution, and which cannot be fully conscious of the risk-transfer represented by the critical paths in the network. Without a full knowledge of the multi-layered network structure no banks can really estimate its exposure to the idiosyncratic risk of the other banks. Moreover, critical multi dimensional paths highlight the risk transformation process. In fact, the deepness with which financial stress can propagate in a financial system is extremely amplified by the ability of a bank to absorb a risk, transform it, and share it with its counterparties under a different shape.

Those concepts are illustrated in the following subsection where we shows how the aggregation algorithm can be used to identify systemic important banks.

4.6.2 Results

To better clarify the working and the outputs of the aggregation algorithm, we analyze one particular scenario, and we show how it is possible to simplify the financial structure of the banking network. This benchmark example also illustrates the origins of the non-linear behavior in such propagation within the network.

Let's consider a multi-layered financial network $\mathfrak{G}$, and a bank b_0 for which we want to know the systemic importance in $\mathfrak{G}$. The two outputs of the algorithm, $\{I_s\}$ and $\{C_s\}$, can be used to simplify the network structure as illustrated in Fig. 4.14. The figure shows the three steps involved in the algorithm for this particular configuration $\mathfrak{G}$ (the first step $s = 0$, where the super-node is composed only by the initial failed node, is not reported in the figure). In each step, the super-node is highlighted in red color, and it contains all the nodes involved in the previous steps, including the previous super-node. The Figure represents also the critical links reported by the algorithm (blue links represent critical links in layer l_1, green links in layer l_2 and purple links in layer l_3). The algorithm reports a final number of defaults equal to 18. In the left part of the figure one can see the initial failing bank, $b_0 = 11$, which is the only member of the super-node in step $s = 0$; in step $s = 1$, one can see the multi-dimensional tree on the three layers involving additional 8 defaults as a result of the default of $b_0 = 11$. In step $s = 2$, the super-node aggregates all the 9 nodes already defaulted, whose simultaneous failures in turn produce 5 further defaults. Finally, in the last step, one can see how the simultaneous failures of the previous 14 banks results in 4 more defaults.

Figure 4.14 clearly shows the non-linear nature of the contagion problem when accounting for multiple layers of interconnectedness. It is clear from the picture that if we repeat the same algorithm but only with layer l_1 activated, the total number of defaults triggered by the failure of bank 11 will be 5 (namely banks 9, 10, 13, 21 and

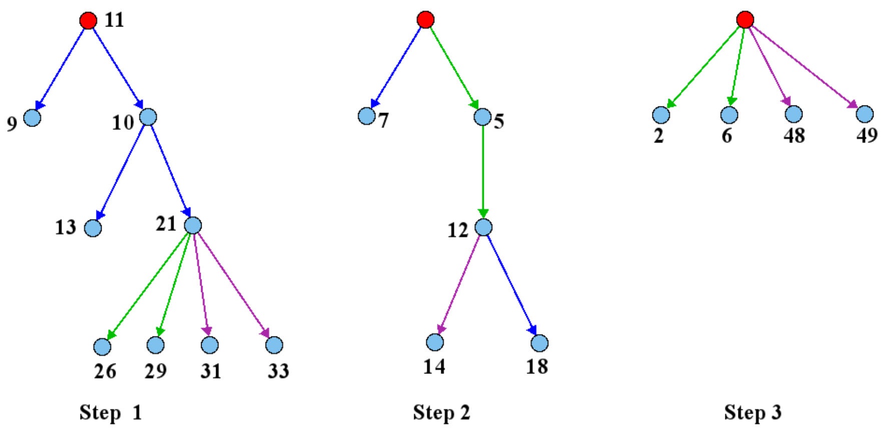

Figure 4.14: The figure shows a representation of the outputs of the aggregation algorithm for one particular multi-layered financial system $\mathfrak{G}$ and the initial defaulting bank $b_0 = 11$. The color of the edges reflects their nature (blue edges belong to layer l_1, green edges to layer l_2 and purple edges to layer l_3). Three steps are involved in this process; in the first one on the left, the tree shows how the failure of bank 11 can bring to default of banks 9, 10, 13 and 21 because of the losses transmitted through layer l_1, banks 26, 29 and 31 fail become illiquid, and bank 33 fails because of its common exposures with bank 21. All these 9 nodes are then aggregated into the super-node of step 2 (red node); the defaults of this super-node triggers other 5 failures. In the last step (last tree on the right) the 5 banks (5,7,12,14,18), aggregated into the super-node, bring to the failure of other 4 banks.

7), meanwhile no defaults at all would be triggered in case of only layer l_2 or l_3 are active. Therefore, the non-linearity which appears for example in Fig. 4.7 is due to the creation of critical paths in the multi-dimensional space, which amplifies the range of propagation of the initial shock. This highlights also the fact that when considering the three single layers in isolation the systemic risk in the banking system would be heavily underestimated. As the large number of defaults in the complete scenario (when all the three layers are activated simultaneously) is due to multi-dimensional critical paths that can reach also remote banks in the system, the removal of one layer can interrupt these critical paths and so underestimate the number of banks involved in the propagation process. Moreover, the identification of critical paths is necessary in order to understand how the idiosyncratic risk taken by the single institutions can affect the stability of the system. It is evident that there is a strong interaction among the different risks embedded in our model: a well working interbank market has to be able to properly share these risks among the different financial institutions in such a way that the system can absorb local shocks without propagating them to the entire system.

We highlight here a fundamental point of the whole paper, made clear by the example reported in Fig. 4.14. In the first step of the algorithm, bank 21 plays a fundamental role in increasing the extent to which the shock can propagate in the financial system. In fact, losses materialize for node 21 in the form of interbank counterparty risk. Nevertheless, the bank transmit stress to other institutions in the form of funding and market risk. The banks behavior assumed in the model enables the risk to be transformed from one shape into an other, and this transformation-and-sharing risk process is a the very core of the high level of systemic risk we report in our simulations.

A natural measure of systemic importance for a bank in the system is immediately achieved through the aggregation algorithm. A bank becomes systemically important if its failure materializes in substantial losses for the other institutions, leading to other defaults and eventually a significant impact on the real economy. The aggregation algorithm has the advantage that it does not take into account the reasons why a bank fails: once it does, it is aggregated into the super-node. The size of the super-node when the algorithm converges therefore reflects the order of magnitude of the spillovers produced by that particular bank, which in turn depends both on the composition of the banking system (i.e. balance sheet information are included when computing the threshold values for the critical links) and on the multi-layered network structure itself. The size of the super-node, which should reproduce the number of defaults obtained from the simulation engine, is an approximation in two main respects: (i) losses directly affecting the capital from different layers (for example layer l_1 and layer l_3) are not summed up together to trigger the default of a bank, but the bank will fail only if losses from separate layers trigger the threshold for that particular layer. This shortcut can be avoided at the price of a more complicated algorithm, while we prefer to keep a good trade-off between simplicity and interpretability, and correctness. (ii) Liquidity spirals are only partially reproduced with the algorithm: if a bank fails at some point in the algorithm, its borrowers in the short-term interbank market will experience a liquidity shock, that can in turn trigger their defaults, and so on. However, in reality (and also in our simulations) banks start withdrawing liquidity before they fail, because of liquidity needs or because they have to fulfill their Risk-weighted Capital Ratio. This mechanism of *precautionary* withdrawal of liquidity is not captured by the algorithm, and it is difficult to include if we want to keep its iterative nature, which has the advantage to be easily understandable. In the light of these observations, we cannot expect that the number of defaults in the simulations will be exactly reproduced by the size of the super-node. Nevertheless, to its advantage, the algorithm is able to simplify the network structure and to reproduce the non-linearity we find in the simulations.

To assess the validity of the aggregation algorithm, Fig. 4.15 show the comparison

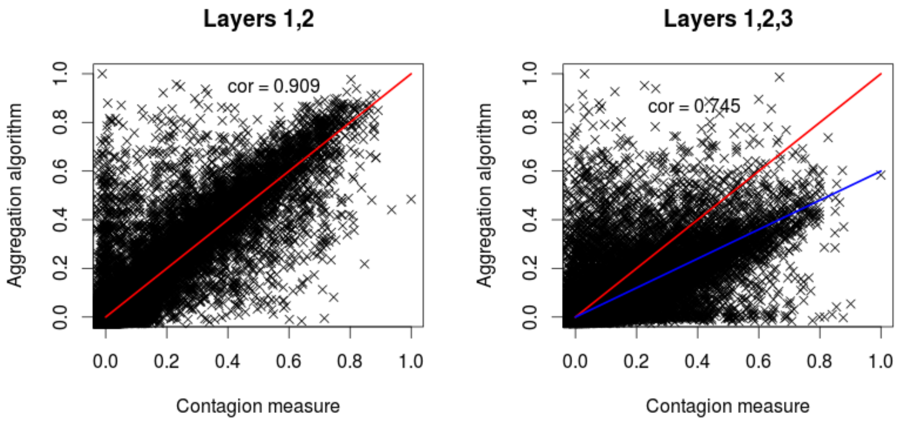

Figure 4.15: In the left-side panel of the figure we report the comparison between the number of defaults obtained from the simulation engine (horizontal axes) and the size of the super-node as output of the aggregation algorithm (vertical axes), for 10^5 random realizations of the multi-layered interbank network. For each realization, we randomly select one of the 50 banks as initial defaulting bank. The red line is the unitary slope dependency $y = x$. On the right-side panel of the figure, we report the same results when all the three layers are activated simultaneously, and the blue line is the best linear regression $y = a \cdot x$, where $a = 0.59$. All the values are normalized to the maximum number of defaults reported in the simulations.

between the results from the simulation engine (number of defaults) and the size of the super-node computed with the aggregation algorithm. In particular, on the left-side panel there is the comparison when only two layers are activated (namely layer l_1 and l_2), and in the right-side panel the same comparison is reported when all the layers are activated simultaneously. In both cases, there is a significant level of correlation among the two measures, highlighting the good performance of the aggregation algorithm, especially if compared to the classical network measures reported in Fig. 4.12, or the balance sheet-based measures shown in Fig. 4.13. The larger accordance in the case of just two active layers has already been explained in point (i) above. In fact, the differences in the number of defaults can be attributed to those banks who fail because they receive losses from different layers, a mechanism which is absent in the aggregation algorithm, that instead aggregates losses from different counterparties only within the same layers.

It should be noted that the main scope of the aggregation algorithm is not to reproduce the number of the defaults we obtain in the simulation engine, but approximate it with the advantage of having some more clues about how the network structure propagates local shocks to a global scope. Given the correlation between the simulation results and the recursive algorithm, and given that there is no other way for the algorithm to produce non-linear effects a part of the creation of multi-dimensional paths, we can conclude that also in the simulations the non linear effects are generated through the same mechanism. We note, moreover, that the algorithm is easily customizable to take into account different choices for the banks micro-behavior; in fact, the good performance of the algorithm reported in Fig. 4.15 is also due to the choice of the criticality conditions appearing in eq.s (C.2)-(C.6), which reflect the micro behavior of banks in the system. Changing the banks micro-behavior, or including other, will reflect in different condition for the links criticality, but the algorithm can still be used to simplify the financial network structure.

4.7 Conclusions and policy implications

The agent-based, multi-layered interbank network model presented in this paper illustrates the importance of taking a holistic approach when analysing the contagion risks related to the interconnections between banks. The main finding is that looking at segments of banks' interconnections in isolation, without considering the interactions with other layers of banks' interrelationships, can lead to a serious underestimation of interbank contagion risk. In other words, by taking into account the various layers of interbank relations and the interactions between them the contagion effects of a shock to one layer can be significantly amplified, compared to the situation where contagion risks are assumed to be confined within the specific layer where the initial shock arose. This finding points to the existence of important non-linearities in the way bank-specific shocks are propagated throughout the financial system.

Another important finding of the paper is that the structure of the network and the underlying balance sheet positions of the banks (nodes) in the network matter in terms of resilience to shocks. In many, in fact the majority, of our simulated network structures financial contagion is likely to be limited. However, in certain network constellations, also depending on the financial soundness of the central players in those networks, contagion risk is substantially more pronounced.

Furthermore, by considering not only contagion via direct bilateral exposures but also via banks' common exposures (through their securities holdings) we are able to demonstrate a trade-off between risk diversification decisions and financial stability. In other words, due to the potential contagion risks related to banks' common exposures decisions to diversify their investments in securities that may be optimal at the individual bank level can in fact imply higher contagion risks for the system as a whole.

In view of these findings, the paper proposes a “systemic importance” measure that accounts for the multi-dimensional aspect of banks’ interrelations. That is, based on our multi-layered network model and taking into account individual banks’ balance sheet structure the approach provides a single measure of banks’ systemic importance that outperforms standard network centrality measures as well as typical balance sheet indicators.

The observation that unless a holistic view of banks’ interrelations is taken the analysis of interbank contagion risk is likely to underestimate the true contagion risk has major policy implications. From both a micro-prudential and in particular a macro-prudential perspective the findings of this paper suggest that it is insufficient to analyse contagion within specific market segments in isolation. Indeed, according to the findings presented here, a major component of the propagation mechanism that transmits losses in one bank to the rest of the system derives from the interactions between the multiple layers of interactions that banks have with each other. On this basis, an immediate policy prescription emerging from this analysis is the importance of collecting adequate supervisory data that allows for assessing in a holistic way the interconnectedness of the banking system and thus account for the non-linearities that the existence of multi-layered interbank networks may induce.

5

On the Link between Derivatives and Leverage

5.1 Introduction

The current regulatory framework relies on *risk weights* to compute the regulatory capital that banks have to hold against their portfolio of assets. This approach is meant to guarantee that the default probability of a bank is bound by a given threshold, independently of its business and investments strategies. By weighting each asset class by its relative risk weight, all assets become risk equivalent and therefore they can be summed up. Thereafter regulation chooses the amount of capital which a financial institution will have to hold as a fraction of risk weighted assets. This capital provides an upper bound concerning the financial institution's probability of default.

However, the risk weights approach suffers from two main drawbacks. First, ex-ante, risk weights are likely to underestimate the probability of rare events – e.g. a very large drop in the price of the asset. The reason is that, in the current regulatory framework, risk weights are usually computed by using Value at Risks (VaRs) of distributions which do not necessarily capture the likelihood of such events[1]. As a consequence, ex-post, if risk weights lead to a relatively low regulatory capital in absolute terms, in case a rare event materializes, a large amount of equity is wiped out. This, in turn, might trigger fire-sales and systemic crises. Second, the risk weights approach may be plagued by the

[1]To capture tail risk, one should use moments higher than the second one. The Standardized Approach, however, models risk as the variance of the loss distribution of a portfolio, without looking at higher moments. This does not account for tail events. More advanced methodologies used in Internal Rating Based Models can take into account moments higher than the second one, especially for assets held in the trading books. See for example BCBS (10).

discretion that regulators leave to banks when computing such weights. Complex and large banks typically compute their risk weights through their internal rating-based models. This may leave space for financial engineering to calibrate internal models so as to free up regulatory capital.

Given these limitations of the risk weights approach, the regulator imposes a cap on leverage as a backstop to enhance the resilience of individual banks and of the whole financial system. As the recent financial and debt crises have vividly shown, leverage is a key systemic factor amplifying vulnerabilities. Therefore, imposing limits on leverage contributes to mitigating the capital erosion due to tail events. To this end, it is crucial to measure leverage accurately.

Against this background, the goal of this paper is to address the question of whether commonly used measures of leverage L (e.g. the ratio between the total assets (A) and the total equity (E), i.e. $L = \frac{A}{E}$) adequately capture the "effective" leverage that a financial institution takes on, in particular for the case of net positions in derivatives. After showing that banks' net positions on derivatives contribute to increasing their leverage beyond the level which is captured by the ratio currently proposed by regulators, this study also investigates whether the effective leverage embedded in a derivative contract allows banks to engage in capital arbitrage.

The closest work to ours is Breuer (20), who uses an equivalent portfolio technique to show how derivatives' and repurchase agreements' (*repo*) contracts can generate levels of leverage not captured by standard measures. Our contribution develops on two main directions: first, we homogenize standard and effective leverage, and we use empirical balance sheets data to show how the *real* level of leverage in the banking system evolved over time. Second, we show how this loophole in the standard computation of leverage brings to capital arbitrage opportunities, i.e. the amount of risk per unit of capital is larger when regulated banks take exposure through the derivatives market instead of direct investing in the underlying assets.

5.2 Regulatory Treatment of Derivatives

This section discusses how a derivative contract can be replicated with an equivalent portfolio made of own funds and debt on the liability side, and of the security underlying the derivative itself on the asset side. The equivalent portfolio exactly replicates the pay-off and risk of the derivative position. This replica portfolio technique enables us to compute the regulatory capital necessary to hold a derivative contract and to measure its implicit leverage.

5.2.1 Derivatives and Equivalent Portfolios

The intuition behind the Black and Scholes pricing equation (Black and Scholes (17)) is that, under the assumption of no arbitrage opportunities, it is always possible to build a portfolio strategy which reproduces the derivative's payoff and risk profile during the whole life-time of the contract, without using the derivative itself. The model assumes that there are no transaction costs or other financial frictions. It follows that the implicit leverage embedded in the derivative contract is equivalent to the leverage of the equivalent portfolio. The methodology can therefore be used to compute the correct level of leverage in derivative positions.

Forwards and futures are among the most commonly traded derivatives. Forward contracts are traded Over the Counter (OTC), while their standardized forms, futures, are traded on exchange platforms. The party going long in these contracts has the obligation to purchase a certain amount of the underlying asset, called notional amount, at a given time in the future, the maturity, at the price specified in the contract. On the other hand, the party going short has the obligation to sell the notional amount at maturity. Currencies constitute the bulk of the underlying assets for the forward contracts, since these instruments represent the most natural way to hedge against exchange rate risk.

Forward and future contracts are easy to replicate with an equivalent portfolio. Fig. (5.1) shows the balance sheet expansion of the forward contract into its equivalent portfolio. On the left-hand side, the market value of the forward contract is matched with a given amount of capital, which is used to purchase it. On the right hand side, the same amount of capital plus an appropriate amount of debt are used to go long on the underlying asset. The two positions, properly calibrated, are perfectly equivalent in terms of risk and payoff, and abstracting from transaction costs, their price would be the same. The proof is based on the initial Black and Scholes ideas (see Black and Scholes (17)). We report here the main algebra only for forward and future contracts, while the proof for other kind of derivative contracts can be found e.g. in Breuer (20).

Consider a long forward contract on an underlying asset which, for simplicity, is assumed to provide no income. The value of this contract at time t is f_t^l, is the difference between the current price of the underlying asset, S_t, and the discounted value of the price, X, at which the security has to be delivered at maturity, T, given the risk-free interest rate r:

$$f_t^l = S_t - Xe^{-r((T-t)} \tag{5.1}$$

In a nutshell, assuming no arbitrage, an investor can replicate the forward contract by borrowing an amount of cash equal to $Xe^{-r((T-t)}$, supplement it with its own equity equal to f_t^l, and invest the total in the underlying asset $S_t = f_t^l + Xe^{-r((T-t)}$. It is easy to see that at maturity T, the payoffs of the two positions, and therefore their risk, will be the same.

The degree of leverage embedded in the forward position is therefore the ratio of investor's total assets, $S_t = f_t^l + Xe^{-r((T-t)}$, and its equity, f_t^l. In plain English, the implicit leverage in a forward contract is the ratio between the current notional value of the forward contract and its market value.

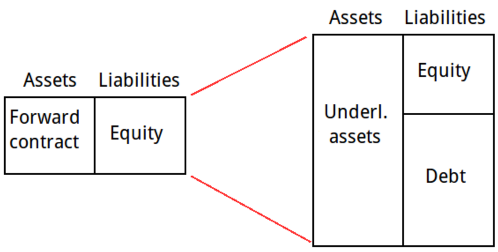

Figure 5.1: The left hand side denotes how a derivative position (forward contract) enters a balance sheet. The right hand side represents the expansion of such derivative position into its equivalent portfolio.

Options are another type of commonly used derivative contracts[1]. Constructing an equivalent portfolio for options is more complicated than doing so for forwards and futures since it involves a continuum time adjustment of the borrowed funds on the liability side, and assets shares on the assets side. The idea is nevertheless the same as forward contracts. An initial amount of equity, augmented by borrowing, is used to go long (short) on the underlying assets, exactly replicating the payoff and risk profile of the call (put) option. Other types of derivatives, like swaps, exotics and

[1] European call options at maturity give the party going long the right, but not the obligation, to buy from the party going short the notional amount of the underlying asset, at a pre-specified price (strike price). The party going short takes a premium at the starting time of the contract, and it has the obligation to sell the notional amount at maturity in case the counterparty calls the option. As for a European put option at maturity the party going long has the right, but not the obligation, to sell the notional amount of the underlying asset at the price specified in the contract (strike price). Differently from American options which can be exercised at any time between the inception of the contract and their maturity, European options can only be exercised at maturity. In a sense, options enable their holders to lever their resources and gain from changes in price of the underlying asset.

credit derivatives, can be viewed as a combination of forward and option contracts working together, and therefore it is still possible to replicate them. For example, a swap is equivalent to a portfolio of futures with the same (time-discounted) underlying notional amount and different maturities, properly selected[1].

5.2.2 Risk weights, Leverage and Derivatives

To compute the risk weights necessary to calculate the regulatory capital which banks need to hold against a derivative position the regulator makes use of the equivalent portfolio technique. In particular, such regulatory capital, e_w, is equal to the capital required to hold the underlying asset in the correspondent equivalent portfolio, corrected by a delta factor δ[2]:

$$e_w = 0.08 \cdot W_a \cdot a \cdot \delta \tag{5.2}$$

where a is the exposure to the derivative's underlying asset and W_a is its associated risk weight.

Basel III provides guidance also for the computation of the leverage ratio. In general, the Basel Committee on Banking Supervision (BCBS) recommends a minimum requirement of 3% for the leverage ratio, which is defined as a capital measure divided by an exposure measure, or equivalently a maximum of 33 for the ratio between exposures and capital[3].

The exposure measure of a derivative contract is the sum of two components. The first one represents the replacement cost, which is obtained by marking-to-market the derivative contract. The second is an add-on component, which reflects potential future exposures over the remaining life of the derivative contract. This last term is obtained by applying an add-on factor to the notional amount. The add-on factor changes depending on the maturity of the contract and on its underlying asset. The maximum value for the add-on factor is 0.15[4].

[1] Swaps can be replicated with different short and long forward contracts with different maturities. When netting such contracts, they will cancel out. Therefore, the real exposure deriving from swaps is considerably lower than their total notional amount.

[2] Regulation (EU) No 575/2013 (CRR). The notional amount needs to be corrected by the delta factor. The delta factor denotes how the price of a derivative varies for a change in the price of the underlying asset. For forward contracts such delta factor is equal to one, while for other derivatives is bound between zero and one.

[3] This rule holds from 1 January 2013 to 1 January 2017. – See BCBS (11).

[4] See BCBS (11).

5.3 Standard vs Effective Measures of Leverage

This section shows how the replica portfolio technique enables us to capture the effective leverage embedded in derivative positions. In contrast, commonly used measures of leverage– which are endorsed by Basel III – are likely to underestimate effective leverage. Next, the section discusses under which conditions the discrepancy between effective and standard measures of leverage can give rise to capital arbitrage opportunities.

5.3.1 Syntethic Leverage

Effective leverage is typically larger than the standard leverage computed with the derivative exposure because the notional values of underlying assets (which constitute the asset side of the replica portfolio) are usually much larger than the derivatives' market values (which constitute the exposure used to compute leverage without expanding the derivative into the equivalent portfolio)[1]. As a consequence, commonly used measures of leverage may not capture the real risk banks are exposed to. The difference between the effective leverage and standard measures of leverage is denoted as "synthetic" leverage.

The equivalent portfolios technique enables us to estimate the effective leverage implied by open positions on derivatives[2]. To illustrate, one can consider a simple balance sheet composed of a single derivative position only, for instance a forward contract. Looking at Fig. (5.1), the standard measure of leverage implied by an open position on this forward contract and computed without using the equivalent portfolio is equal to:

$$L_{standard} = \frac{\text{market price of the forward}}{\text{equity}} \tag{5.3}$$

When using the replica portfolio, the effective leverage would be:

$$L_{effective} = \frac{\text{notional amount of the underlying assets}}{\text{equity}} \tag{5.4}$$

which is much larger than $L_{standard}$. In the example in Fig. (5.1) $L_{standard} = 1$, while $L_{effective} >> 1$. Synthetic leverage is defined as the difference between the two:

$$L_{synthetic} = L_{effective} - L_{standard} \tag{5.5}$$

[1] Derivatives used for trading purposes are recorded in the banks' trading book and are booked at their market value.

[2] Breuer (20) firstly employed the replica portfolio technique to map the individual components of a derivative contract into own funds equivalents (equity), borrowed funds equivalents (debt), and the underlying assets.

and in this example it is strictly positive. The same conclusion can be easily drawn for the case of options, swaps and credit derivatives. All in all, for any asset class, a bank can increase its effective leverage beyond the regulatory threshold by entering a derivative contract instead of outright purchasing the underlying asset.

In practice when a bank enters a derivative position, it funds it with its own equity and debt, as it does for any other investment. Since it is impossible to determine the combination of capital and debt which a bank employs to enter a derivative contract, it is assumed that it purchases it with equity only, which therefore must be equal to the derivative contract's market value. This assumption provides a conservative estimation of the leverage embedded in derivative positions.

The effective leverage implicit in derivative contracts, like the standard measure of leverage, varies with the price of the underlying assets. Although such implicit leverage is not captured by the standard measures of leverage, it can amplify banks' probability of default: as synthetic leverage increases, the variance of the returns on equity will also go up, which will affect the default probability.

Formally, leverage is defined as the elasticity of the value of equity with respect to the value of assets, $L = dE/E \cdot A/dA = A/E$. The last equality holds since equity is the residual value and captures the gains or losses on assets, i.e. $dE = dA$. Rearranging the first equation, it is easy to show that

$$RoE = L \cdot RoA \tag{5.6}$$

where RoE denotes the returns on equity and RoA the returns on assets. It follows that the variance of the returns on equity equals the square of leverage multiplied by the variance of the returns on assets:

$$Var(RoE) = L^2 \cdot Var(RoA) \tag{5.7}$$

Since the right hand side of the last equation is proportional to a bank's default probability, increasing leverage has a direct impact on financial stability. Therefore, downward biased estimates of leverage produce distorted measures of risk.

5.3.2 Capital Arbitrage Opportunities

This section investigates whether the effective leverage embedded in a derivative contract can allow banks to engage in capital arbitrage. The answer depends on the link between regulatory capital and leverage. While capital requirements bind leverage, in the sense that risk weights affect the leverage ratio which a bank can achieve, a cap on the leverage ratio can also bind regulatory capital, in the sense that it affects banks' minimum capital requirements. For given asset classes – for instance government bonds, whose risk weights are equal to zero – it is the leverage ratio (as opposed to the risk weights) which binds banks' capital requirements. For other assets, instead, risk weights (as opposed to the leverage ratio) determine the minimum regulatory capital which a bank has to hold.

If it is the risk weights approach which determines the minimum regulatory capital, then no capital arbitrage opportunities can arise since the risk-weighted requirement for derivatives is exactly equal to the requirement for the underlying portfolio. In this case, whether a bank is exposed to an asset through a derivative contract or via outright purchase, it is subject to the same capital requirements.

In contrast, if it is the leverage ratio which binds the minimum capital requirements and if leverage is not measured correctly, then capital arbitrage opportunities can arise. Such opportunities are likely to surface when banks enter a derivative contract to get exposure to asset classes with low risk weights. For these assets the leverage ratio is likely to provide the binding constraint. Since the market price of a derivative contract is usually far lower than the notional amount of its underlying asset, the effective leverage of a bank exposed via derivatives is significantly higher than the leverage captured by standard measures. If L denotes the standard leverage ratio between the underlying assets, with nominal value equals to 100 euro, and the equity necessary to back it up, since L has to be smaller than 33, then the equity will have to be larger than 3 euro. Let L_d denote the standard leverage ratio for a derivative contract on the same underlying assets worth 100 euro. In general the associated equity E will be smaller than 3 euro, since the market value of the derivative is smaller than the notional value of the underlying asset. The leverage ratio L_d is equal to M_v/E, where M_v is the derivative market value. Since M_v is smaller than 100 euro, if the bank targets a leverage ratio equal to 33 then the equity E will have to be smaller than 3. Equivalently, if the bank employs the same amount of capital to get exposure in the derivative market, the notional amount of this position will be larger than 100.

For the sake of the argument let us assume that at time t_1 a bank holds only one asset class and its exposure is equal to a_1. Regulatory requirements impose the bank to hold capital, e_1, equal to at least 8% of its risk-weighted assets:

$$e_1 \geq 0.08 \cdot W \cdot a_1 = e_{W,1} \tag{5.8}$$

where W is the risk weight associated to the bank's asset. In addition, the regulator imposes that the bank's leverage ratio (expressed as a ratio between equity over assets) must be equal to at least 3%:

$$e_1 \geq 0.03 \cdot a_1 = e_{L,1} \tag{5.9}$$

These two regulatory requirements have to be satisfied simultaneously. Assuming that the bank is operating at the minimum capital requirement, i.e. it does not have any capital in excess of the minimum amount imposed by the regulator, the capital e_1 that it has to hold is given by the maximum between $e_{W,1}$ and $e_{L,1}$:

$$e_1 = max\left\{0.08 \cdot W \cdot a_1; 0.03 \cdot a_1\right\} \tag{5.10}$$

If the risk weight W is very low (for instance, for domestic government bonds it is equal to zero), then $0.08 \cdot W \cdot a_1 \approx 0$ and the capital that the bank has to hold is derived by the regulatory requirement on the leverage ratio, i.e. $e_1 = 0.03 \cdot a_1$. On the other hand, if the risk weight W is sufficiently large, then $0.08 \cdot W >> 0.03$, which means that by fulfilling its capital requirement the banks also meets its leverage ratio requirement. In this case the leverage ratio is equal to:

$$L_1 = \frac{a_1}{e_{W,1}} = \frac{1}{0.08 \cdot W} \tag{5.11}$$

which shows that leverage is bound by the risk weight W. It is easy to generalize the case of one security to a portfolio composed of n securities, with different risk weights $W_1, W_2, \ldots, W_n$. The upper bound for leverage will be equal to:

$$L_1 = \frac{a_1}{e_{W,1}} = \frac{1}{0.08 \cdot min_i W_i} \tag{5.12}$$

When the two regulatory requirements are equivalently binding in terms of minimum capital requirement, i.e. when:

$$0.08 \cdot W \cdot a_1 = 0.03 \cdot a_1 \tag{5.13}$$

then $W = 0.375$. In plain English, this means that if the risk weight W (or, for many different assets, the weighted average of risk weights W_i) is larger than 0.375, then risk weights provide the binding constraint for the minimum regulatory capital. On the other hand, if W is smaller than 0.375 the leverage ratio provides such binding constraint.

Suppose that at time t_2 the bank decides to increase its exposure by Δa through an outright purchase of the asset. As a consequence, because of the regulatory requirements, the bank will have to increase its capital. Assuming again that the bank is operating at the minimum capital requirement, the capital e_2 which it will have to hold is given by the maximum between capital and leverage requirements at time t_2, i.e. $e_{W,2}$ and $e_{L,2}$:

$$e_2 = max \{e_{W,2} = 0.08 \cdot W \cdot (a_1 + \Delta a); e_{L,2} = 0.03 \cdot (a_1 + \Delta a)\} \tag{5.14}$$

At time t_2 leverage is:

$$L_2 = \frac{a_1 + \Delta a}{e_2} \tag{5.15}$$

which again has to be smaller than (or equal to) the threshold 33. Indeed, when the binding constraint for the minimum capital requirement is $e_{L,2}$, i.e. when $e_{L,2} > e_{W,2}$, the leverage ratio will be exactly equal to 33:

$$L_2 = \frac{a_1 + \Delta a}{e_{L,2}} = \frac{1}{0.03} = 33 \tag{5.16}$$

In contrast, when the risk weights provide the binding constraint, i.e. when $e_{W,2} > e_{L,2}$, or equivalently when $W > 0.375$, the leverage ratio will be strictly smaller than 33:

$$L_2 = \frac{a_1 + \Delta a}{e_{W,2}} = \frac{1}{0.08 \cdot W} < 33 \tag{5.17}$$

Suppose now that at time t_2 the bank decides to increase its asset exposure still by Δa, but through entering a derivative position instead of purchasing outright the asset itself. The derivative contract will have a market value equal to c while its underlying notional amount will be equal to Δa. Once again, at time t_2, the capital e_2 which the bank will have to hold is given by the maximum between capital and leverage requirements:

$$e_2^* = max \left\{e_{W,2} = 0.08 \cdot W \cdot (a_1 + \Delta a); e_{L,2}^* = 0.03 \cdot (a_1 + c)\right\} \tag{5.18}$$

The capital requirement computed with the risk weights approach is exactly the same as the case where the bank decides for an outright purchase of the asset. The reason is that when the bank enters a derivative position, the computation of the capital requirement it is based on the exposure to the underlying asset of the replica portfolio. However, $e_{L,2}^*$ is smaller than $e_{L,2}$, since the former is based on the market value of the derivative contract which is smaller than its notional amount Δa.

When the bank gets exposure via a derivative position, its leverage is equal to:

$$L_2^* = \frac{a_1 + c}{e_2^*} \tag{5.19}$$

while effective leverage is:

$$L_{effective,2} = \frac{a_1 + \Delta a}{e_2^*} \tag{5.20}$$

and $L_{effecive,2} > L_2^*$. Also in this case the binding constraint for the minimum capital requirement is given by the maximum between $e_{W,2}$ and $e_{L,2}^*$. If it is the risk weights approach which constrains the minimum capital requirement, the effective leverage can never be above 33. The following inequalities show why this is the case:

$$L_{effective,2} = \frac{a_1 + \Delta a}{0.08 \cdot W \cdot (a_1 + \Delta a)} < 33 \tag{5.21}$$

Since the observed effective leverage is often larger than 33, as we will show in the next Sections, then it is the standard leverage ratio $e_{L,2}^*$ which provides the binding constraint to capital. But since the standard measures of leverage are typically underestimated, i.e. $e_{L,2}^* < e_{L,2}$, then capital arbitrage opportunities materialise: for a given amount of risk (i.e. the risk deriving by the Δa exposure), the use of derivatives enables the bank to save an amount of capital equal to $0.03 \cdot (\Delta a - c)$. In other words, for a given level of regulatory capital, a bank could increase its exposure to an asset class (whose risk weight is “low enough”) beyond the regulatory limit by entering a derivative position instead of outright purchasing the asset itself.

5.4 Empirical Analysis

By looking at the OTC derivative market, this section provides estimates of effective leverage and quantifies the difference between the leverage computed using standard measures and the leverage computed using the equivalent portfolio technique. In addition, it provides an estimate of the additional capital that banks should hold to bring down the effective leverage to the regulatory leverage threshold.

5.4.1 Effective Leverage in the Derivatives’ Markets

Although it is not possible to exactly measure the effective leverage of a financial institution without knowledge of its open derivative positions, the Bank for International Settlements’ (BIS) aggregate statistics on outstanding OTC derivatives enable us to obtain a rough estimate of such effective leverage in the OTC derivatives' market[1].

The left hand side of Fig. (5.2) plots the notional outstanding amount of derivatives in OTC markets, as reported by the BIS. The chart shows that the notional amount of OTC derivatives grew exponentially in the first half of 2000s, it stabilised during the financial crisis and then it picked up again, although at a moderate pace. At the end of 2013 the total aggregate notional value of OTC derivatives was approximately about 700 USD trillion[2].

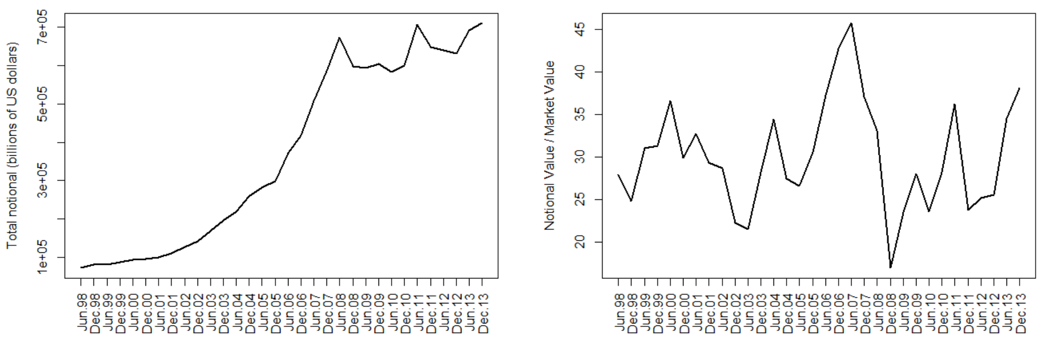

Figure 5.2: LHS chart: total notional outstanding amounts in OTC derivative market, defined as the gross notional value of all deals concluded and not yet settled on the reporting date. RHS chart: ratio between total notional outstanding amount and total gross market value in OTC derivative markets. Source: BIS data.

From a financial stability perspective, a key question is to quantify the difference between the leverage computed using standard measures and the leverage computed using an equivalent portfolio. This can be done as follows. Given a derivative exposure, the resulting standard measure of leverage is equal to the market value of the derivative (M_v), – possibly adjusted by an add-on factor –, divided by the equity (E) needed to hold that position:

$$L = \frac{M_v}{E} \tag{5.22}$$

According to the methodology proposed in this paper, instead, the leverage embed-

[1]The BIS reports aggregate data on OTC derivative positions for 13 jurisdictions, which are: Australia, Belgium, Canada, France, Germany, Italy, Japan, Netherlands, Spain, Sweden, Switzerland, United Kingdom and United States. The market share of dealers that participate in the BIS's semi-annual survey of OTC derivative markets varies across risk categories, but it is always larger than 90%.

[2]he BIS survey only provides a measure of the aggregate size of OTC derivatives' notional amount, but it does not give any indication regarding the gross exposures of financial institutions. For the sake of simplicity, it is assumed that banks purchase derivatives with equity only, and without any debt. This assumption provides a conservative measure of the effective leverage in the derivatives' market.

ded in the derivative should be equal to the notional amount of the underlying asset (N) divided by its corresponding equity, that is:

$$L^* = \frac{N}{E} \tag{5.23}$$

The ratio between L^* and L is equal to:

$$\frac{L^*}{L} = \frac{N}{M_v} \tag{5.24}$$

When a bank purchases a derivate contract with equity only, the standard leverage L is equal to one (see Sections 2.1 and 3.1). However, since the effective leverage is larger than one, the ratio L^*/L indicates the extent to which it is possible to generate synthetic leverage using derivatives. In particular, when the ratio L^*/L is equal to 1 it is not possible to create synthetic leverage. On the other hand, if this ratio is larger than 1, the banks' exposure increases but the standard leverage does not. The ratio L^*/L can be computed for any financial contract. In case of a loan, for example, since the market price and the notional amount are the same, such ratio is equal to one. In addition, the ratio changes over time. This is due to the fluctuations of derivatives' prices, which are not necessarily anchored to the prices of the underlying assets.

The right hand side of Fig. (5.2) reports such ratio[1]. The ratio varies overtime since the price of derivatives changes with the price of the underlying assets. It ranges between 18 and 46, reaching its peak at the end of 2007.

Fig. (5.3) reports the aggregate effective level of leverage implicit in the OTC derivative markets divided by the standard measure of leverage for derivatives taking netting into account (in contrast, in right hand side of Fig. (5.2) the ratio is not netted)[2]. Therefore, it can be viewed as the effective level of leverage embedded in derivative positions for the banks included in the BIS survey.

Fig. (5.3) shows that after reaching its peak at the end of last century, effective leverage decreases with the burst of the dot.com bubble. From 2005 until 2007, in the

[1]The ratio L^*/L essentially represents the notional amount which a financial institution can be exposed to per unit of derivative bought on the market.

[2]Such leverage is computed as the ratio between the aggregate notional amounts of the underlying assets and the total derivative gross market values (i.e. the sum of the absolute values of all open contracts with either positive or negative replacement values evaluated at market prices prevailing on the reporting date), multiplied by a scaling netting factor. The scaling netting factor represents the ratio between gross credit exposures (i.e. the derivative gross market values minus the amounts netted with the same counterparty across all risk categories, under legally enforceable bilateral netting agreements) and gross market values, and therefore provides an approximation of the percentage of netted position over total position. Note that the netting factors used to compute leverage can differ from netting factors used in the risk-weight approach.

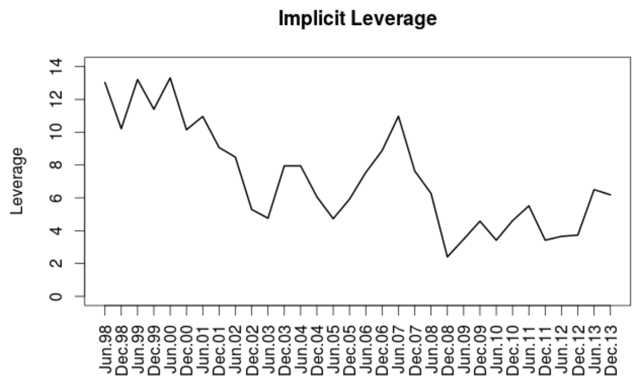

Figure 5.3: Ratio between total notional outstanding amount and total gross market value in OTC derivative markets taking netting into account. The notional outstanding amounts are used as a proxy for the current notional amounts. Source: BIS data.

run-up to the financial crisis, effective leverage more than doubled, growing from 5 to more than 10. At the end of 2007 it started to decline, likely as a consequence of the turbulence in US money markets, and it reached its minimum value after the demise of Lehman in September 2008. In the last part of the sample, effective leverage peaks up again.

BIS statistics also report a breakdown by risk category (i.e. underlying asset) and by instrument (i.e. type of derivative). Fig. (5.4) repeats the exercise carried out in Fig. (5.3) with a higher degree of granularity.

The left panel of Fig. (5.4) plots the effective leverage with a breakdown by underlying asset[1]. The chart shows that the largest level of leverage arose from derivatives (mainly swaps and forwards) on interest rates and foreign exchange markets. Developments are similar to those reported in (5.3). The right panel of (5.4) reports a breakdown by instrument. In the run-up to the financial crisis, credit default swaps (CDS) and forward contracts played the most significant role[2]. Interestingly, after Lehman collapsed forward contracts regained importance rapidly, and at the end of 2013 the effective leverage embedded in those contracts was as large as 15.

[1]Note that the sum of the 4 levels of leverage in Fig. (5.4) is not equal to the total implicit leverage plotted in Fig. (5.3). In fact, since the gross market values and notional amounts are not split proportionally, their ratio cannot be simply aggregated to get the total value. In other words, there is no a rigorous way to arrive from the four levels of leverages in Fig. (5.4) to the aggregate measure in Fig. (5.3).

[2]Since 2011 regulation imposes that for credit derivatives the notional amount should be used to compute their exposure. See BCBS, January 2014, ibidem.

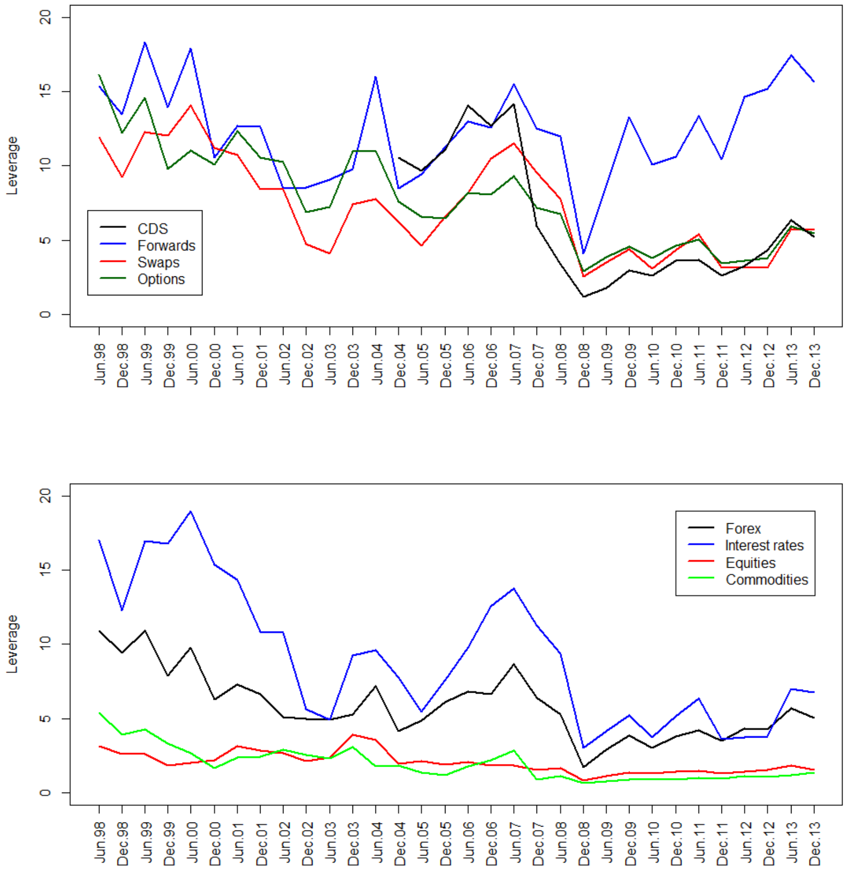

Figure 5.4: Ratio between effective leverage and standard measure of leverage by underlying asset class (top graph) and by derivative instrument (bottom graph). Effective leverage takes into account netting. Source: BIS data.

5.4.2 Effective vs Regulatory Leverage in the Banking System

By correcting the standard measure of leverage using the exposures implicit in derivative contracts, this paper also estimates by how much the banking system aggregate leverage varies when accounting for the leverage embedded in net derivative positions. To this end, the aggregate net market value of derivative contracts is subtracted from the banking system's total assets. The result is then summed up to the aggregate net notional amounts underlying derivatives contracts and divided by the total equity of the banking system.

As shown in Fig. (5.5), the resulting banking system's aggregate effective leverage (red line) is always larger than the standard measure of leverage (blue line) and it is roughly almost twice as high. Moreover, while the standard leverage is always lower than the regulatory leverage threshold (green line), the aggregate effective leverage lies above it most of the time. Such underestimation of leverage has likely led to an underestimation of risk in the banking system. While standard leverage exhibited a modestly declining trend until approximately 2007, aggregate effective leverage increased significantly in the run up to the crisis growing from 38 in 2005 to around 60 in 2008.

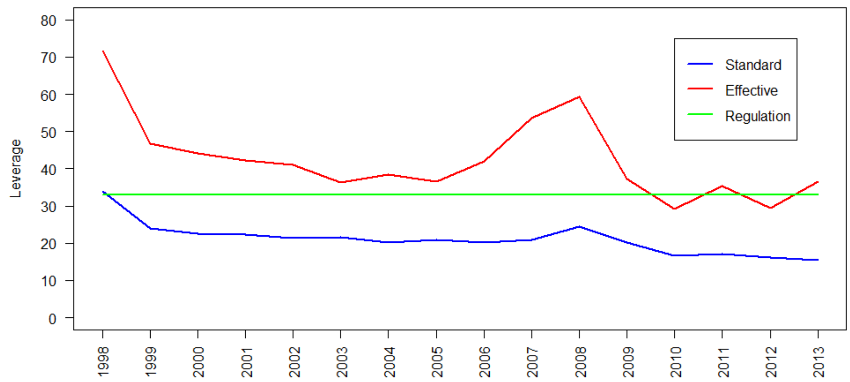

Figure 5.5: Effective leverage is computed as follows. The aggregate net market value of derivative contracts is subtracted from the banking system's total assets. The result is then summed up to the aggregate underlying assets' net notional amounts and divided by the total equity of the banking system. Sources: BIS, OECD Banking Statistics, FED, HelgiLibrary, World Bank, Reserve Bank of Australia, Bank of England, CANSIM, Swiss National Bank, Bloomberg.

Fig. (5.6) replicates the exercise of Fig. (5.5) with a breakdown by country. With the exception of Italy, for the other countries in the sample the aggregate effective leverage is much larger than the leverage estimated with standard measures and often lies above the regulatory threshold. Moreover, the aggregate effective leverage shows higher variability than standard measures of leverage. Since 2012 while the aggregate effective leverage in France, the Netherlands and the UK tends to increase, in Belgium and Italy it is characterized by a downward trend and it remains constant in Germany.

The developments shown in Fig. (5.5) and Fig. (5.6) imply that, most of the time, capital arbitrage opportunities have materialised. Indeed, if it is the risk weights approach which constrains the minimum capital requirement, the effective leverage can never be above 33. The reason is that if banks decide to expand their asset exposures via derivatives and the risk weights are the binding constraint, banks will need to increase their capital for an amount which will bring leverage down to at most 33. However, since the observed effective leverage is often larger than 33 (see Fig. (5.5) and Fig. (5.6)), then the regulatory cap on leverage should provide the binding constraint to capital. But as the standard measures of leverage are typically underestimated, then capital arbitrage opportunities materialise: for a given amount of risk, the use of derivatives enables the bank to save an amount of capital equal to the difference between the effective and regulatory measures of leverage. On the other hand, when the aggregate effective leverage is below the regulatory threshold but still above the standard measure of leverage, there is no capital arbitrage even though banking system's riskiness is underestimated.

If banks decide to expand their balance sheets with an outright asset purchase which gives the same exposure of the derivative portfolio, the standard leverage will be equal to the effective leverage. If this leverage is larger than 33, regulation would require additional capital. In reality, despite effective leverage is larger than 33, banks do not top up their capital since standard measures of leverage are downward biased. In order to better understand the implications in terms of concentration of risk, a more granular approach would be needed, requiring data at banks portfolio level.

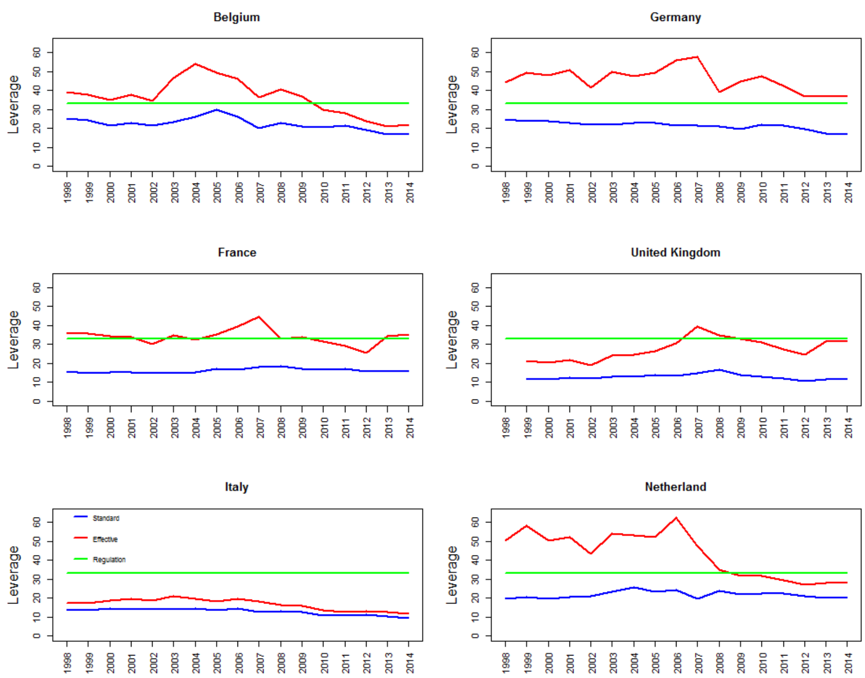

Figure 5.6: Sources: BIS, OECD Banking Statistics, HelgiLibrary, CANSIM, Bloomberg.

Fig. (5.7) plots the additional capital that banks should hold to bring down the effective leverage to the regulatory leverage threshold, which is equal to 33 (blue line). This capital is computed by dividing the effective exposures of banks – i.e. the total assets derived by expanding their derivative portfolios – by the leverage regulatory threshold. The calculation assumes that it is the cap on leverage which constrains the minimum capital requirement. When this resulting "effective" capital requirement is larger than the banks' actual capital (which reflects Basel regulation – red line), capital arbitrage occurs. The gap between the effective capital requirement and actual capital reached its peak in the run-up to the financial crisis. Moreover, Fig. (5.7) reports the capital which would be required according to the 3% regulatory leverage cap (green line).

Fig. (5.8) replicates the exercise carried out in Fig. (5.7) with a breakdown by country. Consistently with the consolidated figures, in all countries the gap between effective capital requirement and actual capital reaches its apex just before the financial crisis. After the demise of Lehman, capital arbitrage tends to fade away. Germany stands out since effective capital requirement is always larger than actual capital, while Italy experiences an opposite situation.

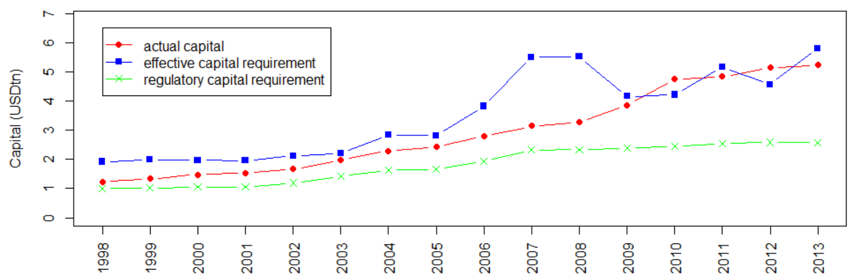

Figure 5.7: "Actual capital" refers to the banks' current capital, which meets Basel standards. "Effective capital requirement" is computed as follows: the aggregate net market value of derivative contracts is subtracted from the banking system's total assets and the net notional amount is added to such assets. The result is then divided by the leverage regulatory threshold which is equal to 33. "Regulatory capital requirement" is computed as follows: the banking system's total assets are divided by the leverage regulatory threshold. Sources: BIS, OECD Banking Statistics, FED, HelgiLibrary, World Bank, Reserve Bank of Australia, Bank of England, CANSIM, Swiss National Bank, Bloomberg, own calculations.

5.5 Policy Implications

From a financial stability perspective, leverage plays a key role. At the level of an individual financial institution, it can increase the probability of default beyond what is captured by the risk weights approach because of the limitations of the latter. At the systemic level, it can amplify shocks and produce contagion. Correct estimates of leverage are therefore crucial to properly assess riskiness of individual banks and of the whole financial system. Against this background, this paper shows how standard measures of leverage can underestimate the effective leverage of financial institutions because of their derivative portfolios. Potentially, the effective leverage embedded in derivative contracts can be very large and can give rise to capital arbitrage opportunities. To rule out this possibility and produce more precise measures of risk, leverage should be computed accurately, using notional rather than market values for net derivative positions.

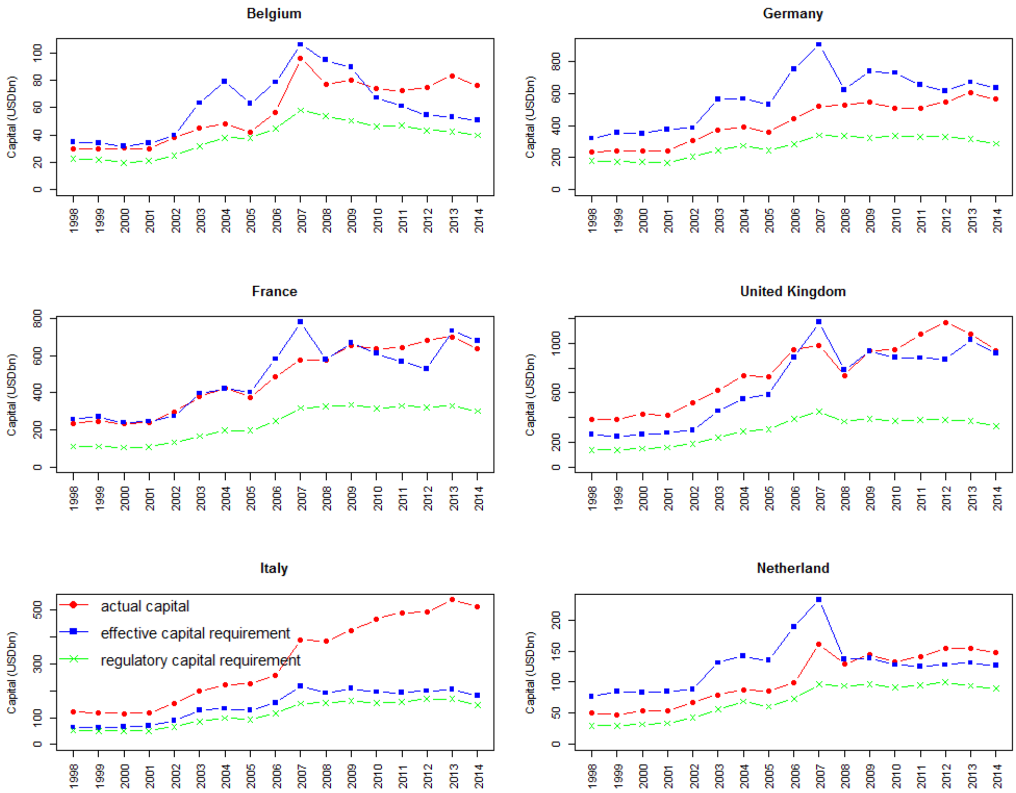

Figure 5.8: "Actual capital" refers to the banks' current capital, which meets Basel standards. "Effective capital requirement" is computed as follows: the aggregate net market value of derivative contracts is subtracted from the banking system's total assets and the net notional amount is added to such assets. The result is then divided by the leverage regulatory threshold which is equal to 33. "Regulatory capital requirement" is computed as follows: the banking system's total assets are divided by the leverage regulatory threshold.Sources: BIS, OECD Banking Statistics, FED, HelgiLibrary, World Bank, Reserve Bank of Australia, Bank of England, CANSIM, Swiss National Bank, Bloomberg, own calculations.

6

Conclusion

This thesis tries to shed some more light on the link between the structure of a financial system, and systemic risk. Chapter 2 introduces a simple but powerful model to generate banking systems with most of the characteristics of a real interbank market. The model has been used to investigate how balance sheets related quantities and different topologies affect the ability of the interbank network to absorb idiosyncratic shocks. The main message is that the level of systemic risk in the system is very much affected by the structure of the system itself, and therefore to prevent and counteract systemic events macroprudential regulations must be put in place. Chapter 3 develops a mathematical framework able to explain the results presented in Chapter 2. Such a framework can also be used to quantify network risk, i.e. the risk coming from the uncertainty about the structure of the financial system. A part of the academic interest in solving the problem, and given the high level of opacity in real financial networks, such tools are becoming urgently needed by regulators.

Chapter 4 presents a multi-layer model to assess systemic risk. The main conclusion of the paper is that systemic risk is underestimated if the different kinds of links among financial institutions are not taken into account. The economic explanation can be found in the ability of banks to transform different kinds of risks one into the other. This underlying ability of banks has the effect to amplify local shock to a systemic extent. Moreover, we propose a measure of systemic importance for the financial institutions composing the system. The measure merges information related to the balance sheets of the banks with information regarding their positions in the multi-layer network in which they are immerse.

Chapter 5 deals with derivative products: using an equivalent portfolio technique, it is shown that (i) classic measures of leverage are misleading when used for derivative products; and (ii) banks can use such loophole to perform capital arbitrage, i.e. to increase the amount of risk per unit of capital by moving their exposures to derivative products.

The research on systemic risk in financial systems is very vivid at the time of writing. Lot of steps have been done so far in the understanding of how the structure of the banking system affects systemic risk. In particular, it is clear now that the internal structure of a financial system is affecting the level of systemic risk, and that idiosyncratic shocks can be amplified into systemic crisis. In other words, the financial system can *endogenously* generate a certain amount of risk that can be larger than the real risk, ultimately generated by the real economy. Network theory has been successfully employed to identify systemic important banks and systemic important markets. We are able by now to say a lot concerning the resilience of a financial system against idiosyncratic shocks, and the major contribution of this thesis is exactly in this direction. Lot of efforts, however, needs to be done to understand the endogenous formation of interbank networks. This implies to model banks' micro-behaviors and their interactions, the latter being responsible for the network structures we see in reality. Given the knowledge concerning the link between the topology of the interbank networks and financial stability, this last step pave the way to understand the link between the incentives of economic agents and systemic risk. The complete understanding of such phenomena would open the door to new macroprudential policies, more oriented to attack banks incentives, than risk *per se*.

From a policy perspective, indeed, the research on systemic risk is becoming more and more needed. Macroprudential policy is very close to both microprudential regulation and to monetary policy (see Buch (23) for a wide discussion on this topic). Microprudential regulation has the final goal to ensure the safety and soundness of individual financial institutions, considered as isolated entities. Several tools are already available to policy-makers and regulators, both for measuring the stability of single financial institutions (the most common tool in this scope is probably the Value at Risk), and to control their default risk (e.g. through appropriate liquidity and solvency requirements). There is obviously a strong interaction between microprudential and macroprudential regulation, since in general both target the same quantities, like banks' capital and liquidity reserves.

Microprudential supervision and macroprudential policy complement each other over a medium term horizon. Microprudential measures, by increasing the resilience of single financial institutions, can also contribute to counteract systemic risk. Similarly, macroprudential instruments (e.g. the countercyclical capital buffer), by mitigating the accumulation of imbalances, can also contribute to make single financial institutions more resilient.

Macroprudential and monetary policies interact with each other mainly via their respective transmission channels. Monetary policy has a clear objective, which can be identified as keeping prices stability, and its effectiveness can be measured through inflation. By now, a large set of established empirical and theoretical tools is available to assess and evaluate the effects of monetary policy. However, monetary policy can also have impact on financial stability. For instance, a low interest rate environment can create incentive for risk-taking behaviors, or quantitative easing can create a reshuffling in the securities portfolios of many economic agents, increasing concentration and affecting therefore financial stability. The two policy domains can complement each other in ensuring concurrently price stability and financial stability.

The main challenge when conducting macroprudential policy is due to the lack of well-defined policy goals and concrete instruments. Macroprudential regulation has the general goal to protect the stability of the whole financial system or, in other words, to mitigate systemic risk. However, since knowledge is still limited, macroprudential policy can not be targeted perfectly, and therefore it may not fully offset financial instabilities. Therefore, in the future, monetary policy may have to take a greater role to prevent financial crisis (see IMF (44) for a discussion on this point).

Lot of experience still needs to be gained on how to better calibrate macroprudential tools, e.g. capital buffers. This lack of experience, which translates into lack of data, implies that researchers face a further obstacle when investigating the origin of systemic risk and the effects of macroprudential policies on it. In turn, this affects accountability of macroprudential measures: since a clear and commonly accepted measure of systemic risk is still missing, it is hard to evaluate and judge the effects of a particular measure which has been set in to place. For those reasons, in the next years policy makers and researchers will have to work in strict cooperation, sharing knowledge, experience, ideas and data, with the final goal to shed light on the roots of systemic risk and how to prevent its materialization in the future.

Bibliography

[1] Acemoglu, Daron, Asuman Ozdaglar, and Alireza Tahbaz-Salehi (2015), "Systemic risk and stability in financial networks." *American Economic Review*, 105, 564–608, URL http://www.aeaweb.org/articles.php?doi=10.1257/aer.20130456. 1, 7

[2] Acharya, Viral, Lasse Pedersen, Thomas Philippon, and Matthew Richardson (2010), "Measuring systemic risk." Working Paper 1002, Federal Reserve Bank of Cleveland, URL http://EconPapers.repec.org/RePEc:fip:fedcwp:1002. 1

[3] Acharya, Viral V., Tanju Yorulmazer, Denis Gromb, Jose Liberti, Erlend Nier, Sypros Pagratis, Enrico Perotti, Raghu Sundaram, and Lucy White (2008), "Cash-in-the-market pricing and optimal resolution of bank failures." *Review of Financial Studies*, 2742. 4

[4] Allen, Franklin and Douglas Gale (2000), "Financial contagion." *The Journal of Political Economy*, 108, 1–33. 2, 7, 11, 36, 66

[5] Bargigli, L., G. di Iasio, L. Infante, F. Lillo, and F. Pierobon (2015), "The multiplex structure of interbank networks." *Quantitative Finance*, 15, 673–691, URL http://dx.doi.org/10.1080/14697688.2014.968356. 80, 82

[6] Battiston, Stefano, Domenico Delli Gatti, Mauro Gallegati, Bruce Greenwald, and Joseph E. Stiglitz (2012), "Default cascades: When does risk diversification increase stability?" *Journal of Financial Stability*, 8, 138 – 149, URL http://www.sciencedirect.com/science/article/pii/S1572308912000125. 7

[7] Battiston, Stefano, Domenico Delli Gatti, Mauro Gallegati, Bruce C. Greenwald, and Joseph E. Stiglitz (2009), "Liaisons dangereuses: Increasing connectivity, risk sharing, and systemic risk." Working Paper 15611, National Bureau of Economic Research, URL http://www.nber.org/papers/w15611. 11

[8] Battiston, Stefano, Michelangelo Puliga, Rahul Kaushik, Paolo Tasca, and Guido Caldarelli (2012), "DebtRank: Too central to fail? financial networks, the FED and systemic risk." *Scientific Reports*, 2, URL http://dx.doi.org/10.1038/srep00541. 67

[9] BCBS (2011), "Basel iii: A global regulatory framework for more resilient banks and banking systems." Consultative document, Basel Committee on Banking Supervision, Bank For International Settlments, URL http://www.bis.org/publ/bcbs189.htm. 4

[10] BCBS (2013), “Fundamental review of the trading book: A revised market risk framework.” Consultative document, Basel Committee on Banking Supervision, Bank For International Settlments, URL `http://www.bis.org/publ/bcbs265.pdf`. 109

[11] BCBS (2013), “Revised basel iii leverage ratio framework and disclosure requirements.” Consultative document, Basel Committee on Banking Supervision, Bank For International Settlments, URL `http://www.bis.org/publ/bcbs251.pdf`. 113

[12] Beale, Nicholas, David G. Rand, Heather Battey, Karen Croxson, Robert M. May, and Martin A. Nowak (2011), “Individual versus systemic risk and the regulator’s dilemma.” *Proceedings of the National Academy of Sciences*, 108, 12647–12652, URL `http://www.pnas.org/content/108/31/12647.abstract`. 95

[13] Benito, Enrique (2008), “Size, growth and bank dynamics.” Banco de España Working Papers 0801, Banco de España, URL `https://ideas.repec.org/p/bde/wpaper/0801.html`. 13, 38

[14] Bernanke, Ben and Mark Gertler (1989), “Agency Costs, Net Worth, and Business Fluctuations.” *American Economic Review*, 79, 14–31, URL `https://ideas.repec.org/a/aea/aecrev/v79y1989i1p14-31.html`. 7

[15] Bernanke, Ben, Mark Gertler, and Simon Gilchrist (1998), “The financial accelerator in a quantitative business cycle framework.” "Working Paper 6455, National Bureau of Economic Research, URL `http://www.nber.org/papers/w6455`. 7

[16] Bisias, Dimitrios, Mark Flood, Andrew W. Lo, and Stavros Valavanis (2012), “A Survey of Systemic Risk Analytics.” *Annual Review of Financial Economics*, 4, 255–296, URL `https://ideas.repec.org/a/anr/refeco/v4y2012p255-296.html`. 1, 67, 95

[17] Black, Fischer and Myron S Scholes (1973), “The Pricing of Options and Corporate Liabilities.” *Journal of Political Economy*, 81, 637–54, URL `https://ideas.repec.org/a/ucp/jpolec/v81y1973i3p637-54.html`. 111

[18] Bluhm, Marcel, Ester Faia, and Jan Krahnen (2013), “Endogenous banks’ networks, cascades and systemic risk.” SAFE Working Paper Series 12, Research Center SAFE - Sustainable Architecture for Finance in Europe, Goethe University Frankfurt, URL `http://EconPapers.repec.org/RePEc:zbw:safewp:12`. 36, 67

[19] Boss, Michael, Helmut Elsinger, Martin Summer, and Stefan Thurner (2004), “Network topology of the interbank market.” *Quantitative Finance*, 4, 677–684, URL `http://EconPapers.repec.org/RePEc:taf:quantf:v:4:y:2004:i:6:p:677-684`. 12, 13, 37, 38, 80

[20] Breuer, Peter (2002), “Measuring off-balance-sheet leverage.” *Journal of Banking & Finance*, 26, 223–242, URL `http://EconPapers.repec.org/RePEc:eee:jbfina:v:26:y:2002:i:2-3:p:223-242`. 110, 111, 114

[21] Brunnermeier, Markus K. (2009), "Deciphering the Liquidity and Credit Crunch 2007-2008." *Journal of Economic Perspectives*, 23, 77–100, URL `https://ideas.repec.org/a/aea/jecper/v23y2009i1p77-100.html`. 36, 65, 71

[22] Brunnermeier, Markus K. and Yuliy Sannikov (2014), "A macroeconomic model with a financial sector." *American Economic Review*, 104, 379–421, URL `http://www.aeaweb.org/articles.php?doi=10.1257/aer.104.2.379`. 7

[23] Buch, Claudia M. (2015), "Macroprudential policy: what do we need to know?" In *Putting Macroprudential Policy to Work*, 78 – 93, de Nederlandsche Bank, URL `http://www.dnb.nl/en/binaries/416362_DXO_OS_Vol12_WEB_tcm47-313965.pdf`. 130

[24] Caldarelli, G. (2007), *Scale-Free Networks: Complex Webs in Nature and Technology*. Oxford University Press. 3, 12, 14, 19, 37

[25] Cappiello, Lorenzo, Linda Fache Rousová, and Mattia Montagna (2015), "Systemic risk, contagion and fire sales." memeo, forthcoming, European Central Bank. 4, 5

[26] Censor, Yair Al and Stavros A. Zenios (1997), *Parallel Optimization: Theory, Algorithms and Applications*. Oxford University Press. 28

[27] Cocco, João F., Francisco J. Gomes, and Nuno C. Martins (2009), "Lending relationships in the interbank market." *Journal of Financial Intermediation*, 18, 24–48, URL `https://ideas.repec.org/a/eee/jfinin/v18y2009i1p24-48.html`. 16

[28] De Masi, G., G. Iori, and G. Caldarelli (2006), "Fitness model for the italian interbank money market." *Phys. Rev. E*, 74, 066112, URL `http://link.aps.org/doi/10.1103/PhysRevE.74.066112`. 13, 37, 39, 80

[29] Delpini, Danilo, Stefano Battiston, Massimo Riccaboni, Giampaolo Gabbi, Fabio Pammolli, and Guido Caldarelli (2013), "Evolution of Controllability in Interbank Networks." *Scientific Reports*, 3, URL `http://dx.doi.org/10.1038/srep01626`. 67

[30] Diamond, Douglas W and Philip H Dybvig (1983), "Bank Runs, Deposit Insurance, and Liquidity." *Journal of Political Economy*, 91, 401–19, URL `https://ideas.repec.org/a/ucp/jpolec/v91y1983i3p401-19.html`. 66

[31] Eisenberg, Larry and Thomas H. Noe (2001), "Systemic Risk in Financial Systems." *Management Science*, 47, URL `http://dx.doi.org/10.2307/2661572`. 67, 75

[32] Ennis, Huberto (2001), "On the size distribution of banks." *Economic Quarterly*, 1–25, URL `http://EconPapers.repec.org/RePEc:fip:fedreq:y:2001:i:fall:p:1-25`. 13, 38

[33] Finger, Karl, Daniel Fricke, and Thomas Lux (2012), "Network analysis of the e-mid overnight money market: The informational value of different aggregation levels for intrinsic dynamic processes." Kiel working papers, Kiel Institute for the World Economy, URL `http://EconPapers.repec.org/RePEc:kie:kieliw:1782`. 13, 38

[34] Gai, Prasanna and Sujit Kapadia (2010), "Contagion in financial networks." *Proceedings of the Royal Society of London A: Mathematical, Physical and Engineering Sciences*, 466, 2401–2423. 37, 66

[35] Georg, Co-Pierre (2011), "The effect of the interbank network structure on contagion and common shocks." Discussion Paper Series 2: Banking and Financial Studies 2011,12, Deutsche Bundesbank, Research Centre, URL `http://EconPapers.repec.org/RePEc:zbw:bubdp2:201112`. 36, 68

[36] Gerali, Andrea, Stefano Neri, Luca Sessa, and Federico M. Signoretti (2010), "Credit and Banking in a DSGE Model of the Euro Area." *Journal of Money, Credit and Banking*, 42, 107–141, URL `https://ideas.repec.org/a/mcb/jmoncb/v42y2010is1p107-141.html`. 7

[37] Gertler, Mark and Peter Karadi (2011), "A model of unconventional monetary policy." *Journal of Monetary Economics*, 58, 17–34, URL `https://ideas.repec.org/a/eee/moneco/v58y2011i1p17-34.html`. 7

[38] Glasserman, Paul and H. Peyton Young (2015), "How likely is contagion in financial networks?" *Journal of Banking & Finance*, 50, 383 – 399, URL `http://www.sciencedirect.com/science/article/pii/S0378426614000600`. 37, 38

[39] Gómez, S., A. Díaz-Guilera, J. Gómez-Gardeñes, C. J. Pérez-Vicente, Y. Moreno, and A. Arenas (2013), "Diffusion dynamics on multiplex networks." *Phys. Rev. Lett.*, 110, 028701, URL `http://link.aps.org/doi/10.1103/PhysRevLett.110.028701`. 68

[40] Hansen, Lars Peter (2013), "Challenges in Identifying and Measuring Systemic Risk." In *Risk Topography: Systemic Risk and Macro Modeling*, NBER Chapters, 15–30, National Bureau of Economic Research, Inc, URL `https://ideas.repec.org/h/nbr/nberch/12507.html`. 1

[41] Hałaj, Grzegorz and Christoffer Kok (2013), "Assessing interbank contagion using simulated networks." *Computational Management Science*, 10, 157–186, URL `http://dx.doi.org/10.1007/s10287-013-0168-4`. 67, 79

[42] Hałaj, Grzegorz and Christoffer Kok (2014), "Modeling emergence of the interbank networks." Working Paper Series 1646, European Central Bank, URL `http://EconPapers.repec.org/RePEc:ecb:ecbwps:20141646`. 68

[43] Imakubo, Kei and Yutaka Soejima (2010), "The transaction network in japan's interbank money markets." *Monetary and Economic Studies*, 28. 12, 13, 37, 38

[44] IMF (2013), "The interaction of monetary and macroprudential policies." Consultative document, International Monetary Fund, URL `https://www.imf.org/external/np/pp/eng/2013/012913.pdf`. 131

[45] Inaoka, Hajime, Takuto Ninomiya, Ken Taniguchi, Tokiko Shimizu, and Hideki Takayasu (2004), "Fractal network derived from banking transaction – an analysis of network structures formed by financial institutions –." Bank of Japan Working Paper Series 04-E-4, Bank of Japan, URL `http://EconPapers.repec.org/RePEc:boj:bojwps:04-e-4`. 13, 38

[46] Iori, G., S. Jafarey, and Padilla (2006), “Systemic risk on the interbank market.” *Journal of Economic Behaviour and Organization*, 61, 525–542. 66

[47] Iori, Giulia (2008), “A network analysis of the Italian overnight money market.” *Journal of Economic Dynamics and Control*, 32, 259–278, URL http://dx.doi.org/10.1016/j.jedc.2007.01.032. 12, 16, 36, 38

[48] Iori, Giulia, Saqib Jafarey, and Francisco G. Padilla (2006), “Systemic risk on the interbank market.” *Journal of Economic Behavior & Organization*, 61, 525–542, URL http://EconPapers.repec.org/RePEc:eee:jeborg:v:61:y:2006:i:4:p:525-542. 7

[49] Janicki, Hubert and Edward Prescott (2006), “Changes in the size distribution of u.s. banks: 1960-2005.” *Economic Quarterly*, 291–316, URL http://EconPapers.repec.org/RePEc:fip:fedreq:y:2006:i:fall:p:291-316:n:v.92no.4. 13, 38

[50] Johnson, Neil and Thomas Lux (2011), “Financial systems: Ecology and economics.” *Nature*, 469, 302–303. 11

[51] Kiyotaki, Nobuhiro and John Moore (1997), “Credit Cycles.” *Journal of Political Economy*, 105, 211–48, URL https://ideas.repec.org/a/ucp/jpolec/v105y1997i2p211-48.html. 7

[52] Ladley, Dan (2013), “Contagion and risk-sharing on the inter-bank market.” *Journal of Economic Dynamics and Control*, 37, 1384–1400, URL http://EconPapers.repec.org/RePEc:eee:dyncon:v:37:y:2013:i:7:p:1384-1400. 68

[53] Lengnick, Matthias, Sebastian Krug, and Hans-Werner Wohltmann (2013), “Money creation and financial instability: An agent-based credit network approach.” *Economics: The Open-Access, Open-Assessment E-Journal*, 7, URL http://dx.doi.org/10.5018/economics-ejournal.ja.2013-32. 66

[54] Luttmer, Erzo G. J. (2007), “Selection, growth, and the size distribution of firms.” *The Quarterly Journal of Economics*, 122, 1103–1144, URL http://qje.oxfordjournals.org/content/122/3/1103.abstract. 38

[55] Lux, Thomas and Daniel Fricke (2012), “Core-periphery structure in the overnight money market: Evidence from the e-mid trading platform.” Kiel Working Papers 1759, Kiel Institute for the World Economy, URL https://ideas.repec.org/p/kie/kieliw/1759.html. 16, 80

[56] May, Robert M. and Nimalan Arinaminpathy (2010), “Systemic risk: the dynamics of model banking systems.” *Journal of The Royal Society Interface*, 7, 823–838. 12, 36, 37

[57] Montagna, Mattia and Thomas Lux (2013), “Hubs and resilience: towards more realistic models of the interbank markets.” Kiel Working Papers 1826, Kiel Institute for the World Economy, URL https://ideas.repec.org/p/kie/kieliw/1826.html. 39, 44, 45, 52

[58] Newman, M. E. J. (2002), "Random graphs as models of networks." *eprint arXiv:cond-mat/0202208.* 37

[59] Newman, Mark (2010), *Networks: An Introduction.* Oxford University Press, Inc., New York, NY, USA. 3

[60] Nier, Erlend, Jing Yang, Tanju Yorulmazer, and Amadeo Alentorn (2007), "Network models and financial stability." *Journal of Economic Dynamics and Control*, 31, 2033 – 2060, URL `http://www.sciencedirect.com/science/article/pii/S0165188907000097`. Tenth Workshop on Economic Heterogeneous Interacting AgentsWEHIA 2005. 11, 12, 15, 16, 36, 37, 43, 44, 55, 65, 66

[61] Rajan, Raghuram (2005), "Has financial development made the world riskier?" *Proceedings - Economic Policy Symposium - Jackson Hole*, 313–369, URL `http://EconPapers.repec.org/RePEc:fip:fedkpr:y:2005:i:aug:p:313-369`. 1

[62] Reinhart, Carmen M. and Kenneth Rogoff (2009), *This Time Is Different: Eight Centuries of Financial Folly*, 1st edition edition. Princeton University Press, URL `http://www.amazon.com/exec/obidos/redirect?tag=citeulike07-20&path=ASIN/0691142165`. 1

[63] Rosengren, Eric (2010), "Asset bubbles and systemic risk." Speech 32, Federal Reserve Bank of Boston, URL `http://EconPapers.repec.org/RePEc:fip:fedbsp:32`. 1

[64] Sole, Juan and Marco A Espinosa-Vega (2010), "Cross-Border Financial Surveillance: A Network Perspective." IMF Working Papers 10/105, International Monetary Fund, URL `https://ideas.repec.org/p/imf/imfwpa/10-105.html`. 8

[65] Soramäki, Kimmo, Morten L. Bech, Jeffrey Arnold, Robert J. Glass, and Walter E. Beyeler (2007), "The topology of interbank payment flows." *Physica A: Statistical Mechanics and its Applications*, 379, 317–333. 12, 37

[66] Tasca, Paolo and Stefano Battiston (2011), "Diversification and financial stability." Working Paper Series 11-001, CCSS, URL `http://ssrn.com/abstract=1878596orhttp://dx.doi.org/10.2139/ssrn.1878596`. 95

[67] Upper, Christian (2011), "Simulation methods to assess the danger of contagion in interbank markets." *Journal of Financial Stability*, 7, 111–125, URL `http://EconPapers.repec.org/RePEc:eee:finsta:v:7:y:2011:i:3:p:111-125`. 14, 39, 65, 67, 95

[68] Upper, Christian and Andreas Worms (2004), "Estimating bilateral exposures in the german interbank market: Is there a danger of contagion?" *European Economic Review*, 48, 827–849, URL `https://ideas.repec.org/a/eee/eecrev/v48y2004i4p827-849.html`. 27

[69] Vasicek, Oldrich (1987), "Probability of loss on loan portfolio." Technical report, KMV Corp, URL `https://www.kmv.com`. 4

Appendices

Appendix A

Computation of the degree distribution via the probability function

We provide here the derivation of the equations stated in sec. 3.3. Starting from a particular probability function $P_S(A_i, A_j)$, and a distribution for the *size* parameter $\rho(A_i)$, we can write the mean in-degree of a vertex as:

$$k_{in}(A_i) = N \int_a^b P_S(t, A_i)\rho(t)dt = N \cdot F_{in}(A_i) \tag{A.1}$$

and, similarly, for the out-degree we can write:

$$k_{out}(A_i) = N \int_a^b P_S(A_i, t)\rho(t)dt = N \cdot F_{out}(A_i) \tag{A.2}$$

where N is the number of nodes of the network. Assuming the function $F_{in}(A_i)$ and $F_{out}(A_i)$ to be monotonous in A_i, and for N large enough, we can invert the functions F_{in} and F_{out} in order to find the relationships between the size parameter A_i and the the out-and in-degree of the node:

$$A_i = F_{in}^{-1}\left(\frac{k_{in}}{N}\right) \tag{A.3}$$

$$A_i = F_{out}^{-1}\left(\frac{k_{out}}{N}\right) \tag{A.4}$$

The transformation of the parameter in the size-distribution $\rho(A_i)$, from A_i to $k_{in/out}$, leads us to:

$$P(k_{in}) = \rho\left[F_{in}^{-1}\left(\frac{k_{in}}{N}\right)\right] \cdot \frac{d}{dk_{in}} F_{in}^{-1}\left(\frac{k_{in}}{N}\right) \tag{A.5}$$

$$P(k_{out}) = \rho\left[F_{out}^{-1}\left(\frac{k_{out}}{N}\right)\right] \cdot \frac{d}{dk_{out}} F_{out}^{-1}\left(\frac{k_{out}}{N}\right) \tag{A.6}$$

The density D^l of a network generated according to probability function P_l is computed as follow:

$$D^l = \frac{2 \cdot \langle n_l \rangle}{N(N-1)} = \frac{2 \cdot \sum_{i,j=1}^{N} \langle H(P_{ij}^l - \epsilon_{ij}) \rangle}{N(N-1)} = \frac{2 \cdot \sum_{i,j=1}^{N} P_{ij}^l}{N(N-1)} \tag{A.7}$$

where $\langle n_l \rangle$ is the expectation value of the number of links generated by probability function P_l, ϵ_{ij} are i.i.d. random variables distributed uniformly over the interval $[0,1]$, and $H(\cdot)$ is the Heaviside function.

Appendix B

Computation of the state functions: analytical solutions for first round effects

The purpose of this appendix is to provide the derivation of eqs. (3.21) and (3.22). We first recall the main characteristics of the model; a probability matrix P, with entries $p_{ij} = P_s(A_i, A_j)$ $(s = 1, 2, 3)$, indicates the probability for each possible edge in the system, this is computed after the sequence $\{A_i\}$ has been assigned to the system itself. For each probability matrix P, a large number of realizations for the adjacency matrices are possible. Once an adjacency matrix A has been determined for the system, the weight of each edge is computed according to:

$$l_{ij} = \frac{l_i p_{ij}}{\sum_{j \in \Omega_i} p_{ij}} = \frac{(1-\theta) A_i p_{ij}}{\sum_{j \in \Omega_i} p_{ij}} \tag{B.1}$$

where Ω_i denotes the set of nodes which satisfy $a_{ij} = 1$. We can now start deriving eq. (3.21). First of all, note that with probability $(1 - p_{ij})$, bank i has no link directed to bank i_0, and in that case its net worth η_i in round 1 rests unchanged and remains identical to η_i^0: this situation gives one of the two contributions in eq. (3.21). In the other case $(a_{ij} = 1)$, we have instead:

$$\eta_i^{r=1} = \eta_i^1 = \eta_i^0 - f_{i_0} l_{ii_0} = \eta_i^0 - f_{i_0} \frac{(1-\theta) A_i p_{ii_0}}{c_i} \tag{B.2}$$

where η_i^1 is the net worth of bank i at time $t = 1$, f_{i_0} is the fraction of money that bank i_0's creditors lose due the failure of bank i_0, and $c_i = \sum_{j \in \Omega_i} p_{ij}$. Considering the mechanism of contagion explained in section 3.4, we have:

$$f_{i_0} = f_{i_0}(\theta, \gamma) = min\left[\frac{(1-\theta)\,A_{i_0} - \gamma A_{i_0}}{\sum_j p_{ji_0}}, 1\right] \tag{B.3}$$

To derive the distribution of the random variables η_i we note that on the right side of eq. (B.2) the only random term is c_i, since the other are fixed once the sequence $\{A_i\}$ and the probability matrix P are fixed. We can write:

$$c_i = \sum_{j=1}^{n} \theta\left(P_s(A_i, A_j) - \xi_j\right) \cdot P_s(A_i, A_j) = \sum_{j=1}^{n} c_{ij} \tag{B.4}$$

where $\theta(x)$ denotes again the Heaviside function and ξ_i are *i.i.d.* random variables with uniform distribution between zero and one:

$$\xi_i \sim U_{[0,1]} \tag{B.5}$$

Since we are using $N = 250$, and the variables in eq. (B.4) are simply functions of *i.i.d* random variables with finite mean and variance, we can apply the Central Limit Theorem (CTL) and conclude that c_i can be approximated by a Gaussian distribution with mean:

$$\begin{aligned}
\langle c_i \rangle &= \sum_{j=1}^{n} \langle \theta\left(P_s(A_i, A_j) - \xi_j\right) \cdot p_{ij} \rangle \\
&= \sum_{j=1}^{n} \int_0^1 \rho(\xi)\theta\left(P_s(A_i, A_j) - \xi_j\right) \cdot p_{ij} d\xi \\
&= \sum_{j=1}^{n} p_{ij} \int_0^{p_{ij}} d\xi = \sum_{j=1}^{n} p_{ij}^2 \equiv m_i,
\end{aligned} \tag{B.6}$$

and variance:

$$\begin{aligned}
\sigma_{ij}^2 &= Var\left[\theta\left(P_s(A_i, A_j) - \xi_j\right)\right] = \left\langle c_{ij}^2 \right\rangle - \langle c_{ij} \rangle^2 \\
&= \left(\int_0^1 d\xi \left[\theta\left(P_{ij} - \xi_j\right)\right]^2 p_{ij}^2\right) - p_{ij}^4 = p_{ij}^3 - p_{ij}^4,
\end{aligned} \tag{B.7}$$

and so:

$$\sigma_i^2 = \sum_{j=1}^{n} \sigma_{ij}^2 = \sum_{j=1}^{n} \left(p_{ij}^3 - p_{ij}^4\right). \tag{B.8}$$

Therefore, the distribution of the variables c_i can be approximated by:

$$\rho(c_i) = \frac{1}{\sigma_i\sqrt{2\pi}} \cdot exp\left\{-\frac{1}{2}\left(\frac{c_i - m_i}{\sigma_i}\right)^2\right\}. \tag{B.9}$$

Now we have to compute the distribution of η_i^1, which is a simple function of c_i. Rewriting eq. (B.2) as:

$$\eta_i^1 = \eta_i^0 - f_{i_0}\frac{(1-\theta)\, A_i p_{ii_0}}{c_i} = a - \frac{b}{c_i} \tag{B.10}$$

where we indicate the constant terms η_i^0 and $f_{i_0}\,(1-\theta)\, A_i p_{ii_0}$ with a and b respectively. Denoting by $\rho_c(\cdot)$ the pdf of c_i, we obtain the pdf of η_i^1 as follows:

$$\begin{aligned}
\rho\left(\eta_i^1\right) &= \frac{\rho_c\left(\frac{b}{a-\eta_i^1}\right)}{\left|f'\left(\frac{b}{a-\eta_i^1}\right)\right|} = \frac{b}{\left(a-\eta_i^1\right)^2}\cdot\rho_c\left(\frac{b}{a-\eta_i^1}\right) \\
&= \frac{b}{\left(a-\eta_i^1\right)^2}\cdot\frac{1}{\sigma_i\sqrt{2\pi}}\cdot exp\left\{-\frac{1}{2}\left(\frac{\frac{b}{a-\eta_i^1} - m_i}{\sigma_i}\right)^2\right\}
\end{aligned} \tag{B.11}$$

where a and b depend on η and θ. The last equation, combined with the Dirac delta for the variable η_i, leads us to eq. (3.21). Note that in the case of a random network, the individual determinants m_i and σ_i would be constant across banks while they depend on the balance sheet size through eq. (3.15) to (3.17) in the present framework.

As regards the state function of the second round, $\Phi^{t=2}\left(\vec{\eta}|s_{i_0}\right)$, since the variable $\eta_i s$ are now dependent, an explicit closed form becomes difficult to compute (and the same is true for all the other higher rounds). However, it is possible to use different approximations of these state functions. One way is the factorization of the function itself as:

$$\Phi^{t=2}\left(\eta_1, \eta_2, \ldots, \eta_n; s_{i_0}\right) = \prod_{i=0}^{n} \Phi_i^{t=2}\left(\eta_i\right) \tag{B.12}$$

assuming absence of dependency between variables. However, such an approximation leaves out some of the interesting spillover effects that are the focus of our interest. We prefer, therefore, to generate variables η_i and compute the integral in eq. 3.3 numerically. In order to generate the variables, we use the following algorithm, which is built-in into the structure of our model:

- given a probability matrix P and a sequence $\{A_i\}$ for the node's fitness parameters, we generate a $N \times N$ random matrix M, with entries m_{ij} distributed according to:

$$m_{ij} \sim i.i.d.\ ,\ U_{[0,1]}$$

an adjacency matrix A with entries:

$$a_{ij} = \begin{cases} 1, & \text{if } m_{ij} \leq p_{ij} \\ 0, & \text{otherwise} \end{cases} \tag{B.13}$$

and the correspondent weight matrix W with entries $w_{ij} = l_{ij}$;

- for each node we generate its second round net worth $\eta_{i,2}$; with probability $P^I = p_{ii_0}$ it will be:

$$\eta_{i,2} = \eta_i^0 - f_{i_0} l_{ii_0} - \sum_{j=1}^{n} \theta(p_{ij} - m_{ij})\theta(p_{ji_0} - m_{ji_0})\theta(P_1(a_j) - \varepsilon_j) l_{ij} f_j \tag{B.14}$$

with probability P^{II}:

$$\eta_{i,2} = \eta_i^0 - \sum_{j=1}^{n} \theta(p_{ij} - m_{ij})\theta(p_{ji_0} - m_{ji_0})\theta(P_1(a_j) - \varepsilon_j) l_{ij} f_j \tag{B.15}$$

and with probability $1 - P^I - P^{II}$:

$$\eta_{i,2} = \eta_i^0 \tag{B.16}$$

where ε_i are *i.i.d.* variables distributed according to a uniform pdf, $\varepsilon_i \sim U_{[0,1]}$, and $P_1(a_i)$ is the probability that bank i has failed in the first round, computed according to eq. (3.21). In general, to generate the equity levels for higher rounds, one needs to build equations like (B.14) - (B.16) the losses coming from the banks in the lower shells of the system.

In this way the two contributions can be separated, and the output is shown in Fig. 3.4. The advantage of working with state functions instead of Monte Carlo realizations of the system is that we get *closer* to an analytical solution and can decompose the overall effects into their different elements.

The coefficients f_i are obtained directly from the model:

$$f_i \equiv \frac{min\,[p_i \cdot e_i - \eta_i; l_i]}{l_i} = min\left[1, \frac{A_i[p_i\theta - \gamma]}{l_i}\right] \tag{B.17}$$

where λ_i is the size of the shock, according to notation presented in Sec. 3.2, and we can compute a mean-field approximation to l_i as:

$$l_i = n \cdot \int_a^b \frac{1}{c_j}(1-\theta)A_j \cdot p_{ji} \cdot \rho\left(A_j\right) dA_j \tag{B.18}$$

which brings us to:

$$f_i = min\left[1, \frac{(\lambda_i\theta - \gamma)}{(1-\theta)} \frac{A_i}{\sum_j \frac{A_j P_{ji}^2}{\sum_k P_{jk}^2}}\right] \tag{B.19}$$

Note that f_i represents the limited liability condition, which through the minimum functions in eq. (B.17) complicates the problem of finding an analytical solution for the state function at each event time t higher than 1. Since the $c_i s$ are random variables, the expectation of l_i is obtained by substituting c_j with its expectation value, computed using eq. (B.9). Note that, in case the shock consists in wiping out all external assets from the balance sheets of the biggest bank i_0, it is easy to see that $f_{i_0} = 1$ if θ is higher than a certain threshold value: in this case no damping factor will enter in eq. (B.2).

B.1 Mean and variance for the marginal Φ-function

In this section we show how to compute the mean and variance for the state function (3.21). Our goal is therefore to compute mean and variance of the variable (B.10), given that c_i is distributed according to (B.9). In general, given a random variable x, distributed according to $\rho_x(x)$, and a variable y defined as a function of the former, $y = f(x)$, it is possible to find an approximation for the mean and the variance of y through the following method. As regards the mean, we have:

$$< y >=< f(x) >=< f(\mu_x + (x - \mu_x) > \tag{B.20}$$

where we call μ_x the mean value of the variable x. A Taylor expansion around μ_x leads to:

$$< f(\mu_x) + f'(\mu_x)(x-\mu_x) + \frac{1}{2}f''(\mu_x)(x-\mu_x)^2 + \frac{1}{3!}f'''(\mu_x)(x-\mu_x)^3 + \cdots > \tag{B.21}$$

In case of a Gaussian variable, the above equation reduces to:

$$< y >= f(\mu_x) + \frac{1}{2}f''(\mu_x)\sigma_x^2 \tag{B.22}$$

In our case, we know the distribution of the function c_i, which is approximated by a Gaussian distribution, and we want to know the distribution of η_i, defined as:

$$\eta_i = a - \frac{b}{c_i} \tag{B.23}$$

We have, after some algebra:

$$< \eta_i >= \eta_i^0 - p_{ii_0} \left[\frac{b_i}{m_i} + \frac{b_i}{m_i^3} \sigma_i^2 \right] \tag{B.24}$$

and

$$< \eta_i^2 > - < \eta_i >^2 = p_{ii_0} b_i^2 \left[\frac{1}{m_i^2} (1 - p_{ii_0}) + \frac{\sigma_i^2}{m_i^4} (3 - 2p_{ii_0}) - p_{ii_0} \frac{\sigma_i^4}{m_i^6} \right] \tag{B.25}$$

It is easy to see that the above expression approaches zero if all the elements p_{ij} tend to one or to zero: the full information regarding the network structure will restore the determinism and remove all uncertainty about the extent of contagion.

Appendix C

Multi-layered model

C.1 Jaccard index

Among the several measures that can be introduced to measure similarity among set of numerical or binary data (see for example Bargigli *et al.* (2013)), we use in this paper the so called Jaccard index. Given two networks g_1 and g_2, described by the weighted matrix W^1 and W^2, we introduce the following quantities[1]:

- M_{11}: number of entries (i, j) which have non null values both in the matrix W^1 and W^2;
- M_{10}: number of entries (i, j) which have non null values in the matrix W^1 and null value in the matrix W^2;
- M_{01}: number of entries (i, j) which have null values in the matrix W^1 and non null value in the matrix W^2;
- M_{00}: number of entries (i, j) which have null values both in the matrix W^1 and W^2.

We have $M_{11} + M_{10} + M_{01} + M_{00} = N^2$. The Jaccard index is then defined as:

$$J_{12} = \frac{M_{11}}{M_{10} + M_{01} + M_{11}} \tag{C.1}$$

and its value ranges in the interval $[0, 1]$. In particular, J_{12} is equal to 0 if the two networks do not have a single common link, and it is equal to 1 if the two networks are identical.

[1]For simplicity we assume here that both the matrices are $N \times N$, with entries (i, j) belonging to the real space $\Re$.

C.2 Computation of the critical links

The identification of the thresholds for a link weight to be defined critical is at the core of the aggregation algorithm proposed in the paper. In this section we report the details necessary to compute them. We note that the threshold values compute here depend on the micro behavioral rules assumed for the banks. Changing the banks' behavior will of course change threshold values, but the aggregation algorithm will still work as tool for the semplification of the multi-layer network structure[1].

- Layer l_1: given the matrix W^1 whose entries represent the long-term direct exposures among banks, there exists a critical link in layer l_1 between two banks i and j if:

$$W^1_{ji} \cdot LGD_i > \frac{eq_j - \bar{\gamma}\left[RWEA_j + \sum_{\mu=0}^{M} p_\mu w^\mu s^j_\mu + w^{ib} l^l_j\right]}{1 - \bar{\gamma} w^{ib}} \tag{C.2}$$

  Despite the complicated form of eq. (C.2), its meaning is simple: a critical link between nodes i and j exists if node j is not able to absorb the losses transmitted in case of the defaults of node i. In the above equation we introduce the losses-given-default (LGD) of bank i, computed as an estimation of the percentage of loans that bank i is not able to repay in case of its default[2]. We note that the use of LGD is fundamental in order to replicate a more realistic scenario in the simulations, and the quality of its estimation depends on the available data.

- Layer l_2: given the matrix W^2 whose entries represent the short-term direct exposures among banks, there exists a critical link in layer l_2 between two banks i and j if:

$$W^2_{ij} > \left(c_j + l^s_j + \sum_{\mu=0}^{M} \bar{s}^j_\mu \cdot exp\left\{ -\alpha_\mu \frac{\bar{s}^j_\mu}{s^{tot}_\mu} \right\} \right) \tag{C.4}$$

[1] The computation of the thresholds necessary to identify critical links represents the tricky part of the algorithm. In fact, a part of layer l_1 for which one can easily compute the maximum losses each bank can absorb without going below the capital requirements, for the other layers approximations are necessary.

[2] In our framework, this amount to:

$$LGD_i = 1 - min\left[max\left[\frac{c_i + \sum_{\mu=0}^{M} s^i_\mu p_\mu + l^s_i - b^s_i}{l^l_i} ; 0 \right] ; 1 \right] \tag{C.3}$$

Of course, better calibrations are possible depending on data availability and the dynamics used in the model.

The sequence $\left\{\bar{s}^j_1, \bar{s}^j_2, \cdots, \bar{s}^j_M\right\}$ are the roots of the equation:

$$\frac{eq_j + \sum_{\mu=0}^{M} \bar{s}^j_\mu \cdot \left[1 - exp\left\{-\alpha_\mu \frac{\bar{s}^j_\mu}{s^{tot}_\mu}\right\}\right]}{CRWA_j + w^{ib} l^l_j + \sum_{\mu=0}^{M}\left(s^j_\mu - \bar{s}^j_\mu\right) exp\left\{-\alpha_\mu \frac{\bar{s}^j_\mu}{s^{tot}_\mu}\right\}} - \bar{\gamma} = 0 \tag{C.5}$$

Those roots have to found numerically since we have to impose the pecking order, as in the simulator engine, and the non linearities appearing both in the numerator and in the denominator of eq. (C.5) make impossible to find analytical solutions.

Equation (C.4) states that a critical link between i and j exists if bank i can force bank j to liquidate an amount of assets, by withdrawing all its short-term funding, which will reduce the RWCR of bank j beyond the threshold value $\bar{\gamma}$. In other words, bank j is relying too heavily on the funding services provided by bank i. We note that the link between illiquidity and insolvency, in the simulator engine, was properly expressed through the map in eq. (4.9).

- Layer l_3: given the matrix of the portfolios $S_{N\times M}$, whose entries s^i_μ represent the securities μ in the portfolio of bank i, there exists a critical link in layer l_3 between two banks i and j if the liquidation of the whole bank i's portfolio results in the default of bank j, namely when:

$$\frac{eq_j - \sum_{\mu=0}^{M}(1 - p^*_\mu) s^j_\mu}{CRWA_j + w^{ib}(l^s_j + l^l_j) + \sum_{\mu=0}^{M} w^\mu p^*_\mu s^j_\mu} < \bar{\gamma} \tag{C.6}$$

Where we indicated with p^*_μ the price of the security μ after bank i liquidates its portfolio, according to eq. (4.5).

C.3 Simulation results

In this section we report the distribution of the number of defaults for the most important banks in the system.

(DE018)

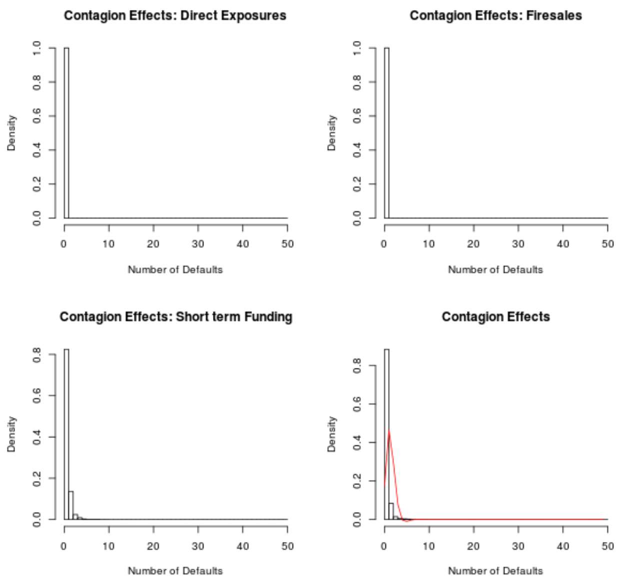
Contagion Effects: Direct Exposures
Contagion Effects: Firesales
Contagion Effects: Short term Funding
Contagion Effects
Density
Number of Defaults

(DE019)

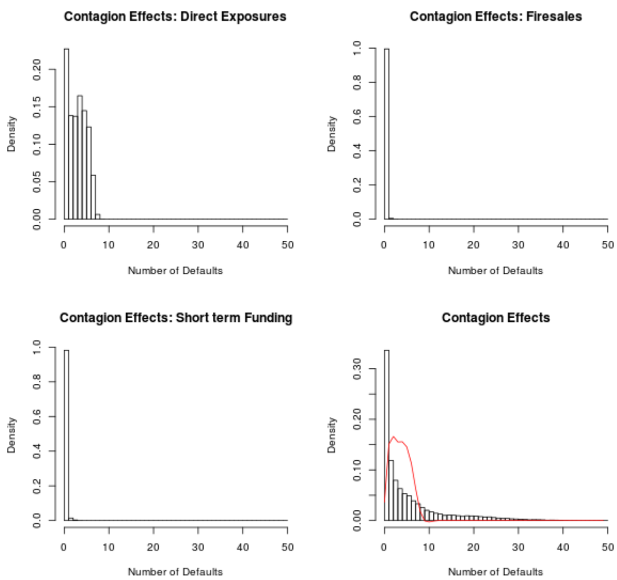
Contagion Effects: Direct Exposures
Contagion Effects: Firesales
Contagion Effects: Short term Funding
Contagion Effects
Density
Number of Defaults

(DE020)

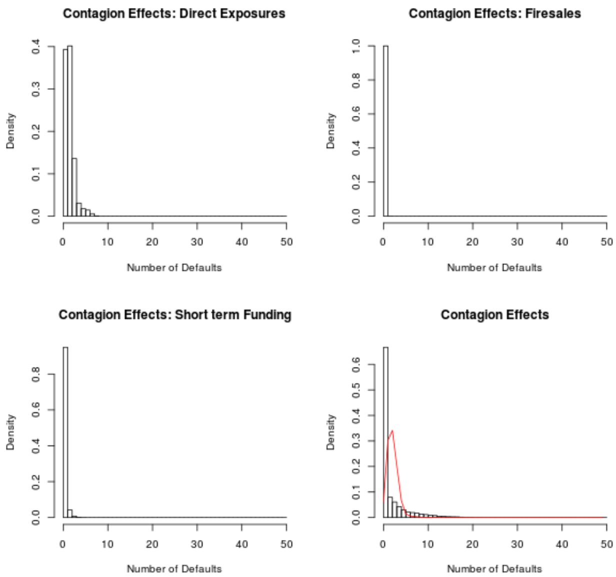
Contagion Effects: Direct Exposures
Contagion Effects: Firesales
Contagion Effects: Short term Funding
Contagion Effects
Density
Number of Defaults

(DE021)

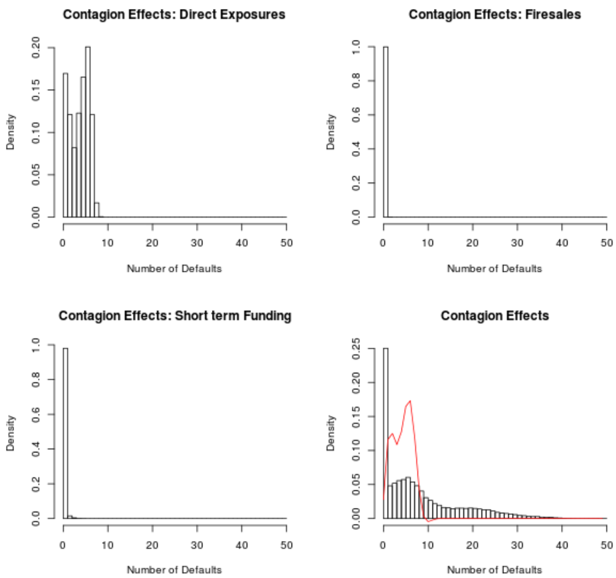
Contagion Effects: Direct Exposures
Contagion Effects: Firesales
Contagion Effects: Short term Funding
Contagion Effects
Density
Number of Defaults

(DE023)

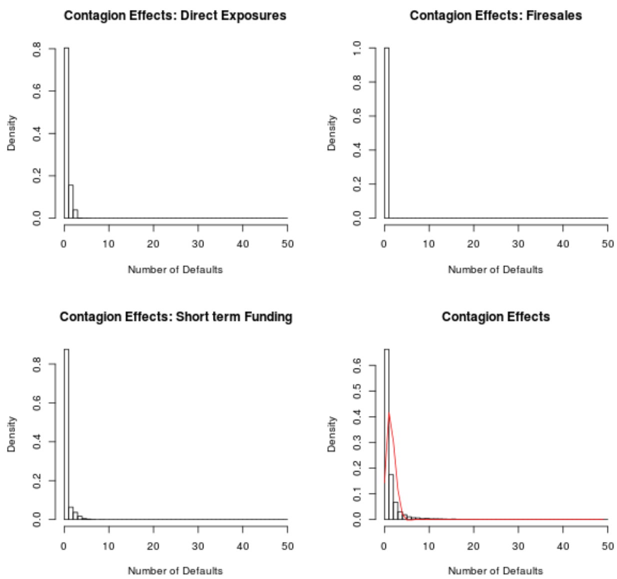
Contagion Effects: Direct Exposures
Contagion Effects: Firesales
Contagion Effects: Short term Funding
Contagion Effects
Density
Number of Defaults

(DE025)

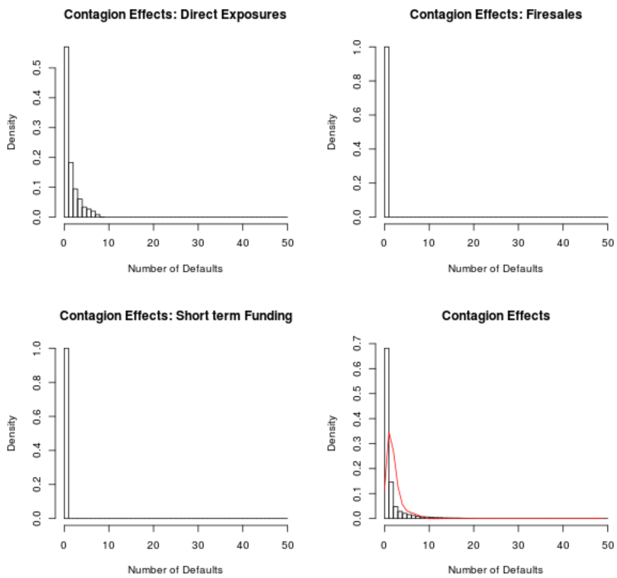
Contagion Effects: Direct Exposures
Contagion Effects: Firesales
Contagion Effects: Short term Funding
Contagion Effects
Density
Number of Defaults

(FR015)

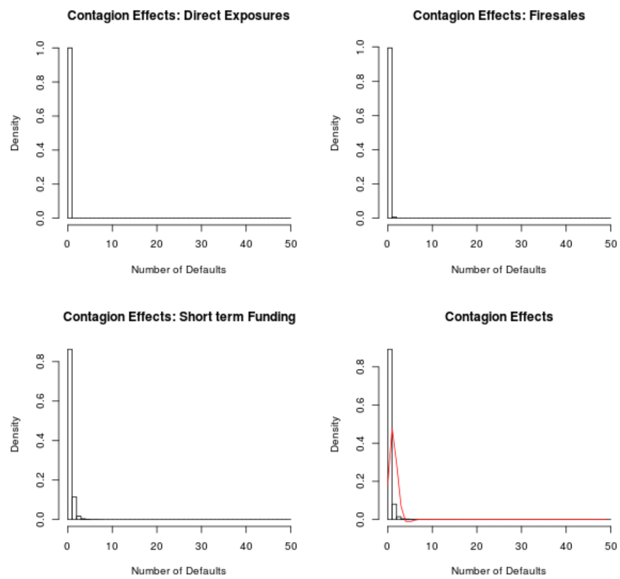
Contagion Effects: Direct Exposures
Contagion Effects: Firesales
Contagion Effects: Short term Funding
Contagion Effects
Density
Number of Defaults

(FR016)

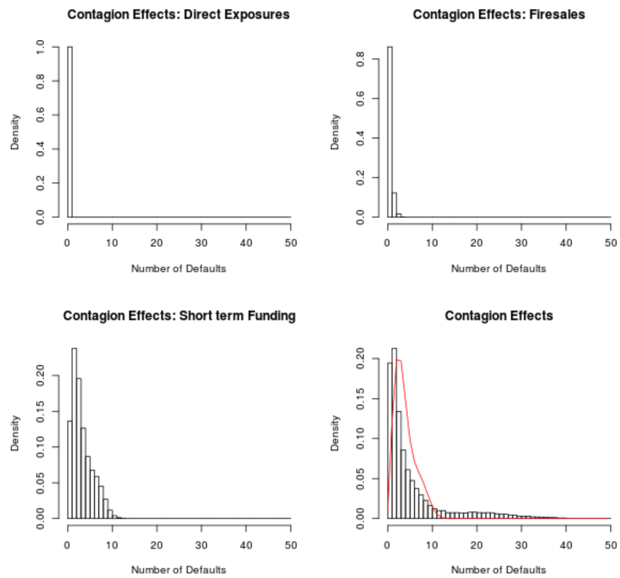
Contagion Effects: Direct Exposures
Contagion Effects: Firesales
Contagion Effects: Short term Funding
Contagion Effects
Density
Number of Defaults

(GB088)

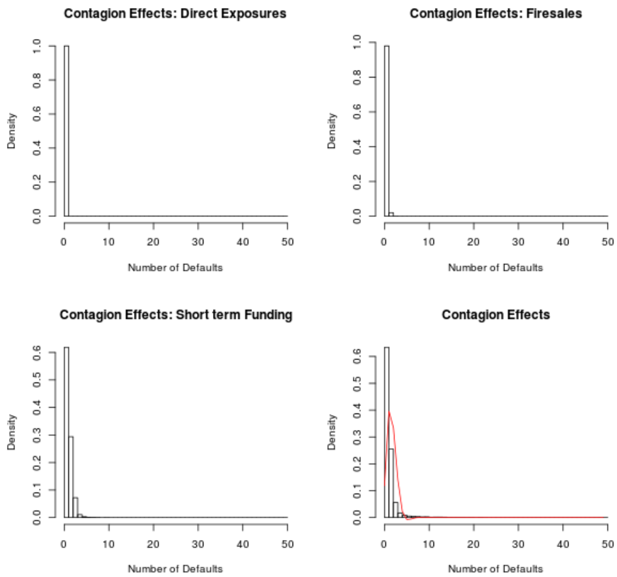
Contagion Effects: Direct Exposures
Contagion Effects: Firesales
Contagion Effects: Short term Funding
Contagion Effects
Density
Number of Defaults

(GB089)

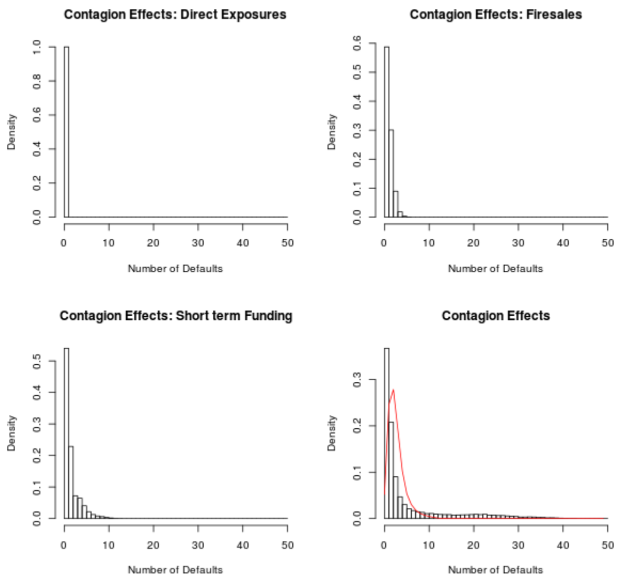
Contagion Effects: Direct Exposures
Contagion Effects: Firesales
Contagion Effects: Short term Funding
Contagion Effects
Density
Number of Defaults

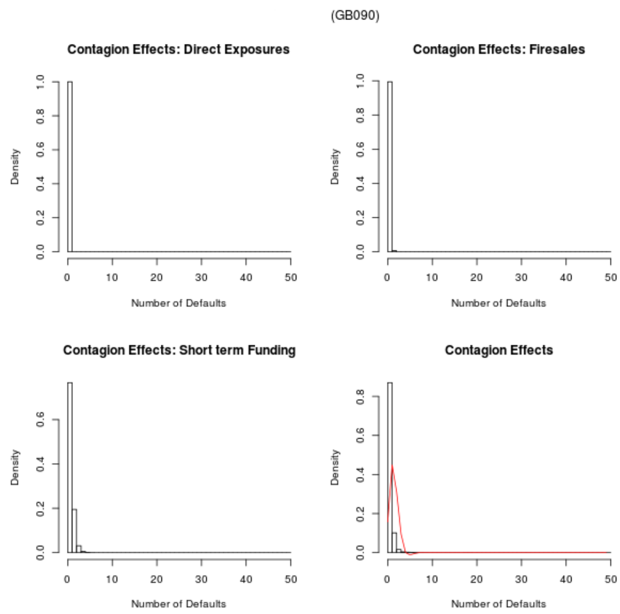
(GB090)
Contagion Effects: Direct Exposures
Contagion Effects: Firesales
Contagion Effects: Short term Funding
Contagion Effects
Density
Number of Defaults

Declaration

I hereby affirm that I have completed my doctoral thesis entitled, "Systemic Risk in Modern Financial Systems" entirely on my own and unassisted, and that I have specially marked all of the quotes I have used from other authors as well as these passages in my work that are extremely close to the thoughts presented by other authors, and listed the sources in accordance with the regulations I have been given.

Date Signature